NASA Contractor Report 4281

Cockpit Ocular Recording System (CORS)

Edward Rothenheber, James Stokes,
Charles LaGrossa, William Arnold,
and A. O. Dick

CONTRACT NAS1-18473
MARCH 1990

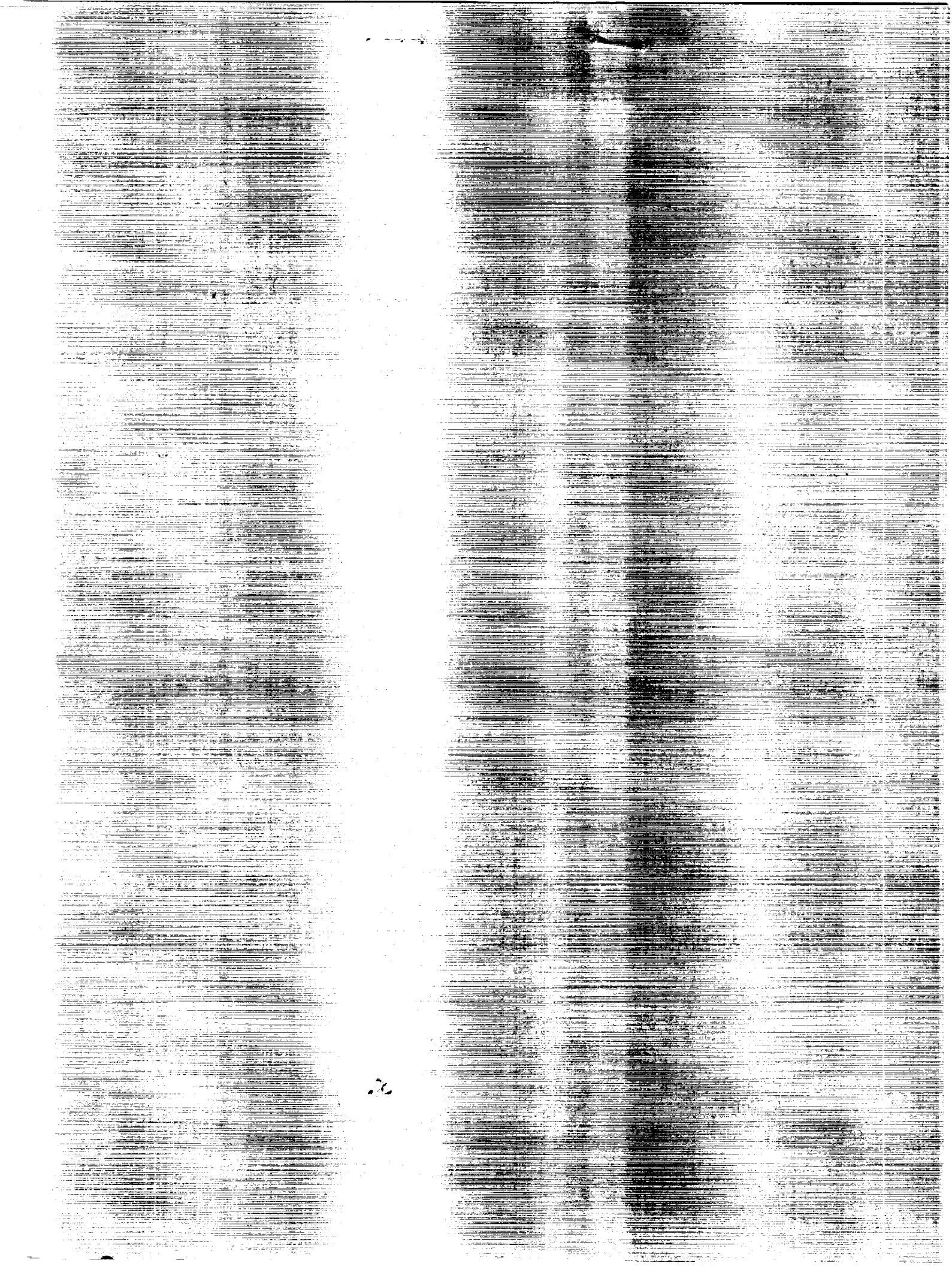

NASA Contractor Report 4281

Cockpit Ocular Recording System (CORS)

Edward Rothenheber, James Stokes,
Charles LaGrossa, William Arnold,
and A. O. Dick
Analytics, Inc.
Willow Grove, Pennsylvania

Prepared for
Langley Research Center
under Contract NAS1-18473

National Aeronautics and
Space Administration
Office of Management
Scientific and Technical
Information Division

1990

Report Documentation Page

1. Report No.	2. Government Accession No.	3. Recipient's Catalog No.
NASA CR-4281		

4. Title and Subtitle
Cockpit Ocular Recording System (CORS)

5. Report Date
March 1990

6. Performing Organization Code

7. Author(s)
Edward Rothenheber, James Stokes, Charles LaGrossa, William Arnold, and A. O. Dick

8. Performing Organization Report No.
TR 2107

10. Work Unit No.
324-02-00

9. Performing Organization Name and Address
Analytics, Inc.
2500 Maryland Road
Willow Grove, PA 19090

11. Contract or Grant No.
NAS1-18473

13. Type of Report and Period Covered
Contractor Report

12. Sponsoring Agency Name and Address
National Aeronautics and Space Administration
Langley Research Center
Hampton, VA 23665-5225

14. Sponsoring Agency Code

15. Supplementary Notes
Langley Technical Monitor--Randall L. Harris, Sr.
SBIR Phase II Final Report

16. Abstract

The overall goal of this project was the development of a Cockpit Ocular Recording System (CORS). The effort consisted of four tasks: (1) the development of the system, (2) the experimentation and improvement of the system, (3) demonstrations of the working system, and (4) system documentation.

Overall, the prototype represents a workable and flexibly designed CORS system. For the most part, the hardware use for the prototype system is off-the-shelf. All of the following software was developed specifically for this effort: (1) setup software that the user specifies the cockpit configuration and identifies possible areas in which the pilot will look, (2) sensing software which integrates the 60 Hz data from the oculometer and head orientation sensing unit, (3) processing software which applies a spatiotemporal filter to the lookpoint data to determine fixation/dwell positions, (4) data recording output routines, and (5) playback software which allows the user to retrieve the data and analyze the data.

Several experiments were performed to verify the system accuracy and quantify system deficiencies. These tests resulted in recommendations for any future system that might be constructed.

17. Key Words (Suggested by Author(s))	18. Distribution Statement
Oculometer Pilot Scan Behavior Data Analysis and Recording	Unclassified-Unlimited Subject Category 52

19. Security Classif. (of this report)	20. Security Classif. (of this page)	21. No. of pages	22. Price
Unclassified	Unclassified	108	A06

NASA FORM 1626 OCT 86 For sale by the National Technical Information Service, Springfield, Virginia 22161-2171 NASA Langley, 1990

TABLE OF CONTENTS

LIST OF FIGURES

LIST OF TABLES

SUMMARY

The overall goal was the development of a Cockpit Ocular Recording System (CORS). This effort was broken into four tasks:

- Development of the system,
- Experimentation and improvement of the system,
- Demonstration of the working system, and
- Documentation.

The System

Overall the prototype represents a workable and flexibly designed CORS system. For the most part, the hardware used for the prototype system is off-the-shelf. The single exception is the flight data acquisition unit emulator (FDAU-M) which was designed, developed, and specially built. These hardware items include:

- A helmet mounted oculometer with a video recording feature,
- A Polhemus magnetic head position sensor,
- A personal computer with a parallel processing and a serial board added,
- A flight data acquisition unit emulator,
- A digital flight data recorder, and
- A time code generator is also used to provide timing signals for the video recording and purposes of validation.

All of the following software was developed specifically for this effort:

- The setup software permits the user to enter the cockpit configuration and to identify dwell regions for use by the CORS system, both in processing and playback.
- Three conceptually different functions are performed within the CORS computer during data collection. These are:
  - The sensing software which integrates the 60Hz data from the helmet mounted oculometer and the head sensing units,
  - The processing software which uses the newly formed position signals, applies a spatiotemporal filter and determines fixation/dwell position,
  - The results are sent out to the recording medium which may be the screen, a disk file, or the flight data recorder.
- The playback software allows the user to retrieve the recorded data and examine them in the context of the regions identified with the setup routine.

Experimentation and Design Improvement

Several experiments are reported which were carried out to test the system accuracy. These experiments show CORS is a viable concept and also highlight some areas where component improvements can be made. The areas of improvement identified include:

- The calibration routines which cannot be modified within the current oculometer. On occasion, the calibration routines preclude obtaining good results.
- The helmet and method of mounting the cameras and visor on the helmet. There is considerable movement of the helmet on the head and of these devices on the helmet.

These improvements can be made and several suggestions are provided in the conclusion section.

Demonstration of the Concept

A demonstration experiment was reported which showed modest accuracy of the system. Additionally, software was developed for the CORS computer to work in conjunction with the flight data acquisition unit emulator and the flight data recorder to write and retrieve data. This effort was successful.

INTRODUCTION

Eye scan data provide an important clue in understanding an operator's acquisition of information, visual workload, strategies, and the associated human performance. With the advent of non-intrusive eye movement recording devices, specifically the oculometer, the feasibility of obtaining such data has increased dramatically. The development of the technology has prompted a number of practical applications in which eye scan data can be used in a variety of ways: evaluating instrument design, as a substitute for manual manipulation, analysis of behavior for training, accident investigations, and a host of other applications.

The potential benefits of developing and using an oculometer for training, and especially accident investigation, resulted in the present project. This report describes the results of Analytics' efforts to develop a prototype Cockpit Ocular Recording System (CORS) for recording pilot eye scan data on a FAA approved Digital Flight Data Recorder. The work was performed under a Phase II Small Business Innovative Research contract sponsored by NASA Langley Research Center, contract NAS1-18473.

The work described in the present report is predicated on the results of the Phase I effort and it will be useful therefore to review, briefly, the issues and results of that study.

Background - Phase I

The objective of the Phase I effort was to investigate the concept of collecting and recording eye movement data on a digital flight data recorder (DFDR). In Phase I, a number of technical issues reviewed and analyzed.

- Is it technically feasible to collect eye movement data in a cockpit environment using an oculometer?
- Is the modern DFDR capable of recording processed oculometer data?
- How useful is pilot eye movement data in accident investigation and reconstructions?
- What other uses exist for pilot eye movement data gathered during actual flight operations?

These issues were investigated in detail and the results were presented in a report (Arnold, Deimler, & LaGrossa, 1986, Analytics Technical Report 2042). In summary the findings were:

- Components of commercially available oculometer systems exist that (with modification) seem appropriate for the intended application.
- Digital flight data recorders have the capacity to store processed output signals.

- Signal characteristics of the processed oculometer data can be made compatible with the input characteristics of the DFDR through a flight data acquisition unit.
- Processing software is currently available for the eye-data processing subsystem.
- System processing requirements can be met by a microcomputer.
- System control and data compression algorithms must be developed but appear to be of low risk.
- The information recorded on the DFDR should have extensive utility.

Based on these findings, the concept was judged to be feasible and warranted development, experimentation, and demonstration. The results of this effort are documented in this report.

Purpose and Goals of the Phase II Project

The overall goal of the Phase II project was to develop a prototype to demonstrate the feasibility of recording eye position data on a DFDR. The specific approach to meeting the overall objective is contained in the following steps:

- Build a fully functional prototype laboratory system.
- Conduct tests to determine system response characteristics.
- Refine and optimize system configuration.
- Design and conduct empirical studies to understand the technical and operational issues of collecting and recording eye movement information on a commercial flight data recorder in a "cockpit-like" environment.
- Demonstrate the utility of the system.
- Prepare system documentation of the prototype design.

The first five steps have been accomplished and are documented in this report.

Organization of the Report

The report is divided into a number of sections. These sections are organized such that each of the three tasks as defined in the statement of work is discussed in a separate section. General material is provided in other separate sections. The sections are:

- Section 2 provides an overview of CORS, including the functional architecture and a brief description of the software and hardware components.
- Section 3 contains a discussion of Task 1 which included developing and integrating the overall system.

- Section 4 presents the results of Task 2 which involved conducting experimental studies to test the initial system and providing suggestions for improvement of the algorithms.
- Section 5 is a discussion of some recommendations and suggestions for the future.
- Appendix A is a glossary providing definitions of the terms used.
- Appendix B contains the data from the initial experiment.
- Appendix C contains an up to date review of available eye scan technology.

OVERVIEW: SYSTEM CONFIGURATION

The purpose of this section is to provide an overview of the CORS system. Here we provide the basic architecture of CORS along with some comments about the function of the various pieces. Details on the algorithms, hardware, software, and functions will be found in the next section.

The primary function of CORS is the collection and recording of eye scan data, stated in terms of positions and instruments scanned in the cockpit. The use of CORS involves more than just data collection, however. One way to consider CORS is in terms of the sequence of activities in the overall application. There are three steps as shown in Figure 2-1:

- Step 1: Setup in which the user defines the various parameters, planes, surfaces and instrument locations, in a cockpit or in a workstation.
- Step 2: Runtime in which the actual data collection, processing, and recording of eye scan data is performed.
- Step 3: Playback with which the retrieval and analysis of the eye scan data is performed at some time after the actual data collection.

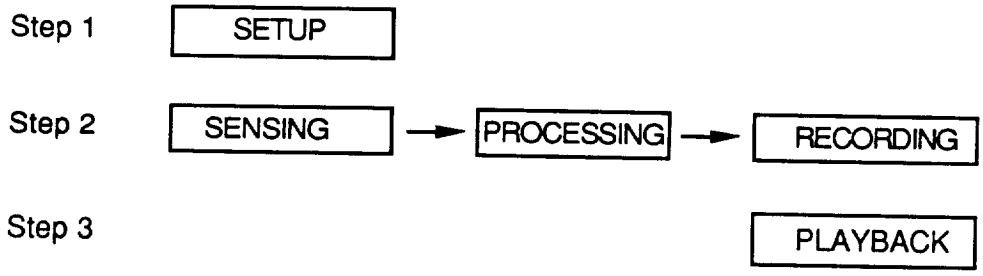

Figure 2-1. Simple diagram showing the relation of the steps and the operations performed within each step of CORS.

The setup step is required before any data collection can be performed. This involves giving the CORS system the necessary information about the location of instruments in the cockpit. Once this is accomplished, it is possible to perform the runtime step.

There are three main functions in Step 2, runtime, of CORS:

- Sensing,
- Processing, and
- Recording.

These three functions are shown across the top of Figure 2-2. The main portion of the figure shows the principal hardware components. The sensing is performed by the oculometer (Eye View Monitor) and the head tracker (Polhemus) sensing devices represented on the left side of the figure. These signals are passed into the CORS computer (represented in the middle of the figure) which performs the processing necessary to determine points of gaze and to convert these eye position signals into real world coordinates (fixations and dwells). The resulting fully processed signals, representing scan data, are then passed to the flight data acquisition unit (FDAU) emulator, shown on the right side of the figure, which transforms the data into the format necessary for the digital flight data recorder (DFDR).

Once the data have been written on the DFDR, the FDAU emulator is also used to perform the third step, that of retrieving the data and sending them back to the computer for playback, display, and analysis.

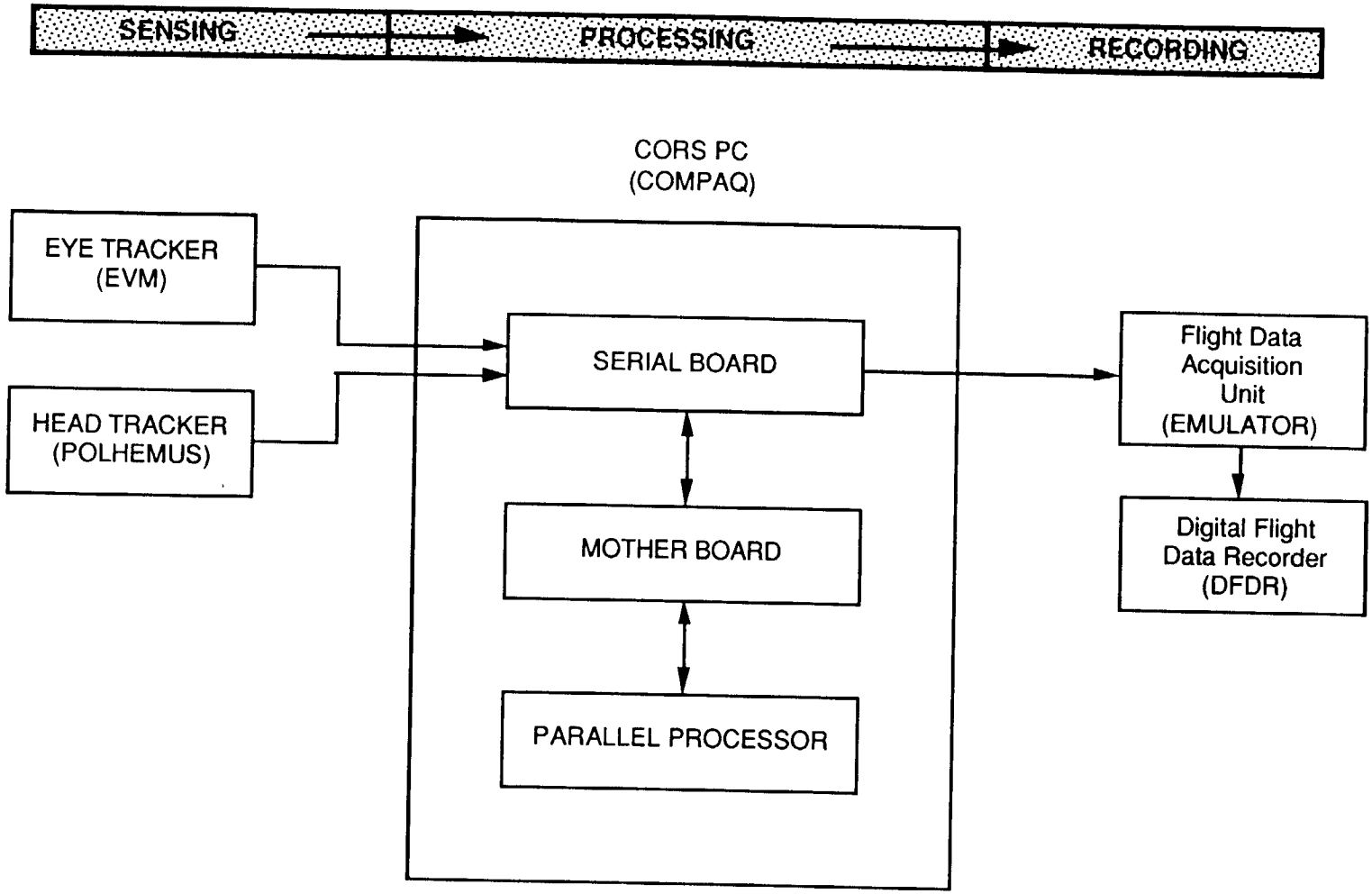

Figure 2-2. Relations between the sensing, processing, and recording portions of CORS runtime.

TASK 1: DEVELOP AND INTEGRATE SYSTEM

The overall goal in Task 1 is: To develop the prototype system. Equipment will be acquired and hardware will be integrated to perform according to the design goals and required capabilities. Software will be developed for subcomponent interfaces. Subcomponent processing and computational software will be developed for data processing, data compression, and system control. The result will be a functional CORS system that will be further refined through experimental studies conducted in Task 2.

Developing the prototype consisted of three separate activities. The first consisted of acquiring off-the-shelf hardware and assembling these components. Much of the Task 1 project effort was centered on the second activity which consisted of tying these components together functionally by developing software. These software components included the setup, runtime, and playback routines. The third activity consisted of developing interface hardware to convert signals between the CORS computer and the DFDR formats.

In the following sections, we discuss the various hardware and software components in terms of Figure 2-2, moving from left to right. After discussing the runtime prototype, we will then consider the system software, including the setup and playback steps illustrated in Figure 2-1.

The Sensing Components

OASIS Eye View Monitor (EVM) Description

The original OASIS (Zaklad, et al., 1986, Analytics Technical Report No. 1977) eye/voice testbed relied on an Applied Science Laboratories (ASL) Eye View Monitor System (EVM), Model 1996. The EVM is a remote-head oculometer. That is, an infrared (IR) source and a pupil camera are both located in a housing which is positioned, on a fixed base, several feet from the subject. On the basis of the IR image captured by the pupil camera, the EVM calculates pupil and corneal reflection centroids. In turn, based on these two centroids and their relationships as established during calibration, the EVM calculates a point in a plane which exists at a fixed distance from the subject's eye. Although the eye turns and points to different locations in the plane, the eye (and therefore also the head) is presumed to be in a relatively fixed location with reference to the plane. The EVM sends x and y eye position and pupil diameter, to the host computer (Masscomp) at a rate of 60Hz.

CORS Upgrade

In the original OASIS EVM, the subject's eye was required to be within a cubic inch volume throughout the calibration and test run. The remote system can be upgraded with mirror tracking to allow for a cubic foot of eye/head movement. However, the head movement restrictions required by a remote oculometer system cannot be tolerated in an operational setting. Accordingly, this alternative was discarded not only for the continued limitation on eye/head movement but also for the space limitations created by a cockpit for installing the associated devices. Instead, the EVM Model 1996 was retrofitted with a helmet mounted oculometer and a magnetic Polhemus head tracker was added to the system.

Helmet Mounted Oculometer (HMO)

In Phase II, the remote head oculometer was upgraded to an HMO. This was done to permit the full range of head motion which would normally be found in an operational setting such as a cockpit. The equipment is mounted on a large regulation motorcycle helmet. This insures that the full range of experimental subjects can use the helmet, but unfortunately this does not preclude the helmet from moving on the subject's head for people with smaller head sizes than the helmet.

Four components are mounted on the helmet: the pupil camera, the visor, the scene camera, and the illuminator. The pupil camera is mounted on the helmet directly above the subject's eye. The pupil camera can be moved laterally to center the pupil horizontally in the field of view (FOV) of the camera. The visor is used to center the pupil vertically in the FOV of the pupil camera. The pupil camera has a 20° FOV with reference to eye rotation and as long as the pupil stays within this FOV the system can function correctly. However, the normal eye movement range of the subject is up to approximately 30° (± 15°) of eye rotation and glances outside the FOV of the camera are lost and cannot be recorded. The pupil camera also has a small depth of focus which requires that the optical path length from the camera to the pupil be constrained to a relatively constant distance.

The visor is a transparent piece of plexiglass which has two films laminated onto the visor. The first film reflects infrared illumination and is used to monitor the pupil and cornea. The second film is a one way mirror allowing the subject to look through the film, while allowing the scene camera to view what the subject is looking at. Two telescoping arms attach the visor to the helmet and there is a joint at the helmet to allow the visor to be shifted away from the helmet. This allows the subject to remove the helmet easily without the visor being in the way. Additionally, the joints and the telescoping arms allow the visor to be positioned at the correct angle and the correct optical path length. Generally, this means that the visor is about four inches from the subject's pupil and at approximately a 45° angle. With repeated use the visor tends to slip during rotation of the head upwards or downwards and will gradually move out position during use.

A provision is available for video recording of the scene through the scene camera. This tape can be viewed at a later time to compare the results provided by the computer against the scene viewed by the test subject at the time of testing. The scene camera is mounted on an arm which is attached to the side of the helmet and then is positioned underneath the visor and directly in front of the subject's nose and mouth. The scene being viewed by the subject is reflected off the visor and onto the scene camera. Before the subject is calibrated, the scene camera must be positioned such that the internal representation of the oculometer calibration points agrees with the image being transmitted by the scene camera. This is crucial since after the subject's head is unrestrained the only external corroboration of the CORS results comes from the data collected from the scene camera. If the camera is not in the correct position the results shown on the scene camera monitor are inaccurate and misleading. Obtaining the correct location can be a difficult task since the arm that the scene camera is attached to has 7 joints. This is a complicated assembly with many degrees of freedom and, like the visor, continued use has loosened the joints and the assembly tends to move if there is any head motion. This made it very difficult to conduct a verification of the head motion algorithms.

The final component of the helmet assembly is the illuminator. The illuminator is mounted next to the pupil camera and contains an infrared LED. The infrared light is reflected from the visor into the subject's pupil. The level of illumination is controlled by the eye view monitor and is adjustable. The illuminator is generally nonintrusive and the subject notices only a slight drying of the eye.

Head Tracker System Description

The Polhemus Navigation Sciences' 3-Space Tracker, which was also added to the CORS system, provides the data necessary to map EVM coordinates into world coordinates as the subject moves about. The system consists of a magnetic source suspended above and behind the subject and a magnetic sensor attached to the top back of the subject's helmet. The tracker can provide Cartesian coordinates and orientation data in one of three forms: 1) orientation angles, 2) direction cosines, or 3) quaternions. For the sake of computational efficiency, the CORS algorithms are configured to use quaternions.

The 3-Space Tracking system utilizes low-frequency, magnetic field technology to determine the position and orientation of a sensor in relation to a source reference frame, providing six degrees of freedom for the movement measurement device. The source unit is mounted on a frame located behind the helmet and the sensor is mounted on the helmet; head motion is calculated from variations in the magnetic fields as measured by the sensor.

The primary operational range of the headtracker is a spacing of 4 to 28 inches between the source and the sensor. The headtracker can resolve a positional change of 0.03 inches and an angular change of 0.1°. The system has a positional static accuracy of 0.1 RMS inches and an

angular static accuracy of 0.5°. Like the EVM eye tracker, the headtracker outputs data at a rate of 60 times/second with a single source/sensor pair.

Algorithmic Integration of Helmet Mounted Oculometer and Head Tracker

As shown in Figure 3-1 calculating the point of gaze (POG) has become more complex than with a fixed oculometer head and additional sources of error have been introduced. In order to reduce overall system error, more care must be taken to assure that the head is initially placed in, and does not vary from, a known position during calibration. The subject's head position must now be adjusted until two LED's, one on the right and one on the left of the cockpit, each become visible through a pin hole frame. Once the subject has been boresighted into the correct head position the helmet is restrained to assure minimal variation from that position during calibration. After the helmet is restrained, the oculometer calibration proceeds normally, although adjustments to visor position may be required for optimal discrimination. Upon completion of calibration, the helmet is unrestrained. CORS software can now calculate a point of gaze in the calibration plane no matter what head position is taken by the subject. In the subsections which follow, the CORS eye/head data integration algorithms are described in detail. A description of the notation is followed by a discussion of calibration, the transformation of EVM coordinates to real world coordinates and extrapolation into the viewing plane.

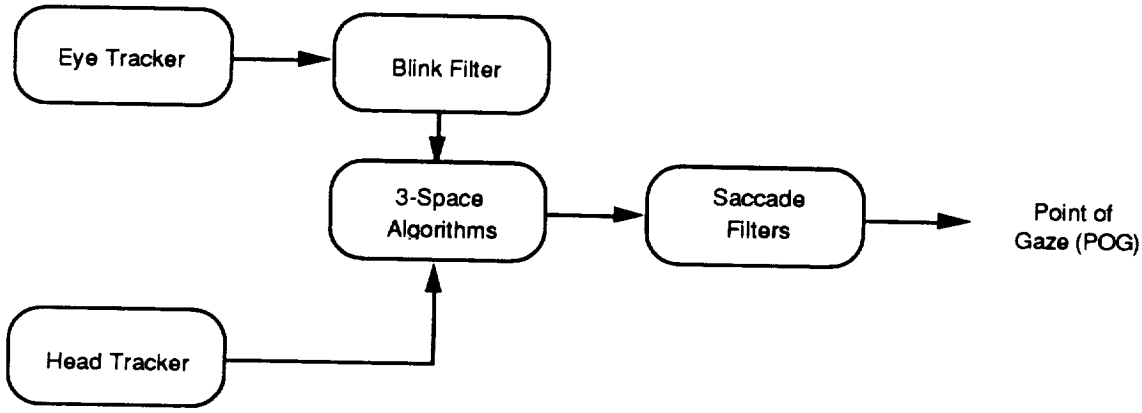

Figure 3-1. Illustration of the relations of the algorithms to calculate real world position.

Notation

A vector is defined as magnitude along a specified direction. Vectors will be written as:

R = <3,4,5>,

meaning vector R has a magnitude of 3 along the x-axis, magnitude 4 along the y-axis and a magnitude of 5 along the z-axis. Vector addition is defined as:

$$R + Q = <3,4,5> + <6,7,8> = <9,11,13> = RQ,$$

where the components of R and Q are added together to produce the resultant vector RQ. A vector can be used to describe the relationship between two points. A point is defined as:

$$P = (2,4,6),$$

and is used to define a specific location in Cartesian coordinates. The vector between two points is the difference of the Cartesian coordinates of the two points:

$$P = (2,4,6) \text{ and } T = (3,5,7) \quad PT = <3-2,5-4,7-6> = <1,1,1>.$$

The vector PT is constant under any orthogonal transformation of the coordinate axes. An orthogonal transformation is a rotation or translation of the coordinate axes of the system. In CORS vectors only undergo a rotational transformation. A rotational transformation is the movement of the coordinate axes through three angles, which are generally called euler angles. To apply a rotational transformation to a vector or a point, a 3 x 3 matrix must be used. A rotational transformation matrix is defined as:

$$\mathbf{R} = \begin{vmatrix} xx & xy & xz \\ yx & yy & yz \\ zx & zy & zz \end{vmatrix},$$

the values of components are calculated from a group of trigonometric identities. Vectors which have undergone an orthogonal transformation are designated with primes.

$$P' = \mathbf{R} * P$$

The combination of the vectors, rotational transform matrices and points are the crucial elements of the algorithms.

All coordinate systems are based on a point of reference or origin. Three different coordinate systems are used in the algorithms, they are world, EVM, and the display. The point of reference for world coordinates is the head tracker source. The origin for the EVM coordinates is defined as C5, the center point of the calibration pattern (see Figure 4-1, in the next section), although this is not the origin for EVM output coordinates. The origin for the display is the lower left corner.

Calibration Procedure with Respect to the Algorithms

The most important assumption made during the calibration procedure is that the vector connecting the eye to the center calibration point (C5) is parallel to the z axis of the real world coordinate system. What this means in practical terms is that the test subject's eye is at the same height as point C5 and is centered directly opposite to point C5. An additional requirement is that the calibration pattern is perpendicular to the z axis of the source. With respect to the algorithms the calibration procedure consists of forcing the subject to align with the solid geometry mathematics by adjustment to the boresight position and then actually calibrating the subject.

Three things must be accomplished during the calibration procedure, vectors *P* and *R* must be established and the boresight command must be given to the head tracker. As shown in Figure 3-2, *P* is the vector between the eye and the point in the EVM plane at which the eye is gazing. (With the head restrained, the EVM plane falls in the same world position as the display plane.) The value of *P* corresponds to the line from the eye directly to point C5 when the subject is in the boresight position. After the head and the eye have been correctly positioned and the head restrained, the boresight command is given to the head tracker. This command causes the head tracker to set azimuth, elevation, and roll to zero for the test subject's orientation during calibration. The remaining action is the calculation of *R*. As shown in the figure, this is the vector connecting the Sensor (B) and the center point of the calibration pattern (C5). *R* is calculated on the basis of the head tracker output with the helmet locked in the boresight position.

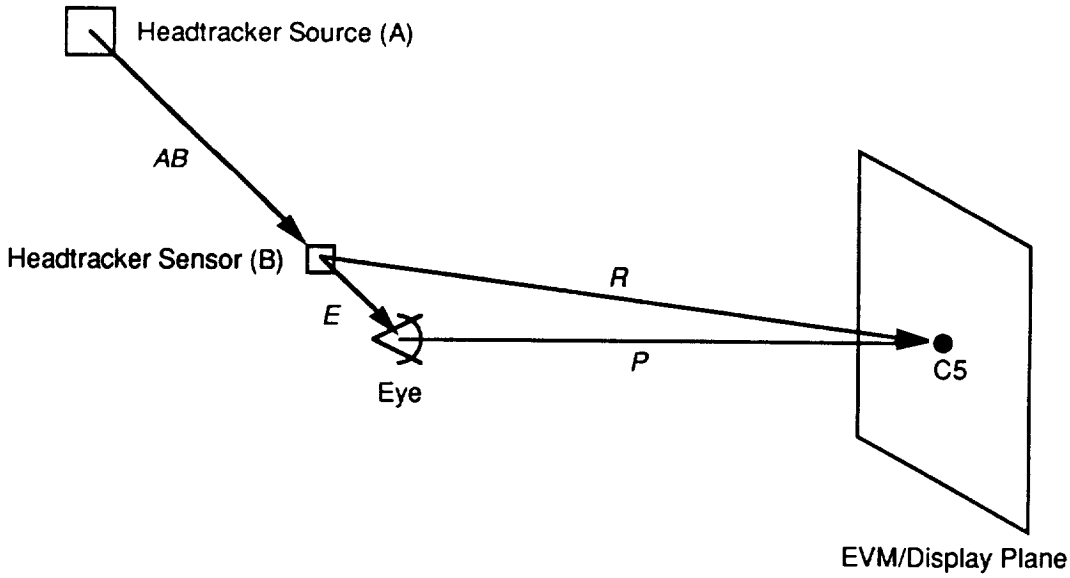

Figure 3-2. Calibration configuration vectors.

Transformation of EVM Coordinates to Real World Coordinates

The transformation of EVM coordinates to real world coordinates begins with the EVM output. Since the EVM cannot be configured to output 0,0 for the center point of the calibration pattern, the EVM output must be put into the proper form;

$$OC_x = (PEVM_x - C5_x) * factor_x \quad \text{and}$$

$$OC_y = (PEVM_y - C5_y) * factor_y.$$

Factor is the multiplier to transform EVM coordinates into world coordinates. *OC* is defined as $<OC_x, OC_y, 0>$, which must be added to *R* to produce *ROC*. These variables are identified in Figure 3.4. *ROC* must be orthogonally transformed using the quaternions provided by the head tracker. The correct orthogonal transform, **Q**, is defined as:

$$\mathbf{Q} = \begin{vmatrix} q0^2 + q1^2 - q2^2 - q3^2 & 2(q1q2 - q0q3) & 2(q1q3 + q0q2) \\ 2(q3q0 + q1q2) & q0^2 - q1^2 + q2^2 - q3^2 & 2(q2q3 - q1q0) \\ 2(q1q3 - q0q2) & 2(q1q0 + q3q2) & q0^2 - q1^2 - q2^2 + q3^2 \end{vmatrix}$$

Applying **Q** results in *ROC'*, the results of all of this can be combined to produce the real world coordinates of P.

$$POG_x = ROC'_x + B_x$$

$$POG_y = ROC'_y + B_y$$

$$POG_z = ROC'_z + B_z$$

Figure 3-3 presents the complete series of computations which are performed to obtain the screen location of the subject's point of regard. Oculometer, calibration, and headtracker data are integrated in this way 60 times a second, allowing interaction between eye position and simulated task to occur in real time.

Extrapolation of the Point of Gaze (POG) into the Panels

To extrapolate the POG into the plane of interest in the operational environment requires combining the POG with *P* and *OC* (see Figure 3-4). *P* is the vector from the subject's eye to point C5 and *OC* is the vector from point C5 to the EVM coordinate point in real world coordinates.

$$POC = P + OC$$

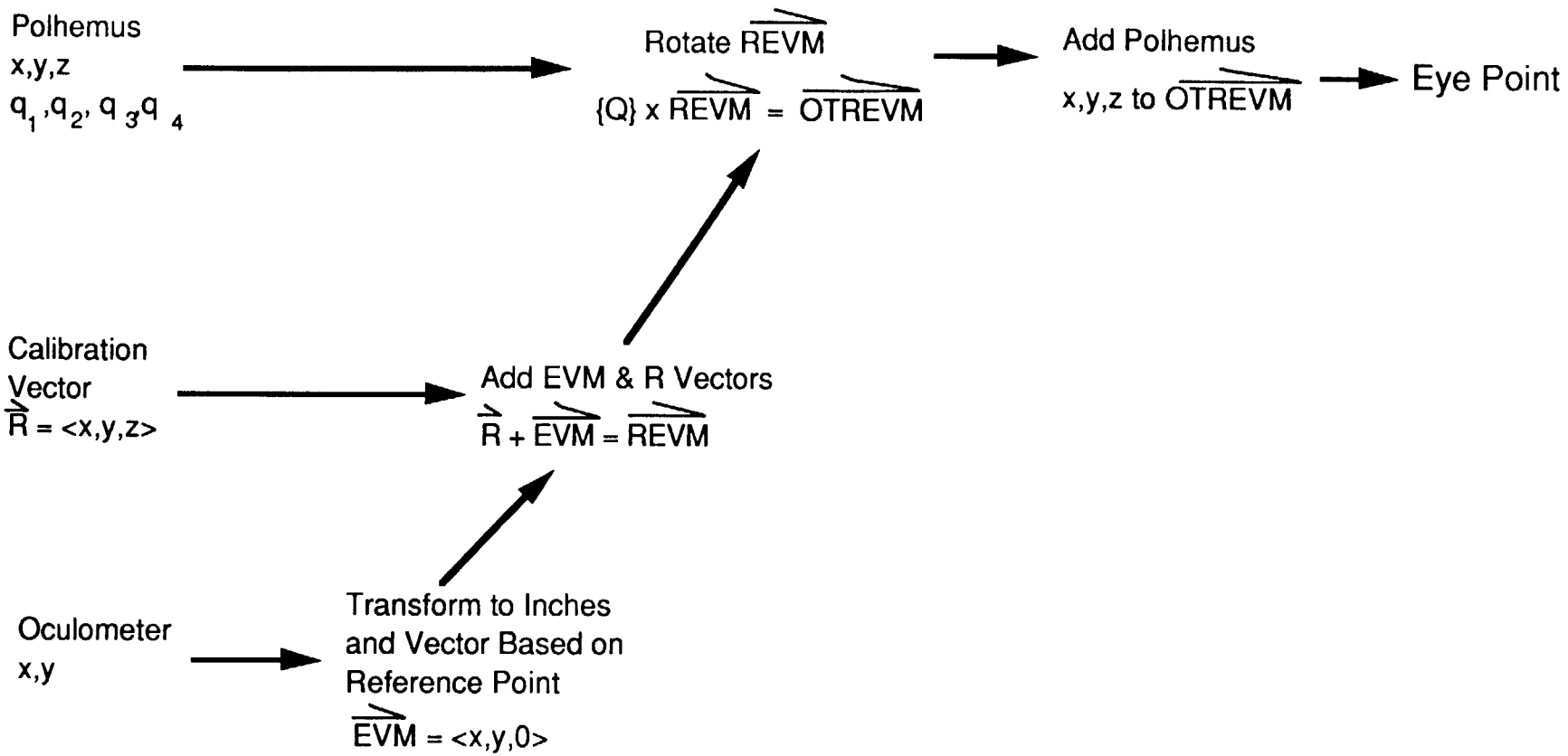

Figure 3-3. Oculometer and Polhemus calculations for integration.

POG and the *POC* represent the line of sight. The next step is to determine the closest plane to the POG. This is accomplished by calculating the distance between the POG and the centers of each of the planes. Once the closest plane has been established, the POG is extrapolated into that plane along the *POC*. The intersection point for that plane and *POC* is calculated. The coordinates of the intersection point are compared against the maximum and minimum values for each Cartesian coordinate. If the intersection point falls between all of the minimums and maximums then the real world point is transformed into coordinates corresponding to that plane. If the intersection point does not satisfy the minimum and maximum conditions, then it is necessary to check another plane. The next plane to be checked is determined from a search order that is part of the definition of the cockpit. The search order is a list of planes that should be checked if a POG is close to that plane, but does not actually intersect that plane. At the top of the search order are those planes which are the closest, since they are the most likely candidates to be the correct plane of intersection.

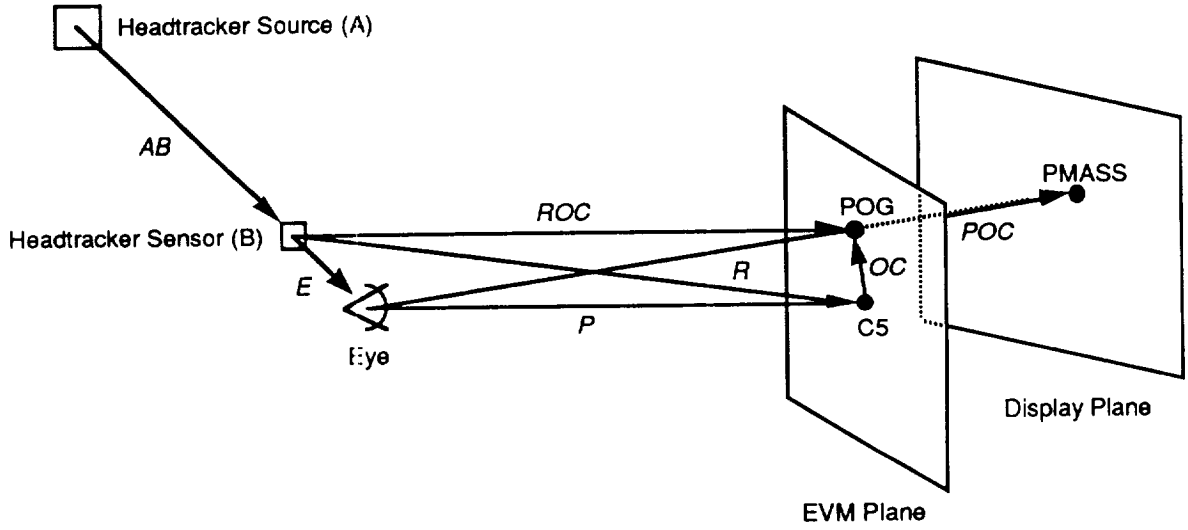

Figure 3-4. Operational configuration vectors.

After a correct intersection point has been found, it is transformed into the coordinates that define that plane. The region ID for that planar coordinate is determined and is the output from CORS along with the plane ID and the time that the fixation occurred. The only exception to this is if the region ID is an invalid region (invalid regions are those regions which are used to make an irregular plane a rectangle). Because an invalid region does not actually exist in the operational environment it is necessary to proceed in the search order to the next plane to determine the correct intersection. If the entire search order is exhausted without a valid intersection being found in any of the planes, then CORS outputs that a fixation occurred at an unknown location.

The Processing Components: The CORS Computer

The CORS computer includes the Model 60 Compaq 386/20 MHz with VGA monitor, disk drives, disk controller cards and various special purpose cards: serial communications, parallel processor card, and 80387/20 math co-processor. A complete list of components is as follows:

Compaq 386/20 MHz, Model 60MB Hard disk, 640K memory,

1 MB RAM Upgrade,

1.2 MB 5 1/4 inch floppy drive,

VGA monitor,

Vega VGA board,

80387/20 MHz Math Co-processor,

Applied Reasoning 386/16 MHz Parallel Board, 1 MB memory,

Applied Reasoning Developer Kit, and

DigiBoard Com/xi, 52K bps maximum.

Description and Purpose of Component Cards

The Compaq 386/20 MHz computer has 8 slots for cards. Five of these are full height 16 bit slots. Two are 8 bit slots, one half height and one full height. Finally, the remaining one is a 32 bit slot.

The Compaq motherboard acts as the controlling processor. It is responsible for memory transfers between the various cards.

The parallel processor board, which has a 80386 processor with a 16 MHz clock, resides in a 16 bit size slot. This board handles the algorithmic processing for CORS. It expects incoming decoded data to be placed in ring buffers setup in a megabyte of memory. The data are the 4 quaternions, 3 Cartesian coordinates, the x and y position of the eye, and pupil diameter. When a new fixation point has been established, it outputs these data to another ring buffer in its memory. These data consist of a number representing a region. The Compaq motherboard has the task of retrieving the data from the parallel processor board memory and sending the data to the FDAU-M.

The Com/xi serial communications card, which also resides in a 16 bit slot, is used to accept data from the head tracker and the EVM. It supports four serial ports, each capable of being configured separately. The Com/xi is a smart communications card with an onboard processor and it performs communications independently of the Compaq motherboard. One of its features is that it can be configured to ring buffer the input automatically. There is 8K of dual-port RAM available for buffering, half of which can be used for any given port.

In the case of communication with the EVM, the Com/xi ring buffers eight byte records every 1/60th of a second at 9600 bps. The motherboard fetches EVM records, one at a time, from the Com/xi and transfers them to one of the parallel processor board input ring buffers in the parallel board memory. Before transferring the data, the processor on the motherboard decodes and verifies that the check sum word indicates that transmission was error free.

In the case of communication with the head tracker, the Com/xi ring buffers 20 byte records every 1/60th of a second at 19.2K bps. The motherboard fetches head tracker records, one at a time, from the Com/xi and transfers them to one of the parallel processor boards input ring buffers in the parallel board memory. The motherboard processor first has to decode the head tracker records and reverse the bytes in the seven words before transferring the data.

The two remaining 16 bit slots are used for the hard disk, floppy disk, and two ports; one parallel and one serial. One of the 8 bit slots, the full height slot, is used for the Vega VGA board. Finally, the 32 bit slot is used for memory expansion to the maximum of 640K of memory addressable by the CORS computer which is more than sufficient for the CORS application.

Runtime Software

The architecture of the runtime software is shown in Figure 3-5. These functional pieces are shown in relation to the three main hardware components, serial board, motherboard, and parallel processor board. The algorithms discussed above for integration of the eye track and head track signals are shown under the parallel processor. The spatial and temporal filters used in processing will be discussed below.

The software was first developed on the Masscomp and then transported to the CORS computer. This provided the dual advantage of not only developing the required CORS software before the CORS computer was available but also provided a separate testbed for evaluating various components of the system. This testbed was utilized in some of the experiments described in Task 2. User manuals for the runtime software are provided in the Supplemental Volume, Part A.

CORS Input

The input to the CORS algorithms consists of Eye View Monitor (EVM) data and head tracker tracking data. Data from both of these sources are communicated sixty times a second. Theoretically, the data could be communicated in serial or parallel fashion. When reading

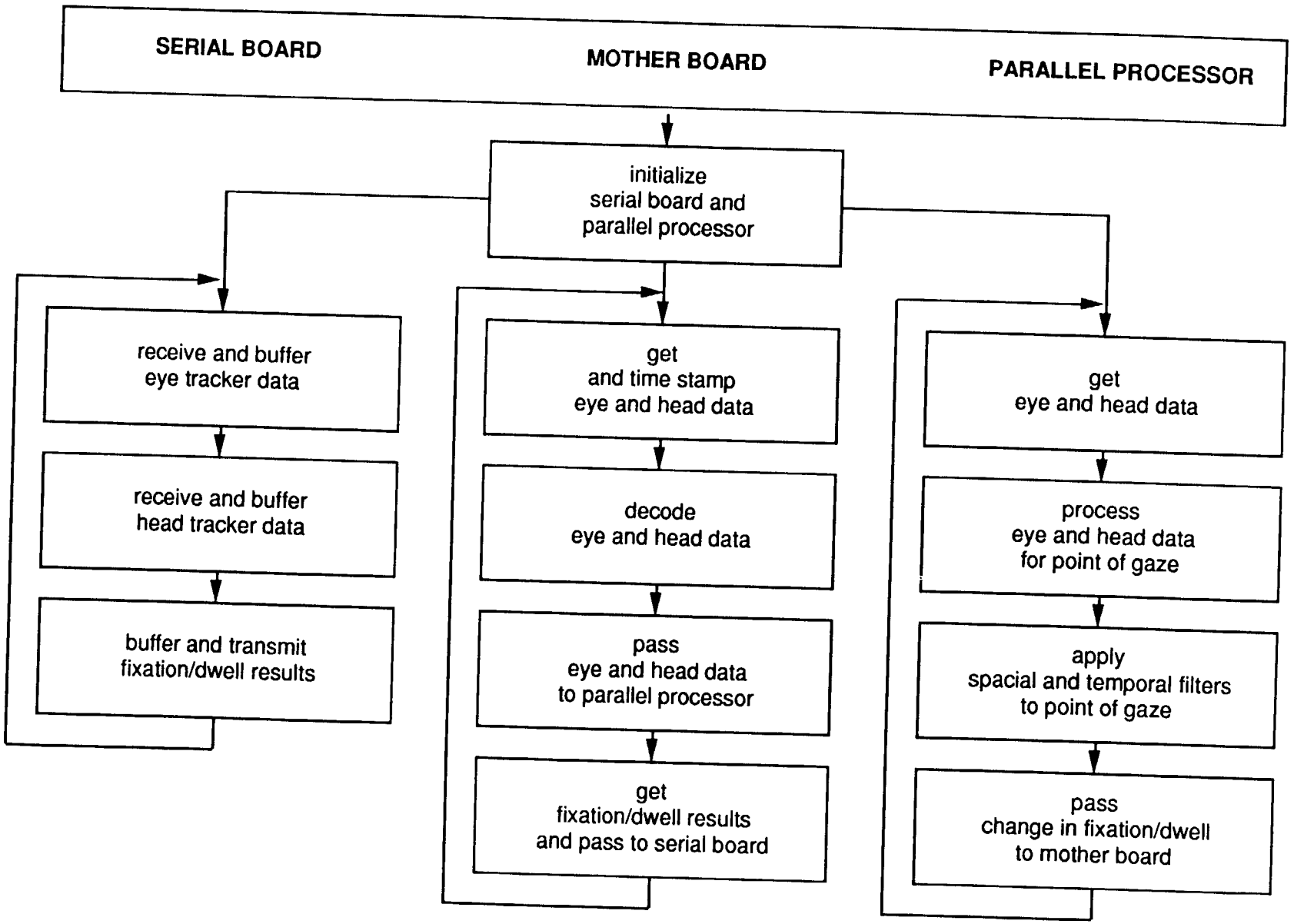

Figure 3-5. Architecture of the runtime software.

data using the motherboard processor, parallel communication is usually preferred because it is faster. Since we cannot afford to burden the motherboard processor, it is essential to have a card perform the communication independently of the motherboard processor. When the hardware for this project was selected, there was not a card available that performed parallel communication independently from the motherboard processor; however, a serial card of this type was available. This independence is preferable so that the motherboard processor is available to do other time critical tasks. Consequently, the EVM and head tracker communication is done serially in CORS.

Communication with the EVM is done at 9600 bps. The algorithms require three words (two bytes per word) of information from the EVM every 1/60th of a second: x position of the eye, y position of the eye, and pupil diameter. Every record that the EVM sends ends with two check sum bytes (check sum word). The check sum word is the sum of the vertical position, horizontal position, and the pupil diameter of the eye. The record transmitted by the EVM is eight bytes (3*2 + 2 = 8 bytes). The check sum bytes are used to identify the boundary between EVM records and to perform error checking on the transmission of the data. Because the words transmitted by the EVM are transmitted a byte at a time, the mother board must perform a decoding process on the EVM input data as well. In this case, the decoding is simple: All that is needed is to put the bytes back together again as words.

Communication with the head tracker is done at 19.2K bps. The algorithms require seven words (2 bytes per word) of information from the head tracker every 1/60th of a second: three Cartesian coordinates and four quaternions. Every record that the head tracker sends begins with three status bytes. The 17 byte record (7*2 + 3 = 17 bytes) is transmitted as 20 bytes because it is in binary encoded format. The most significant bit (MSB) for each seven data bytes are stored in overflow bytes. This encoding makes the MSB in every byte 0, except for the first byte in each record which has a 1 as the MSB. This is done to make it easy to determine the beginning of a head tracker record. In addition, the bytes in words are transmitted backwards, the low order byte followed by the high order byte. The serial board transfers the input data to the mother board memory, the mother board must decode the data before using them.

Explanation of Implementation of CORS Algorithms

The objective of the CORS algorithms is to identify those segments of the positional data (eye and head) which represent the operators points of attention. In order to do this, motion between dwells must be filtered out. In the CORS algorithms, this is accomplished by means of two main loops; the motion loop and the fixation loop. The motion loop is executed whenever the test subject is in transition between points of attention. The fixation loop is executed while the test subject is attending to a specific object in the visual field. Figure 3-6 demonstrates the flow of

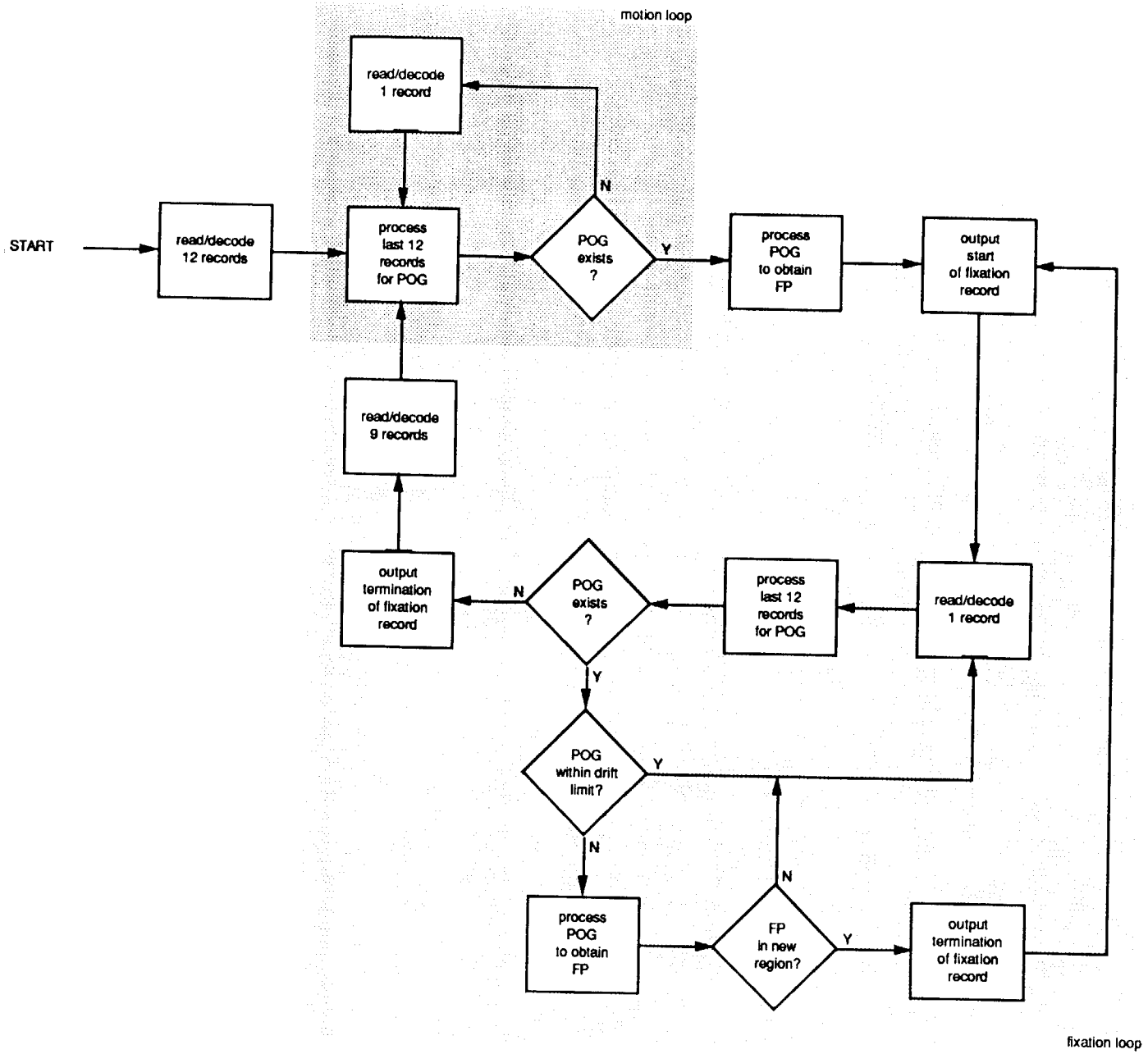

Figure 3-6. Flow chart of the point of gaze (POG)/fixation determination.

these two loops and their relationship. The lowest row of operations in the fixation loop represent that part of the loop which can be omitted when it is not necessary to determine when the test subject stops looking at an object or when the user is only interested in dwells and it is not necessary to identify gaps between successive fixations.

Spatiotemporal Filtering

The motion loop (Figure 3-6) is the processing loop done most often. This loop uses a new single time frame of information, a head tracker record and an Eye View Monitor (EVM) record, and checks to see if a point of gaze (POG) exists. Testing for a POG involves averaging the most recent twelve lookpoints in the EVM imaginary plane and comparing these twelve against the average. If ten or more points fall within a specified radial distance from the average, a POG has been established in the imaginary plane. Where the test subject is actually looking in the world has not yet been determined, only that the test subject is looking at some location and is not currently in transition. If a POG does not exist, the motion loop starts over again. If a POG does exist, the fixation loop takes control. The operation of the spatial component of the spatiotemporal filter is illustrated in Figure 3-7. In each panel, the circle represents the spatial portion of the filter while the dots indicate 12 successive lookpoints in the EVM plane. In the figure, only the leftmost panel shows data that qualify as a POG. For the other two, there is not a sufficient number of points within the circle to qualify. The radius used was 0.316 inches or 52 minutes of arc at the calibration plane.

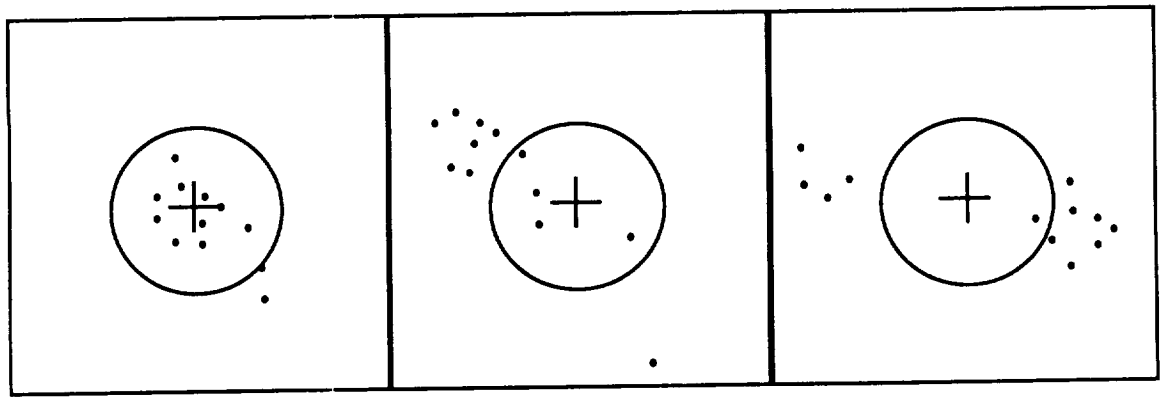

Figure 3-7. Illustration of the spatiotemporal filter operation. The radius is 52 minutes of arc.

A note on the filters. Twelve time frames correspond to 200 msec. There were several reasons for using 10 out of 12 successive frames as the temporal portion of the filter. First, there was some uncertainty with regard to the speed of the CORS computer and whether lookpoint

frames could be processed fast enough in real time. Second, the DFDR writes a 12 bit word in 15.675 msec. For prototype purposes, a number of extra words are written to the DFDR. The CORS computer provided four words and four are generated independently within the FDAU-M. These include time codes from the CORS computer, dwell regions, etc. as well as extra independent time codes generated within the FDAU-M. These FDAU-M generated codes are available to be used for validation. The total time necessary to write eight 12 bit words on the DFDR is 125 msec. Thus, during prototype development, the decision was made to ignore fixations of durations shorter than 200 msec e.g., 'glances' ~100 msec, to make it possible to write the additional information and also to avoid overloading the DFDR and the CORS computer. The time can be defended because it will capture a great percentage (>90%) of instrument 'reads' (Harris et al. 1986; Harris & Christhilf, 1980). Further, because the number of words written to the DFDR can be reduced from the prototype version, this does not represent a serious or permanent limitation for the CORS system.

The first thing done in the fixation loop is to process the POG in the imaginary plane to obtain a real world region in a plane of interest. This region is called the fixation. Using the fixation, a region identification number is looked up. Most of the time, the region ID number will correspond to an instrument in the plane. Alternately, when the dwell is a region in a plane that does not contain an instrument, it is called the background region.

If the previous loop was also a fixation loop, it is possible that the test subject was already looking at the current region. A test is made to check if the region ID number corresponds to a new region. If there is a new region, the region ID is output to the FDAU-M.

The next stage of the fixation loop is to read/decode records until a POG no longer exists. The purpose of this is to determine when the test subject stopped looking at a particular region or object. Once a POG no longer exists, a different POG cannot possibly exist for another ten frames including the lookpoint that caused the termination of the previous POG determination. Thus, nine records are read and decoded without any POG processing. Then, the most recent twelve frames are processed for a POG. If a POG exists, the fixation loop continues. If not, the motion loop takes control again.

The calculation of a fixation point in world coordinates from a POG in EVM coordinates is the heaviest single processing demand imposed by the CORS algorithms. For this reason, entry to the fixation loop occurs only when absolutely necessary. Additionally, the fixation loop can never be exited and reentered without first processing through at least nine lookpoints.

Determining POG Existence

To determine whether a POG exists or not, twelve time samples are used in the moving window. The twelve calculated points in the EVM imaginary plane are compared against their average. (The EVM imaginary plane is located at a fixed distance from the eye and is in a fixed position relative to the head.) If a predefined number of the lookpoints fall within a specified radial

distance from the centroid (average), existence of a POG is established. For prototype purposes, ten is being used as the initial value of the minimum number of lookpoints that must be in range. In the figures that follow, a time line demonstrates the twelve frame windowing process used to determine existence of a POG. The time line scaling is 60Hz because data are input from both the head tracker and the EVM sixty times a second. The black bars within a window represent valid, in range lookpoints. The white gaps within a window represent invalid, out of range lookpoints.

Temporal Processing: An Example

Figure 3-8 demonstrates a possible case that could exist before a fixation actually started. In this case, the twelve points were averaged and only nine of the twelve were found to be in range.

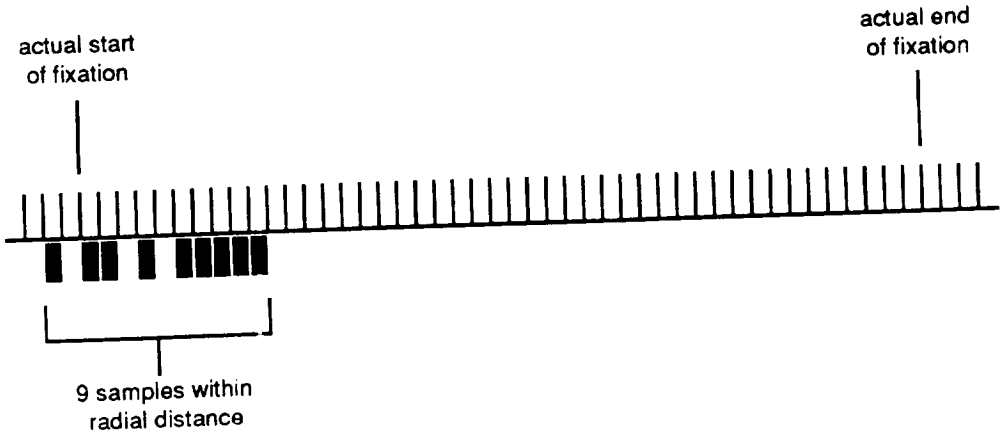

Figure 3-8. An early phase of fixation determination.

Figure 3-9 shows a possible outcome two lookpoint frames later than Figure 3-8. The two additional points changed the centroid (average) to that of ten out of the twelve points in range.

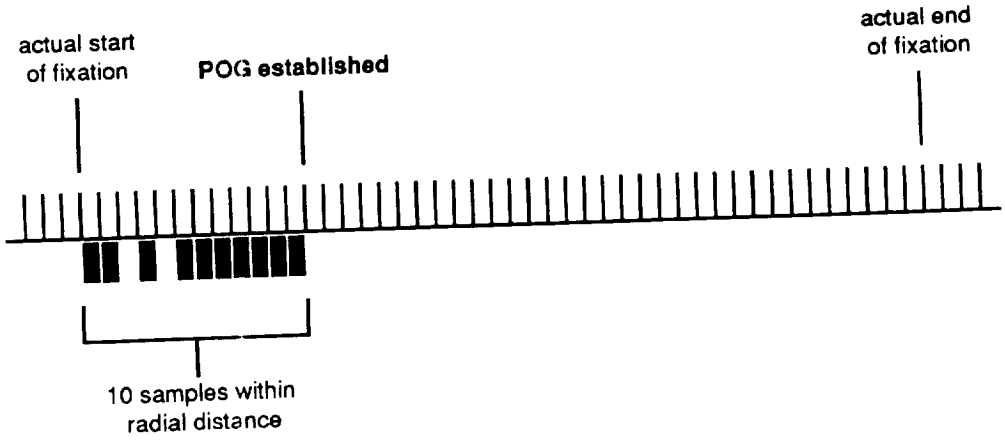

Figure 3-9. Fixation established.

Therefore, a POG exists and a fixation point can be calculated. Note that the POG is not established until twelve frames after the fixation actually started.

Figure 3-10 shows the POG processing continuing to take place. The test subject is still fixating in the same region. In this particular time window, ten out of the twelve points are in range. This is representative of the stage of the fixation loop that continually loops until a POG no longer exists.

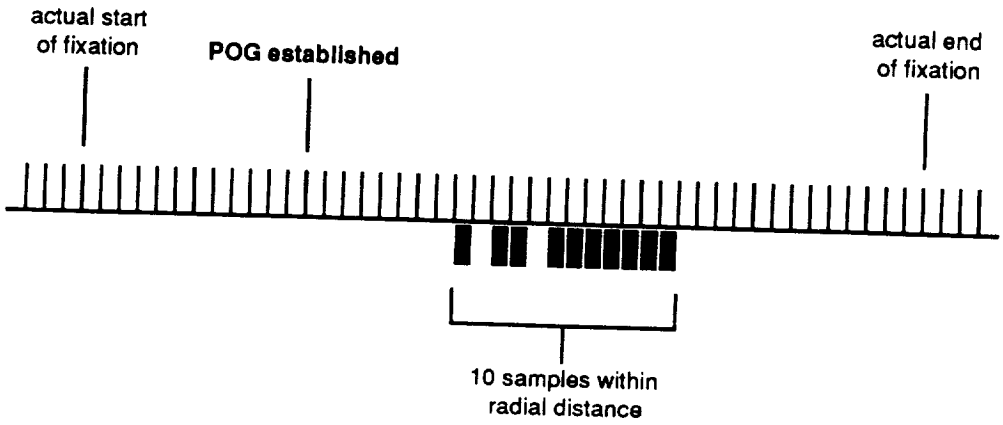

Figure 3-10. Analysis continued with fixation being maintained.

Figure 3-11 demonstrates the termination of a fixation. Only nine of the twelve points are in range. Note that it is not realized that the POG is lost until one or two frames after the fixation actually ended. In the fixation loop, this corresponds to the test for the termination of a POG being true. At this point, nine records can be read and decoded without doing any POG processing. A new POG cannot possibly exist until ten frames after the fixation terminated.

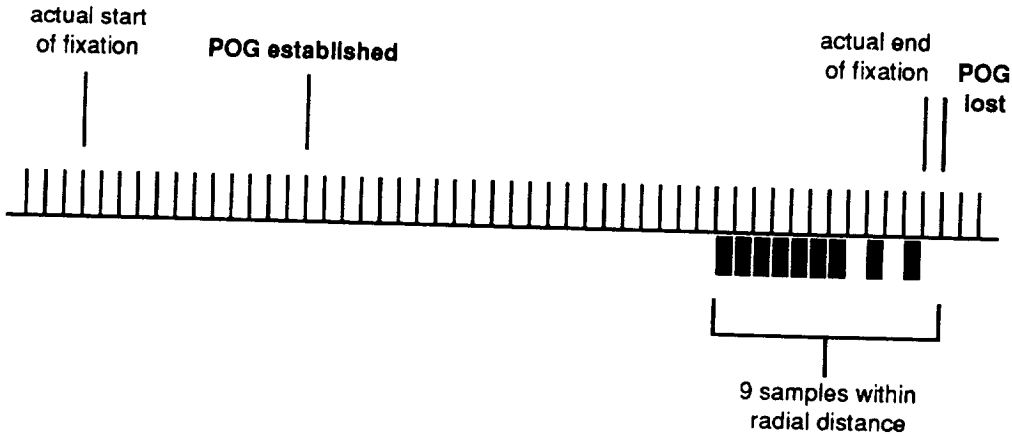

Figure 3-11. Fixation lost, point of gaze changed to another position.

CORS Output

The CORS computer can output data to one of three places: The DFDR, a disk file, or the screen. The data output for CORS consists of a series of six byte records, consisting of four fields as follows:

1. Panel (8 bits, 1 byte) — a number representing a panel area in the cockpit.
2. Region ID (8 bits, 1 byte) — a number representing a region in a panel in the cockpit.
3. Dwell Start Time (24 bits, 3 bytes) — the transmission time of the dwell.
4. Synchronization Time (8 bits, 1 byte) — the difference between data arrival and dwell start transmission.

There are three types of information encoded in the region ID field of data output record: start of fixation or dwell, location of fixation or dwell, and termination of fixation. When a start of record is transmitted, this field will contain either the ID number for an instrument region, or a null ID, indicating a dwell on a region outside of the system-defined cockpit instrument regions. When a termination-of record is transmitted, the region ID field will contain a value simply indicating termination, with no locational information encoded. Writing out termination of information doubles the required space on the DFDR and is necessary only if fixation durations are of interest in specific post analysis applications. In an operational system, only the two bytes represented by points 1 and 2 above are needed, specifically, the panel and region.

Relation of Fixations and Dwells: An Example

Fixations and POGs refer to a specific spatial point in different planes. A dwell consists of one or more fixations (with or without intervening gaps when no fixation is occurring) that occur within a specific region. An instrument may have several areas which contain information and require separate eye movements to these separate areas within the instrument boundaries (Harris et al., 1986). Accordingly, the data sent out of the CORS computer to the DFDR are coded in terms of points and regions.

Data compression occurs by converting the individual lookpoints to POGs and then into fixations and dwells. Yet another level of compression can be used for writing out data. Optionally, either the beginning and end of fixations can be written or the just beginning of dwells. Figure 3-12 illustrates the relation of fixations to the higher level code for dwells. In the figure, there are four dwells which would result in four records. By contrast, there are six fixations in the figure which would result in 12 fixation records.

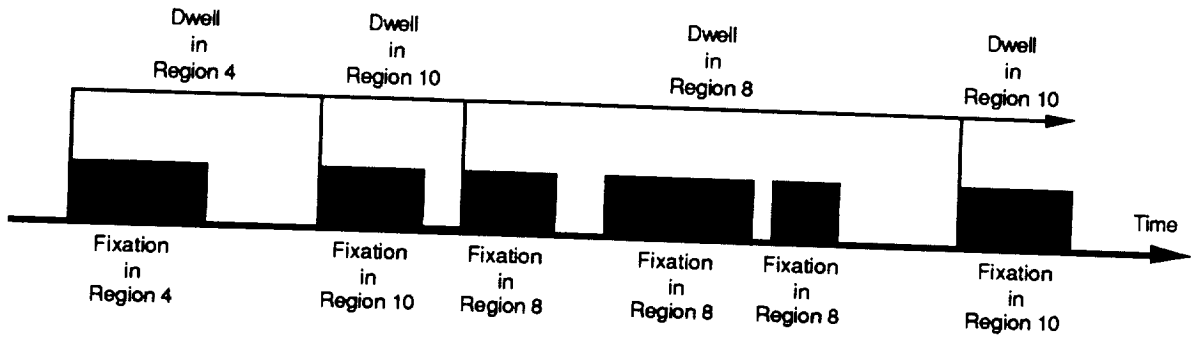

Figure 3-12. Illustration of the conversion of fixations into dwells.

Other Features of the Output

CORS also writes a start-of-run record and an end-of-run record. Byte 1 represents flag bits (11111110 for start and 11111111 for end) and is written to the FDAU-M. The remaining bytes in the record are used for the experiment name (in ASCII) written to both FDAU-M and file.

CORS data output records can be communicated in serial or parallel fashion to the FDAU-M. The FDAU-M tags records it receives with time code generator (TCG) time. This new record is then sent to the DFDR to be stored. Later, post-run analysis can be made by synchronizing the DFDR data with the scene camera recording through comparison of the synchronization time and the TCG time in each record.

It was possible that the TCG clock and the Compaq clock did not measure time at precisely the same rate. The purpose of the synchronization time in the record sent to the DFDR is to correlate (upon retrieval from the DFDR) time tagging in the FDAU-M with the time tagging of region ID records. As a result, no physical connection is required between the CORS computer and the TCG.

The Recording Components

The Flight Data Acquisition Unit Emulator (FDAU-M)

The objective of CORS is to write eye scan data on the DFDR. However, the CORS computer and the DFDR employ different communication standards. Accordingly, the FDAU-M was built to provide the necessary interface between the CORS computer and the DFDR. This unit took the place of a much more expensive, commercially available, FDAU. The FDAU-M provides (bidirectional) data conversion between the CORS computer and the DFDR standards.

Additionally as discussed above, a provision was made to incorporate a TCG signal to allow independent time records to be established on the DFDR. The TCG signal was a validation

to be compared against the time codes provided by the CORS computer. Further, the TCG signals were recorded on the real-time video made through the scene camera.

The high level design and interrelations are shown in Figure 3-13. This figure shows the detailed functional design of the FDAU-M represented by the dotted lines with the CORS computer, the sensor components, the TCG, and the DFDR also depicted, outside the dotted lines.

Theory of Operation

The theory behind the FDAU-M operation is simple; it is a pure hardware/firmware device that performs data format conversion.

Data enter the FDAU-M using RS-232 data format via a universal synchronous/ asynchronous receiver/transmitter (USART). The USART (Intel 8251A) is designed to handle bidirectional communication with the CORS computer. The CORS computer data are input into the FDAU-M in the form of 8 bit words at any (selectable) RS-232 baud rate. TCG data are input into a buffer in parallel format. The correct bits are masked out and arranged. CORS computer data are grouped in bursts that represent dwells. These dwells are then time tagged. All data are then converted into 12 bit format, maintaining data integrity. The newly formed 12 bit words are placed onto a first-in, first-out (FIFO) 12 word buffer. The data are then shifted out of the buffer serially one bit at a time in Harvard biphase format at 768 bps. Sixty-four 12 bit words constitute a subframe. The first word of each subframe is a special identifier (stored in ROM). There are four subframes in each frame. After the first subframe marker, the frame counter word is added. There is also a null word when the data buffer is empty. All words contain special identifier bits used for decoding during playback.

DFDR Playback

The FDAU-M also retrieves data from the DFDR and returns them back to the computer. This is done by using a read amplifier board and a bit synchronization card from a read data unit. The data are retrieved from the DFDR via six unconditioned analog signals recovered from the playback magnetic head. The read amplifier board and bit synchronization cards are then used to filter and condition the signal to a digital (NRZ-L) format and a corresponding clock. These cards provide considerable latitude in allowing the designer to control signal gain in various places which allow noise to be controlled. Also, the output signal choice can be made which increases usability under various conditions. These boards also provide provisions for track selection which is useful during the playback phase. Both cards were furnished by Fairchild Weston. The data are then recovered from the cards in NRZ-L data format. The FDAU-M then converts the data to selectable RS-232 format and outputs the data to the computer.

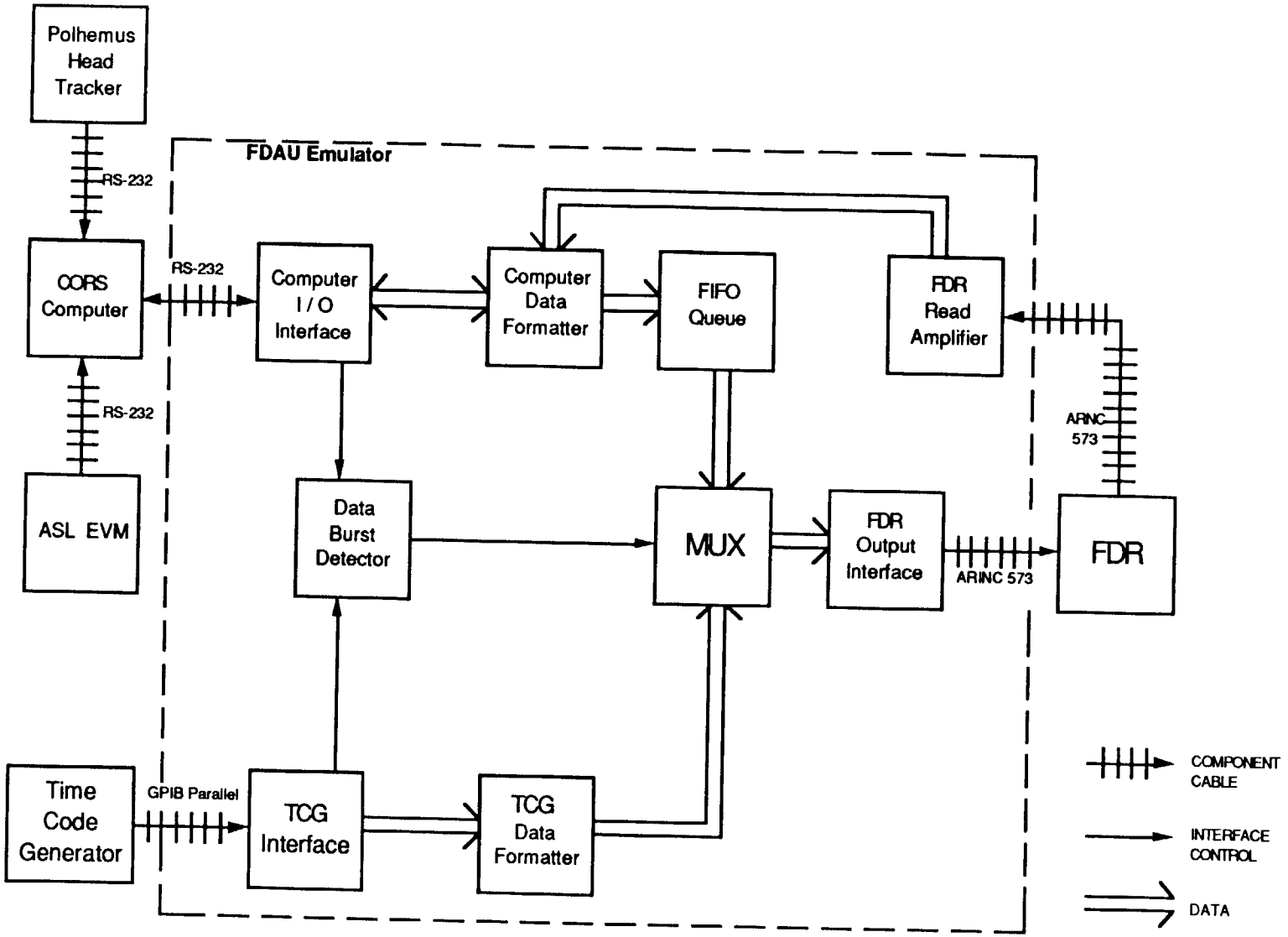

Figure 3-13. Relations between the FDAU-M and other components of CORS.

The Digital Flight Data Recorder

The DFDR used for the CORS system is Model F800 from Fairchild Weston. It is a six track continuous loop magnetic tape device that can withstand 20,000 lbs of force per axis, impacts of 1000 g's per axis for 5 msec and can withstand temperatures of 1100° Celsius. It records at a tape speed of 0.36 inches per second and can record continuously for 25 hours (four hours and ten minutes per track without overwrite). The DFDR accepts ARINC 542 or 573/717 electrical standards. The ARINC 573/717 standard was selected for CORS. It uses 768 bps, Harvard biphase, 12 bit word synchronous serial protocol.

The DFDR can be configured, through FDAU-M control, to operate is such a manner that data can be read three seconds after they are recorded or the data can be read off at a later time as would be done in ground playback of normal DFDR data.

The Time Code Generator (TCG)

The TCG used is model number 9100A built by Datum, Inc. The TCG is a setable time keeping device. The device is set by entering the desired time using a thumbwheel switch/momentary switch combination. By pressing the start button the TCG starts keeping time, as shown on the front LED display. The TCG maintains the Julian day, the military hour, minute, and second. The TCG also maintains time up to 1 ms, but this is not shown on the front display.

Standard outputs include IRIG B (resolution (1 sec.) and 180 degree pulse trains ranging from 1 PPS to 1K PPS). The optional outputs that were used include a 50 bit positive logic parallel signal (resolution, 1 ms) and a video time insertion signal compatible with NTSC signal standards. This mode was used to put a time code on the recording of the scene camera output.

The Cockpit

A 'wire' frame was constructed to serve as a simulated cockpit. Figure 3-14 illustrates a schematic view of the cockpit; Figure 3-15 shows a perspective view, and figure 3-16 shows an unfolded view.. The design goal was to attempt to replicate the panel positions a commercial cockpit as cost effectively as possible while maintaining single pilot occupancy.

The frame was constructed of PCV (1.5" diameter) and serves as support for plastic panels which were attached by means of tie wraps. This approach allows for the rapid replacement/substitution of panels that may be required for different experimental purposes. These panels provided a flat surface upon which instrument facsimiles could be placed. The flat

surface is of considerable convenience in establishing the dwell regions (setup) for CORS. The frame also supports the receiver of the head tracker.

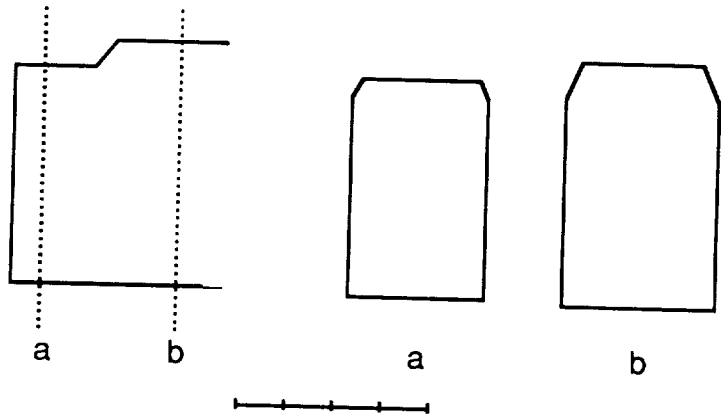

Figure 3-14. Side and cross section views of the cockpit. The left panel is a side view, nose to the left. The other two panels represent cross sections taken at the points indicated in the left panel. *a* corresponds to the lookpoint, *b* corresponds to the eyepoint. (The scale indicates feet.)

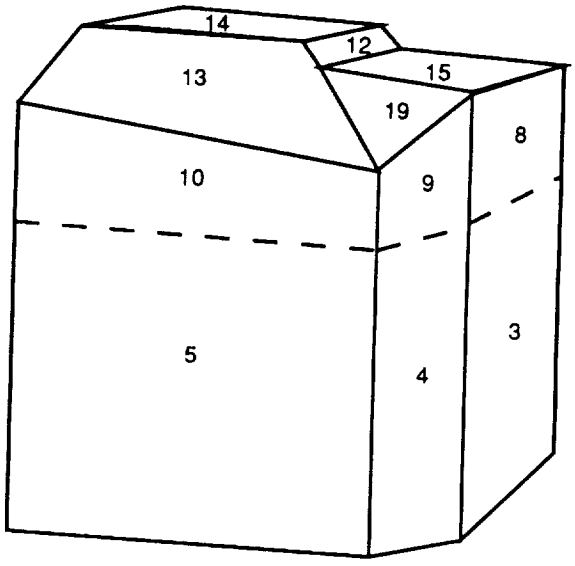

Figure 3-15. A solid perspective view of the cockpit, nose to the right. The panels are numbered to correspond with Figure 3-16, where 3 and 8 represent the front (visible), 16 the back (to the left out of view), and 17 represents the floor .

Boresights were installed to provide references points to establish the head in a known position during calibration. A boresight consisted of a light mounted behind two pinholes about nine inches apart. In order to see the light, the eye has to be positioned directly in line with the pinholes. Two such boresights, located approximately 40° on either side of the midline provided fairly precise positioning of the eye (and head).

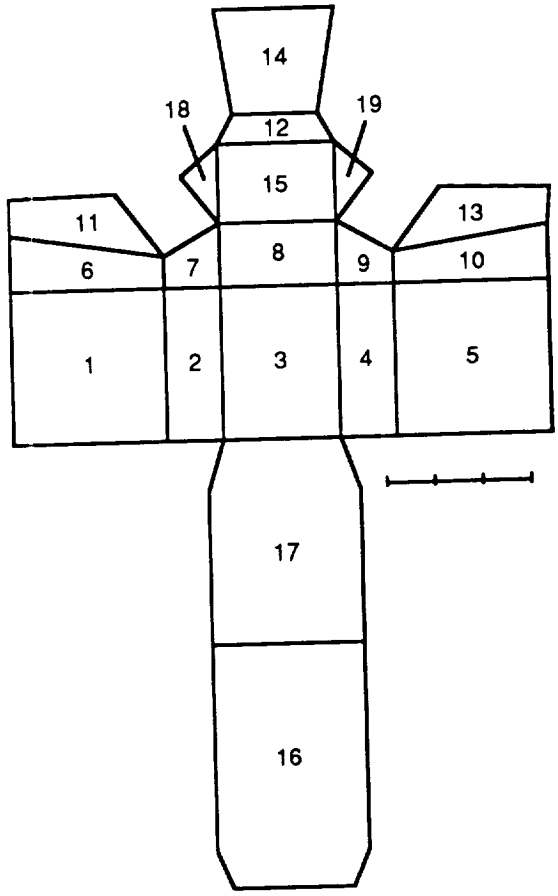

Figure 3-16. Cockpit panel configuration. In this unfolded view, the test subject would be seated on area 17, panel 8 would be at eye level in front, and 16 would be behind him. Panel numbering is the same as in Figure 3-15. (Scale is in feet.)

System Software

Three system software products were developed. The first and second of these were designed to handle setup which involves identification of cockpit regions and planes for the CORS system. The data provided by these programs are then used by the CORS computer during runtime processing. The third piece of software was developed for playback and analysis of the CORS data once they have been recorded.

The Planes Designer Program

The planes designer program permits the user to enter coordinates of the planes and regions within planes so that conversion to dwell regions is possible. For example, the planes in the cockpit illustrated in Figure 3-16 are entered to permit CORS to relate the integrated eye-head position data into panel areas. A few of the highlights of the program are described below. (The user manual is provided in the supplemental volume, complete with an example of a plane being entered.)

- All panels used in the planes program must be represented within a rectangle.
- All panels must be located in a global positioning system. This positioning system is designated as world coordinates and is based on the head tracker sensor units. The head tracker source origin is considered the origin of the CORS world coordinate system. All planes must be referenced with regard to the head tracker source unit.
- The normal for a plane is the vector that originates from the center of the plane and is perpendicular with respect to the plane. This vector must be given in world coordinates and normalized to a unit vector.
- The planes designer program needs the minimum and maximum X, Y, and Z values that occur in each plane.

The Setup Program

A cockpit is composed of a number of planes or panels. The planes designer program discussed above is used to create a separate file for each plane in the cockpit. The execution of both runtime and playback programs require that the user specify a setup file. This file is used to determine which plane files to read and to establish the search priority for each. The setup program provides this cockpit specification for CORS as an integrated set of planes.

The program asks the user for the number of planes in the cockpit, the names of the panel files which represents each panel, and then the search order for each panel. An ascii text file is written out by the program in the following form:

number of planes
panel name 1
.
.
.
panel name n

search order 1

.

.

.

search order n

Replay Software: Function and Application

The CORS replay program allows the user to examine, via a graphical interface, the files dumped from the CORS runtime or FDAU-M reader programs. Various menus are presented to the user at start-up and during replay in order to control the presentation. Based on the setup or cockpit file referenced, the program reads in the panel files and transforms the cell matrix data of each into line drawing specifications for that panel and the regions which it contains. During a replay run, the program presents one of two display formats to the user. In the first format the

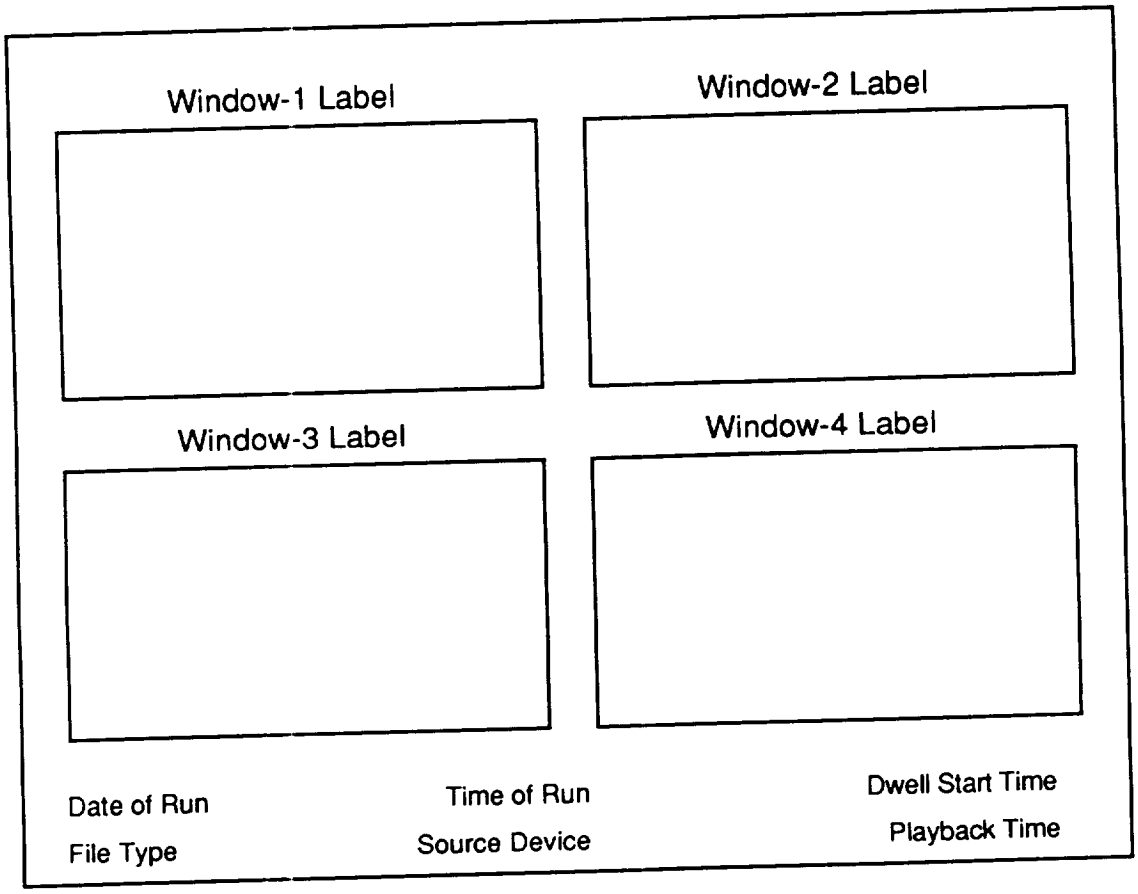

Figure 3-17. Illustration of generic playback window.

display presents a single graphical window, containing the outline drawing of a single panel and its regions, with text material below. In the second, shown in Figure 3-17, the graphical area is broken into four windows with the same text material below. Each of these windows may contain the outline of a single panel and its regions. In both formats, the graphical windows are labeled with the name of the panel files used to construct the images. The text material displayed below the graphical window(s) is the same regardless of the display format.

In the bottom left of the display, four items are shown which remain unchanged throughout a replay run. These include the date and time of the original run, the device utilized (head tracker or helmet mounted oculometer) and the type of file (fixation or dwell, see page 26) upon which the replay is based. In the bottom right of the display two times are shown. The lower of these times represents the current (replay) time while the upper indicates the start time for the fixation or dwell currently presented in the graphical portion of the display. Figure 3-18 presents the appearance of the display during a replay run. The current time indicates that the user is

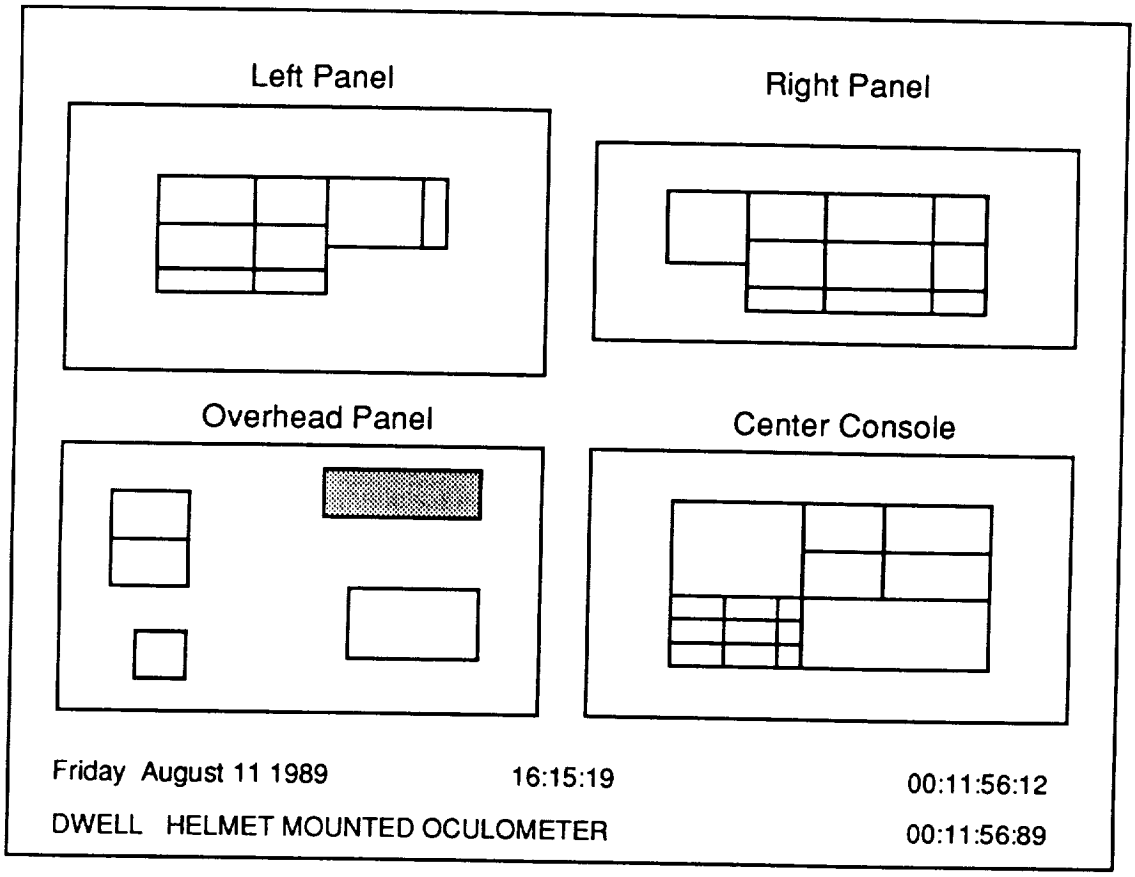

Figure 3-18. Illustration of an example in the display windows.

eleven minutes, fifty-six and eighty-nine one-hundredth seconds into the replay. The dwell start time indicates that the shaded region shown in window three represents a dwell which began seventy-seven one-hundredths of a second before the current time shown.

As a replay progresses, successive fixations or dwells are indicated by changing the color of regions' outline and fill. If replay encounters a fixation or dwell in a panel not currently displayed, a currently displayed panel is erased and the required panel drawn in its place. In the four-panel display format, window 4 is the window used for this type of display update. Windows 1 through 3 retain their original panel assignments throughout the run.

Replay can be paced by the user or by the clock. In the case of user pacing, the program steps from one fixation or dwell to the next, in sequence, in response to keyboard input. In the case of clock or automatic pacing, the program attempts to run in real time. That is, if a dwell was three seconds in length at run time, it should be three seconds in length during replay. However, the drawing speed of the Compaq is such that delays are inserted whenever a drawing operation is required. No attempt is made by the program to compensate for these delays. The program is running real time when the playback time readout is seen to be advancing.

The replay program assumes that the setup file is a local file named SCREENS.DAT and that the replay file is in a local file named TIME.DAT. In order for the replay to execute properly, it is necessary to provide as local files those panel definition files used during the original run. When executed, the replay program immediately presents the user with an assignment menu. A list of all the planes specified for the run is displayed with a space alongside each for the entry of a window number. Function, delete, and up and down arrow keys are used to specify window assignments. If an assignment is made for window 1 and no other, the single window mode is automatically selected. If more than one assignment is made, or if a single window other than window 1 is assigned, the four window mode is selected.

The function key F5 is used to indicate that the window assignment is complete. While the program loads the required panel definition files, a version message is displayed. When the loading operation is complete, the windows are drawn and a start-up menu is displayed. At this point the user may choose either automatic (clock) pacing or stepped (key driven) pacing. Once replay has begun, it will proceed until the end of the replay file is encountered or until the user depresses the escape key. The escape key brings up the control menu, a list of functions with corresponding function keys, giving access to the following operations:

- Change replay pacing - if replay is currently being stepped manually the Auto Step alternative will be shown; if replay is currently clock driven, the Manual Step alternative will be shown.
- Select start time - fast forward to specific point in replay file (not currently implemented).
- Reassign windows - program presents same window assignment menu used at start of program.

- Select event type - set program to replay dwells, the default, or fixations (fixation replay is not currently implemented).
- View algorithm parameters - displays values of all CORS algorithm parameters (number of points for fixation window, maximum number of invalid points in window, square of radius, number of frames skipped, drift limit) as they were set during run being replayed.
- Exit program - terminate replay run.

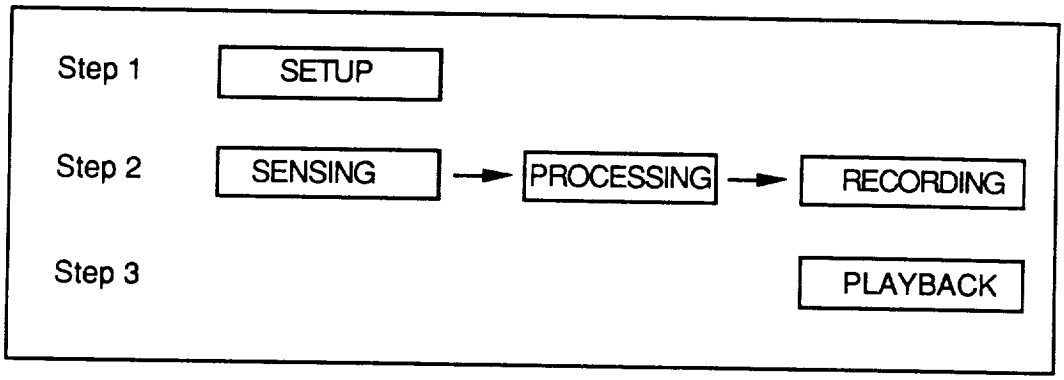

Figure 3-19. Simple diagram showing the relation of the steps and the operations performed within each step of CORS.

System Summary

Overall the prototype represents a workable and flexibly designed CORS system. For the most part, the hardware used for the prototype system is off-the-shelf. The single exception is the FDAU-M which was designed, developed, and built specifically for this effort. All of the hardware items are employed in Step 2 of Figure 3-19 and include:

- The sensing components
  - A helmet mounted oculometer (HMO) with a video recording feature and
  - A head tracker magnetic head position sensor.
- The processing component
  - A personal computer with a parallel processing and a serial board added.
- The recording components
  - A specially built flight data acquisition unit emulator (FDAU-M) and
  - A commercial aircraft digital flight data recorder (DFDR).
- Miscellaneous items
  - A simulated cockpit and

- A time code generator used to provide timing signals for the video recording and purposes of validation.

All of the software was developed specifically for this effort. This includes the following pieces:

- The setup software which permits the user to enter the cockpit configuration and to identify dwell regions for use by the CORS system, during both processing and playback.
- Three conceptually different functions are performed within the CORS computer during data collection. The software functions are:
  - The sensing software which integrates the 60Hz data from the helmet mounted oculometer and the head sensing units.
  - The processing software which uses the newly formed position signals, applies a spatiotemporal filter and determines fixation/dwell position.
  - The recording software encodes the results and transmits them to the recording medium (screen, disk file, or flight data recorder).
- The playback software which allows the user to retrieve the recorded data and examine them in the context of the cockpit regions identified with the setup routine.

TASK 2: CONDUCT EXPERIMENTAL STUDIES

The overall goal in Task 2 is: To conduct experimental studies in the CORS laboratory. Experiments will be performed initially to verify system operability and to provide design feedback. Later experiments will be performed to refine system parameters, develop optimal techniques, and to verify the utility of CORS in reconstructing pilot eye movement history.

The Testbed

Because of the graphics available on the Masscomp computer, some of the experimental work was done using the Masscomp as a testbed. In these cases, the EVM and the head tracker were connected to the input ports of the Masscomp instead of the CORS computer. The helmet mounted EVM was used in all cases. The CORS software and algorithms were utilized whether the work was done on the Masscomp or the CORS computer.

It is also of importance to note that the helmet was always restrained during the Masscomp testbed experiments, effectively eliminating the head tracker sensor inputs from consideration.

Sources of Error and Characterization of Accuracy

Generally, the error for most mechanical systems is directly related to how accurately the system can perform its intended function. CORS has three major components that contribute to the overall system error. Those components are the hardware, the data processing algorithms and the integration scheme of the system. Hardware refers to the oculometer, the head tracker and the computer which integrates the data. The data processing algorithms are the methodology used in the EVM to arrive at a location on the scene camera display where the eye is pointing. Additionally, data processing algorithms are used by the head tracker to calculate the translational and rotational movement of the head tracker sensor which is attached to the back of the oculometer helmet. The integration of the system components is the combining of the output of the helmet mounted oculometer and the head tracker to produce the POG. It is important to remember that the POG must be processed to determine a dwell, which is the combination of a series of lookpoints. An error value can be associated with a POG by evaluating the components described above, but the error associated with the dwell is a combination of the error from the POGs plus an evaluation of the effects of human physiology and saccadic movements which make up a POG.

Hardware and Software Components

There are three hardware components to the CORS system. The first is the oculometer. There are two sources of hardware error in the oculometer, the pupil camera and the scene camera. The resolution of the pupil camera is 103 pixels/inch leading to a positional error ± 0.009 inches with a field of view (FOV) of 11.5°. The resolution of the scene camera is 62 pixels/inch leading to a positional error in the output data of ± 0.016 inches and a FOV of 48°. The second hardware component is the head tracker which has a positional accuracy of 0.1 inch RMS and an angular accuracy of 0.5 degrees RMS. The third hardware component is the Masscomp display; the output data are displayed on the Masscomp display which has a resolution of 59 pixels/inch leading to a positional error of ± 0.017 inches.

Ideally, the overall system accuracy should be a combination of the hardware sources of error, but the software/algorithmic contribution significantly exceeds the hardware contribution. The data processing algorithms used to transform raw data into the desired output can induce an error into the final result. The head tracker integrates the error associated with its algorithms and the resolution of the system to produce a summary system accuracy which was discussed above. Unfortunately, there is no similar value available for the oculometer system. The major data processing algorithms used in the oculometer are those used to discriminate the pupil and cornea, calculate the pupil and corneal centroid, and to fit these data onto points taken during calibration. Based on experience in using this oculometer, the relationship between these algorithms and the human test subject is the primary source of error in the entire system.

The error associated with integrating the output from the head tracker and the EVM should be related to the addition of the eye position / orientation data of the head position data. Unfortunately, the output from the EVM is a screen coordinate on the scene camera monitor. If the test subject's head is immobilized and there is only one plane of interest, it is possible to map directly the screen coordinates to the plane of interest (i.e., the display) with a minimal amount of induced error. The integration algorithms translate the screen coordinates into a real world location as described in the Task 1 discussion. To accomplish this, the display must be kept at a fixed known position and the test subject's left eye must be at a fixed known location during the calibration procedure. Any deviation from these conditions is propagated throughout the entire series of calculations and induces an error in the final result.

Averaging and Transformation

The saccadic and microsaccadic movement of the eye causes the line of sight to fluctuate around the intended point of fixation. Any single lookpoint is likely to be near the actual intended point of attention, but it is only when a group of successive lookpoints are combined that the

actual fixation can be determined. While this is not intrinsically a source of error, the process by which the POGs are transformed into a fixation and the way that these fixations are then evaluated can affect overall system performance.

Work done under this and previous contracts has led to a variety of filters and processing algorithms to transform raw POGs into dwells. Research has shown the filters and processing algorithms to be application specific. For example, instrument scanning results are influenced by the task to be performed (e.g., Dick, 1980). In the piloting task, the periods of fixation/dwells vary over a considerable range (approximately 60 to 600 msec [e.g., Harris et al., 1986]). By way of contrast, in a different task such as reading the range of fixation values is in the range of 200-300 msec. Once an application has been specified, then the effect of utilizing an individual filter can be quantified and folded into the system error calculation. Filters can also be used to aid in compensating for system errors in the processing of the data.

Fluctuations In System Performance: Informal Observations

The goals for any operational system are reliable, consistent, and accurate performance. A reliable system does not require frequent maintenance and the system components are sufficiently rugged to be used in an operational environment. Consistent performance entails having the system produce the same results every time that the system is used. Finally, the system should be as accurate as possible within the limitations of its individual components.

One critical technical issue that needs to be addressed in a future effort is calibration of the human user. Invariably, a test subject must be calibrated more than once before the system has an accurate mapping of POG onto the display system. Generally, one or more of the calibration points are not correctly aligned with the calculated display points. This indicates a deficiency in the calibration procedure, either in execution or internally in the oculometer processor or, alternately, in the test subject failing to look directly at the calibration point. There has been no observed correlation between various "bad" calibrations, i.e., no single source has been identified as a primary variable. Nor is it possible to isolate the source of error because the calibration routines and calibration data cannot be examined separately in this oculometer system.

Another inconsistency in performance is the random fluctuations in the calculated lookpoint produced by the oculometer. Observation during testing suggests that they are caused by the inability of the oculometer to discriminate the pupil. Since the pupil and the cornea can both be observed in the pupil camera image, it is likely the discrimination algorithms have difficulty dealing with fluctuations in image contrast.

The final problem dealing with system consistency relates to degradation in system performance over time. This seems to be related to test subject visual fatigue which causes differences in the pupil and corneal data as the experiment continues. The experiment described

in the next subsection was used to validate these observations of system performance and to provide data on the variations across calibrations.

A primary goal of this effort was to quantify system accuracy. As was implied above, two levels of accuracy need to be addressed. The first is the size of the cluster of lookpoints that make up a fixation and the second is how far the calculated fixation differs from the actual point of interest. The size of the cluster tends to be a function of the human test subject and represents the human limit imposed on system accuracy. The second is a system issue and can be quantified based on the algorithms used to calibrate the test subject and to interpolate the incoming raw data. The performance experiment described below was designed to provide information on both of these issues.

Initial Experimentation

The goals for the experiment were to characterize the overall performance for fixation determination; to characterize the changes across calibrations, across test subjects, and across the field-of-view (FOV); and to relate present system deficiencies to individual system components. These goals were used to define a broad, simple experiment to provide preliminary data on the overall system performance. This was a preliminary experiment designed to pinpoint areas that needed to be explored more thoroughly. The purpose for examining these factors is to identify those system components which require additional development and to develop an approach to improve the performance of those components.

The first goal is to characterize the stability and quality of fixations as assessed by CORS. All static tasks and a high proportion of dynamic tasks require stable fixations. A stable fixation occurs, for example, when an operator identifies a point or region of a display associated with a control action to be taken (i.e., change airspeed). As previously described, the lookpoints must be processed to produce a POG which is then correlated to the desired point. The issue is to determine what is the size of the cluster of lookpoints which represent the POG and the displacement of the POG from the point of interest. Further, because the clustering will be related to calibration, an effort was made to characterize the changes that occur from one calibration to the next.

One of the effects that has been observed during the experimentation conducted in this and in previous efforts has been that system performance degrades in the lower part of the field of view (FOV). Consistent problems in the lower regions of the FOV are related to the optics used to capture the pupil and cornea image and the discrimination algorithms which recognize the pupil and cornea and then calculate their centroids.

A final goal in this experiment was to identify those components in need of improvement. For example, informal observations have suggested that problems exist in the calibration routines.

An objective was to have numeric data to justify the conclusions drawn from the informal observations. Once a more formal connection has been made between system components and poor performance, an approach can be constructed to improve the performance of those faulty components.

Procedure

The approach in this experiment was to examine stable fixations across test subjects. The Masscomp monitor was used to display the screen shown in Figure 4-1. The test subject was calibrated using points C1 through C9, as in any normal calibration. At the start of the experiment itself, a point at E1 would appear on the display, when the test subject felt he was fixating on the point, he would press a key. The test subject was asked to maintain his fixation on the point until it disappeared. For this experiment each of the experimental points stayed on the screen for 10 seconds after the test subject made the keystroke. The keystroke initiated the data recording procedure and stored each lookpoint for the 10 second window. Data were recorded only after each keystroke to eliminate data points relating to acquisition of the experimental point. This allows an estimate of the error based only on the data relating to the static designation of the point.

This procedure was repeated for each experimental point in sequence from E1 to E5. The test subject was recalibrated after the last data point and asked to repeat the procedure using the new calibration data. Each of the test subjects performed ten trials of being calibrated and then fixating on points E1 through E5. The test subjects did not receive any feedback on their performance and all calibrations were used. Three test subjects were used in the experiment representing qualitatively small, medium, and large pupil diameters. All of the other experimental conditions were kept constant to determine if pupil diameter had any noticeable effect on the data.

Data Reduction

Data were recorded as a pair of screen coordinates for each POG. As discussed previously, it is important to examine the size of a cluster and the offset of the cluster from the desired display point. The size of the cluster was evaluated with three different types of measurement. The average value for all of the data points was used as the center of the cluster, with the size of the cluster defined as the distance from the center to the individual points. This distance was calculated as: (a) the average distance from the center to the individual data points; (b) the root mean square (RMS) of the distance from the center to all of the data points; and (c) as the maximum distance from the center to any one data point. From observing the data, it was

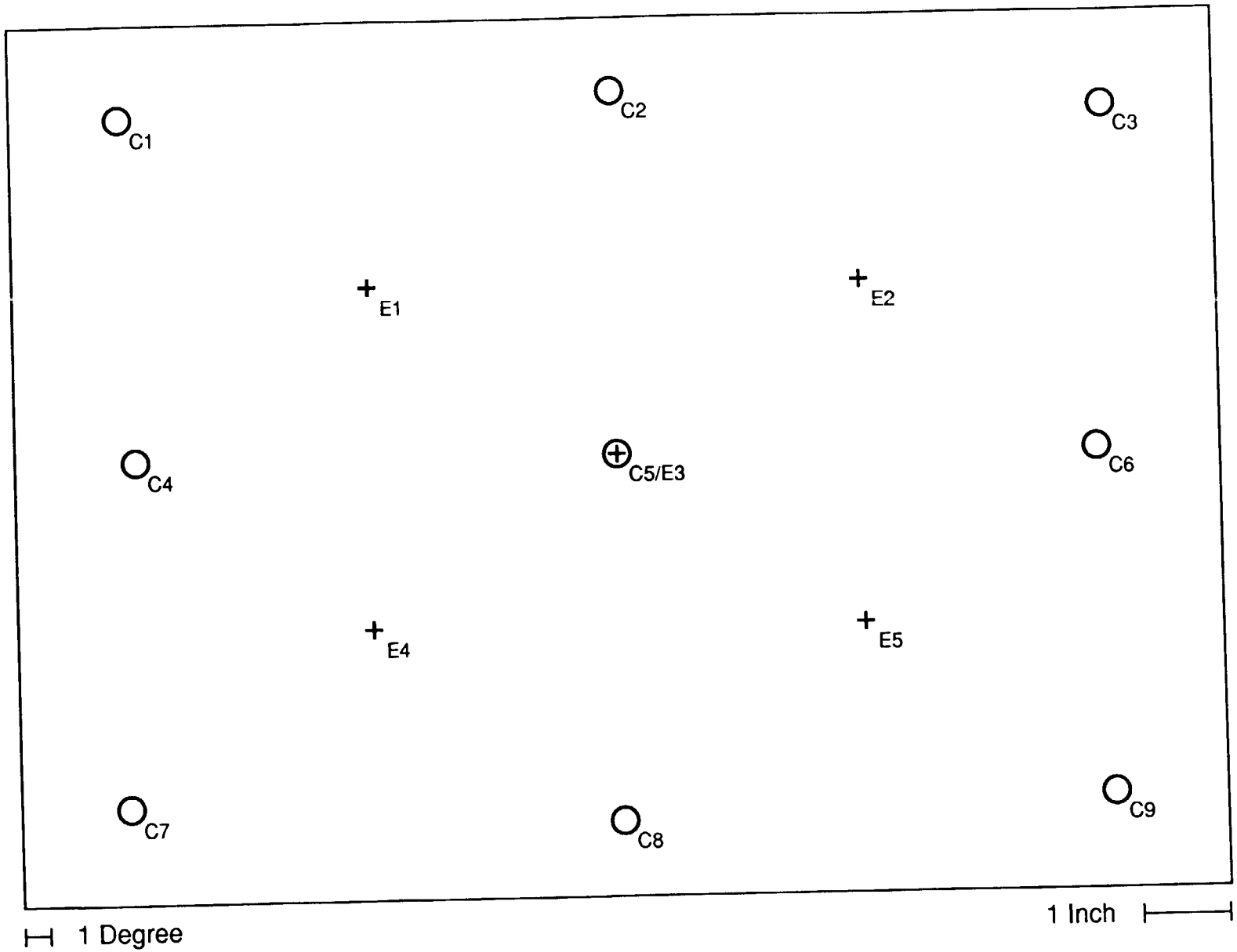

Figure 4-1. Illustration of the calibration points (C) used in the calibration and experimental points (E).

noted that in some runs there was a small fraction of the data points that did not seem to be an integral part of the cluster. The cause of these outlying points seemed to be related to discrimination problems in the oculometer, so when this occurred the data were reevaluated based on the 540 out of 600 (90%) closest data points. As will be discussed below, this produced a significant reduction in the calculated cluster diameters. The displacement from the cluster center to the designated display point was converted to a distance and orientation from the designated display point. The magnitude was calculated as the RMS distance of each point from the designated display point.

Because the data recorded were in screen coordinates, it was necessary to transform these data into a format that could be related to a physical (cockpit) measure. Three types of units were considered: inches, degrees, and milliradians. Inches were not used because the data representing a line of sight value would change based on the distance from the observer from the display. Of the two angular measurements, it was felt that the degrees unit could be more easily understood. Therefore, following standard visual science practices, all of the data presented in this report are in degrees.

System Performance

The data presented in this section were collected during the experiment along with observations made by the staff at Analytics based on their experience with the oculometer system. All of the data collected during the experiment can be found in Appendix B; selected pieces of the data are reported in this section. Overall, these data represent the best that can be realistically expected from the CORS prototype.

Best and Worst Case Performance

Table 4-1 contains the best (smallest) and worst (largest) cluster sizes from the trials of Subject 3. The performance of Subject 3 was the best of the three test subjects in the sense that the results were the most consistent. The best cluster radii are approximately from a quarter of a degree to a third of a degree while the worst does not exceed 0.564 degrees RMS. The radius of the extreme values are two to three times the size of the average or RMS radius and this relationship holds true to a lesser extent for the 90% data. Because this relationship occurs while the average and RMS radii do not significantly decrease when using the 90% data, this leads to the conclusion that the data points are highly clustered within their average and RMS radii. If this conclusion be true, it is reasonable to expect to be able to develop a filtering algorithm which could calculate cluster sizes from a quarter to a half of a degree. This value represents the human limitation inherent in an eye-based system (Hallett, 1986).

Table 4-1. Excerpt of cluster size data for Subject 3 (in degrees).

Subject 3	Run/Point	Avg	RMS	Max	Avg	RMS	Max
	4/2	0.251	0.291	0.717	0.218	0.244	0.444
	5/5	0.264	0.307	0.858	0.227	0.252	0.466
Best Runs	10/3	0.262	0.299	0.814	0.229	0.253	0.457
	1/2	0.260	0.299	0.857	0.228	0.255	0.449
	9/2	0.269	0.323	1.148	0.227	0.255	0.481
	4/4	0.383	0.432	1.017	0.340	0.374	0.669
	10/5	0.392	0.437	1.075	0.351	0.383	0.657
Worst Runs	9/3	0.403	0.435	0.971	0.367	0.387	0.619
	10/1	0.454	0.501	1.292	0.407	0.440	0.739
	6/5	0.501	0.564	1.281	0.443	0.486	0.868

Figure 4-2 is a graphical representation for the best trial of Subject 3. The plus signs represent the five experimental points. The center of the circle is the calculated cluster center. The radius of each circle is based on the point furthermost from the cluster center, the inner radius being the 540th furthermost point and the outer radius being the 600th point. The center of the cluster is very close to the experimental point. Notice, however, that each cluster is located to the left of the experimental point, which indicates a small error induced during the calibration procedure.

Average System Performance

The tabular data in the next two tables represent a composite of all three test subjects. These data represent what would be average system performance without recalibrating the test subject after a poor calibration. Graphical data are illustrative of runs collected during the experiment and were selected on this basis.

Table 4-2 contains RMS cluster radii for 90% and 100% of the data points for each experimental point, for each test subject, and a composite of all test subjects. Table 4-3 lists the cluster offset from the experiment point for each point, for each test subject, and a composite of all of the test subjects. As a composite the RMS cluster radius was approximately 0.75° with an offset of approximately 1.2°. The results for Subject 3 are significantly better than those of Subjects 1 or 2. Furthermore, the difference between the 90% and 100% RMS cluster radius distance is significantly greater for Subjects 1 and 2 than for Subject 3. Obviously the system was having trouble with Subjects 1 and 2, producing data points that were significantly displaced from the overall cluster. Our informal observations of the difference between the test subjects noted

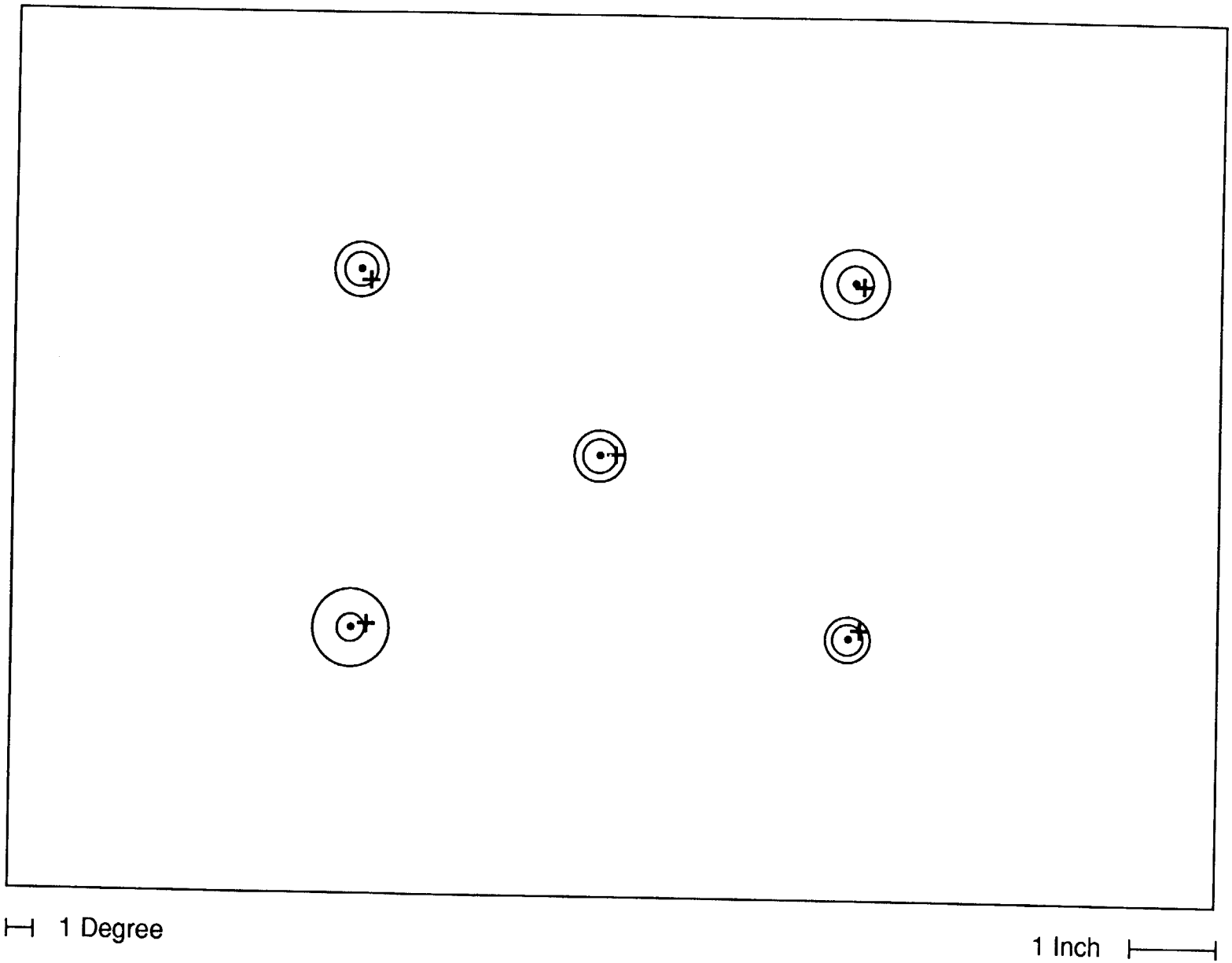

Figure 4-2. Best result. (Subject 3, Run 7.) (Rings denote 100% and 90% of data points.)

that the pupil of Subject 3 is larger than the other two test subjects. Whether this is the primary cause of test differences or there is some other reason is unknown. However, this variable should be explored further to characterize system performance more completely.

Table 4-2. RMS cluster size data for all test subjects (in degrees).

	Subject 1		Subject 2		Subject 3		All Subjects	
%	100	90	100	90	100	90	100	90
Point								
1	0.758	0.662	0.634	0.523	0.350	0.303	0.605	0.518
2	0.617	0.392	0.850	0.423	0.334	0.285	0.636	0.371
3	0.746	0.428	0.839	0.601	0.362	0.312	0.681	0.462
4	1.366	0.736	0.990	0.803	0.359	0.304	0.996	0.653
5	0.661	0.456	1.024	0.682	0.379	0.322	0.737	0.509
All Points	0.873	0.552	0.878	0.620	0.357	0.305	0.744	0.511

Table 4-3. RMS offset data for all test subjects (in degrees).

Point	Subject 1	Subject 2	Subject 3	All Subjects
1	1.182	1.347	0.907	1.160
2	1.327	1.006	1.049	1.137
3	1.906	0.968	0.999	1.362
4	1.455	3.723	1.136	2.399
5	1.391	2.419	1.310	1.773
All Points	1.468	2.167	1.089	1.186

One of our experimental observations was that it is much more difficult to discriminate all test subject's pupil and cornea in the lower part of the FOV than elsewhere and the system performed much worse in this region. Experimental points E4 and E5 are markedly worse than the other three points which are in the upper FOV. If these values were excluded from the composite calculation there would be a significant reduction in the total RMS cluster radius and RMS cluster offset. This points to a system performance deficiency that should be corrected in future work.

Figures 4-3 and 4-4 show two of the trials from the experiment; Figure 4-3 shows an average trial and Figure 4-4 shows one of the worst trials. In Figure 4-3 all of the clusters overlap the experiment point with four of the five points falling in the inner ring, showing that 90% of the values were in this area. Note that the cluster size is larger than was shown in Figure 4-2 and that the worst points are in the bottom of the FOV. The trend observed in Figure 4-3 continues in Figure 4-4 with a much more pronounced effect. The clusters for experimental points E4 and E5 bear no real relation to those points and the data are spread throughout the display. The other three clusters are larger, but the inner 90% of the points are within an acceptable range. The offset is larger and the clusters for experimental points E1 and E2 do not overlap their respective points. Fortunately, results like those shown in Figure 4-4 did not occur often and should be correctable by improvements in the hardware and software algorithms used to process the data.

Correlations between System Deficiencies and Components

There are three components of the oculometer that seem to be the most likely sources of error illustrated in Figures 4-3 and 4-4. Those components are: discrimination, calibration, and the associated interpolation routines. The variabilities of cluster sizes and extraneous data points are most likely related to the discrimination hardware and software. Errors in the calibration process are carried through into the interpolation routines which produce the output from the oculometer. These errors cause an offset between the cluster center and the desired display point.

Errors induced by poor discrimination or the complete inability to discriminate either the pupil or cornea seem to be the likely reasons for the wide fluctuations in cluster size and the random data points that the system produces. The inability of the system to discriminate the pupil has been observed regularly in the lower half of the FOV. Informal observations confirm the above suggestions. The cross hairs displayed on the video output of the pupil camera designate the estimated pupil center. When the fluctuations occur and the test subject is sitting quietly, the cross hairs jitter between two widely separate locations without any noticeable accompanying eye movement, indeed, the jitter is too fast for eye movements to occur. This is most likely caused by the EVM system optics or the hardware processor used to calculate the pupil centroid.

The calibration procedure requires the test subject to fixate on the calibration points in sequence. The values recorded at this time are used as data points to bound curves used in the interpolation routines. If the values recorded during the calibration procedure are inaccurate an offset is induced into the calculated eye point. Figure 4-5 shows the angular offset for the Subject 3 from the experiment. In runs 1, 5, 6, and 10, the angular offset is constant and could be corrected during the data run by recalibrating one point. When angular offset is spaced over a wide arc a specialized calibration routine is required.

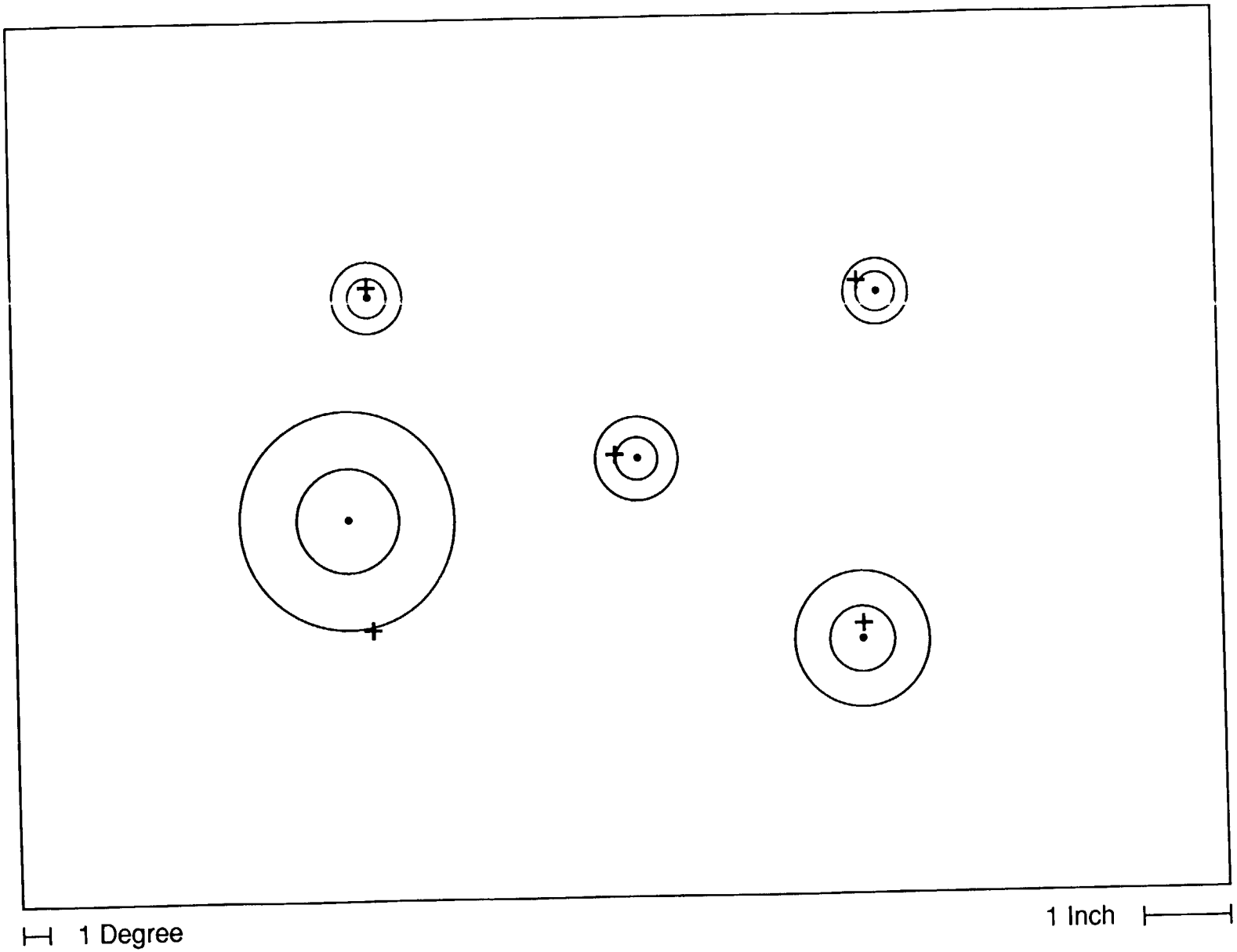

Figure 4-3. Representative result. (Subject 2, Run 2.) (Rings denote 100% and 90% of data points.)

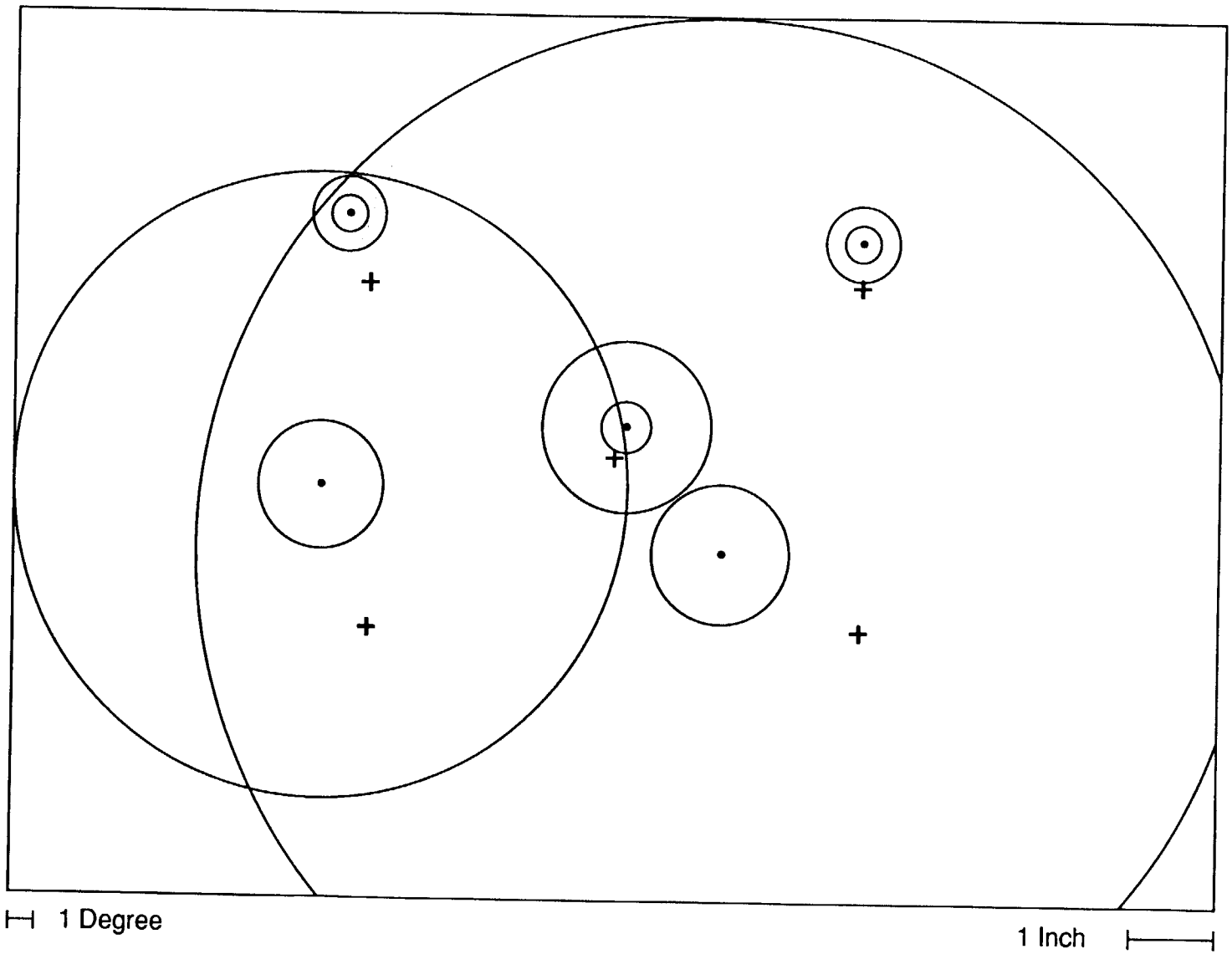

Figure 4-4. Poorest result. (Subject 2, Run 10.) (Rings denote 100% and 90% of data points.)

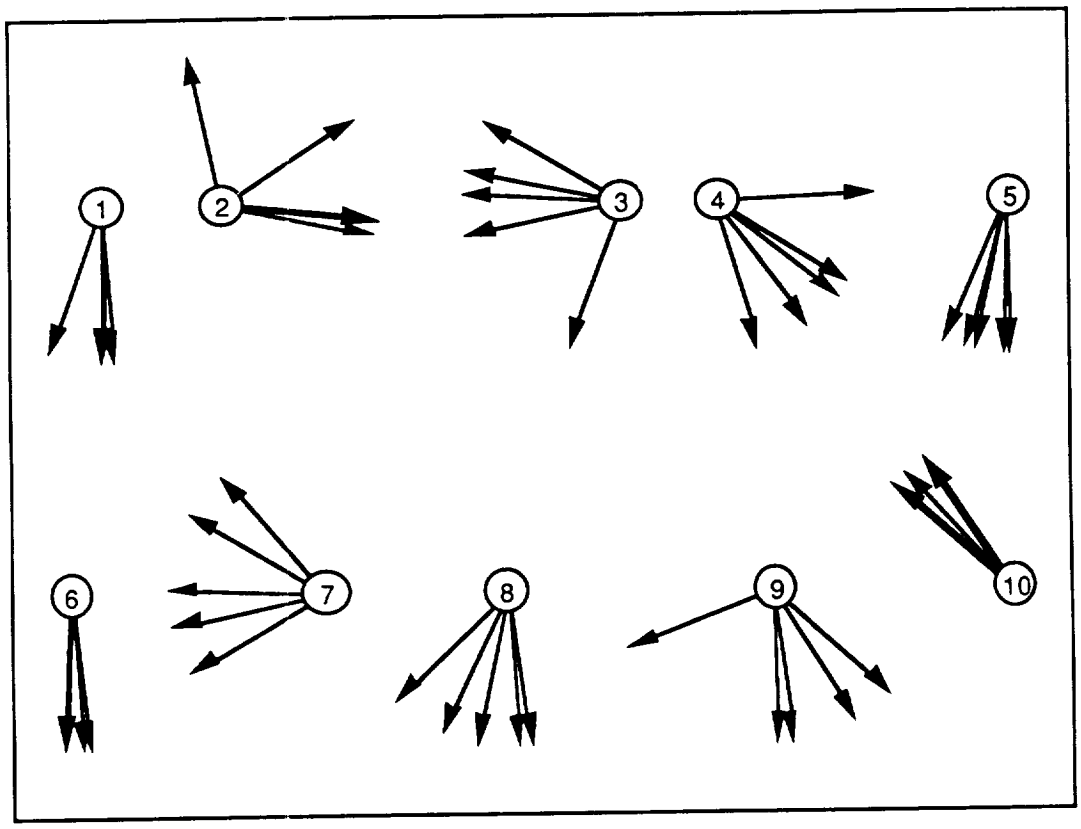

Figure 4-5. Angular orientation of cluster center from desired display point (Subject 3, Runs 1 through 10). (Where there are less than five arrows, dark arrows are used to indicate multiple lines.)

Figures 4-6 through 4-9 display the coordinates of the calculated eye points for Subject 3, run 7 and experimental point 1. The data fluctuate around the center of the cluster. Because

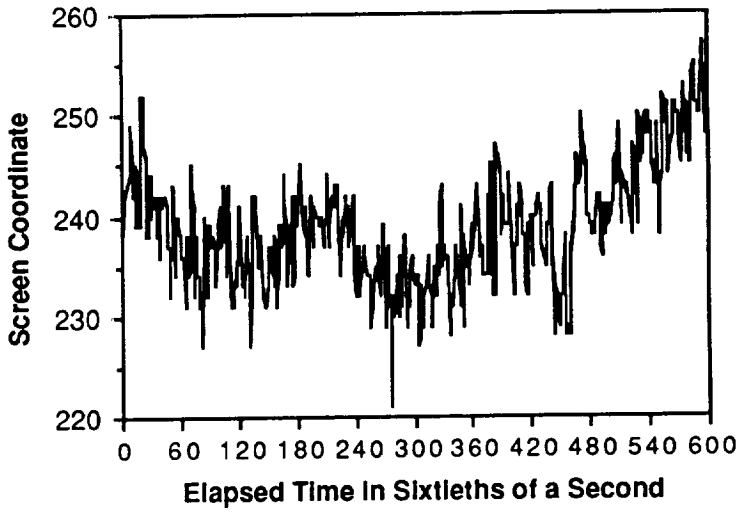

Figure 4-6. Eye lookpoint X coordinate (Subject 3, Run 7, Point E1).

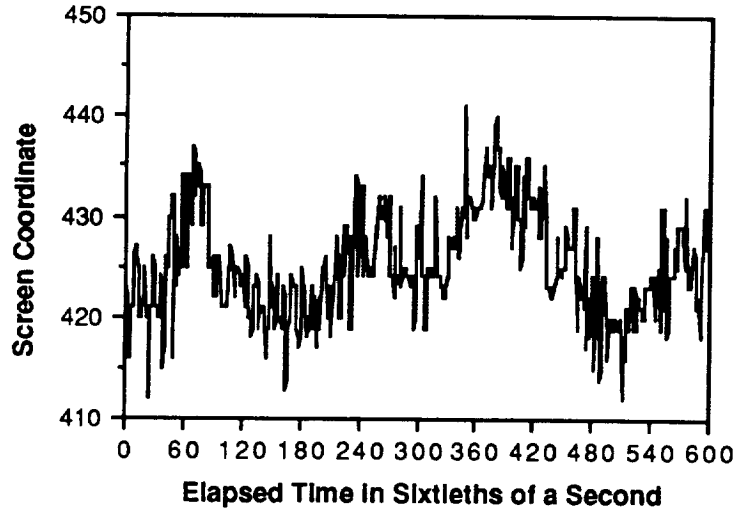

Figure 4-7. Eye lookpoint Y coordinate (Subject 3, Run 7, Point E1).

the interpolation routine utilizes the relationship between the pupil and cornea at each calibration point any deviation leads to an induced offset which is propagated through a sizeable portion of the FOV. The averaged data show how the eye settles on a single point and then slowly drifts to a

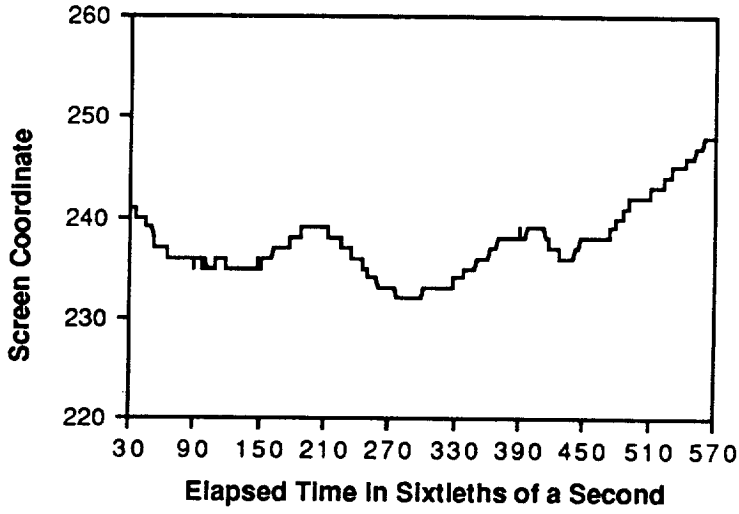

Figure 4-8. Sixty frame average of eye lookpoint X coordinate (Subject 3, Run 7, Point E1). (The plot is a running average of the raw data in Figure 4-6, using 30 frames either side of each plotted point.)

new fixation point. All of this occurred while the test subject focused on the desired display point. Also, there is an initial time at the beginning and end of the data where the test subject has not yet

settled on a specific point. The calibration routine must recognize this and extract its data from the point where the eye has settled to extract a good value for that point. Again the data support the conclusion that a more sophisticated calibration routine is required to improve system performance.

Figure 4-9. Sixty frame average of eye lookpoint Y coordinate (Subject 3, Run 7, Point E1). (Averaging is done in the same way as in Figure 4-8.)

Further Experimentation on System Accuracy

A second experiment was carried out to examine CORS performance in greater detail. The principle behind the experiment was to present stimuli which were sufficiently small to insure that the test subject looked directly at them in order to identify the test items. These acuity targets require foveal vision. By using acuity targets we insured behaviorally where the test subject was looking before responding. By examining those cases in which the test subject responded correctly, we could then examine the performance of CORS. Because the test subject had to look at the stimulus to identify the item correctly, CORS should report a fixation on the target at some time during (or ending slightly after) the stimulus presentation.

The primary goal of the experiment was to isolate system performance from test subject performance. This is possible by means of examining the relations of the possible outcomes for a given experimental trial. Figure 4-10 represents a 2 x 2 contingency table and shows the possible outcomes for the experiment. When CORS 'missed' the fixation and the test subject correctly identified the stimulus (upper right cell of Figure 4-10), represent cases in which the filter settings may be too stringent. That is, if CORS were functioning perfectly, there would be no entries in

this cell. A second goal is to examine the positioning of the fixation in the area around the stimulus in the context of human performance. That is, CORS may report fixations but these may or may not be close to the stimulus position.

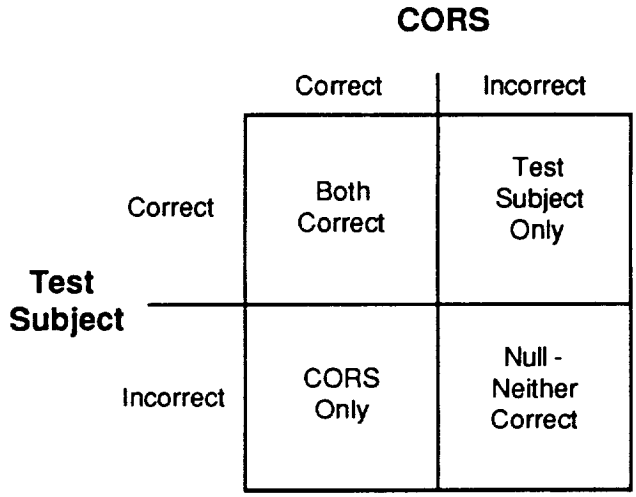

Figure 4-10. Illustration of the possible outcomes for the acuity experiment.

Procedure

On a given trial, two letters were presented. These were selected randomly from the set, ACEFHKMNOTVWXYZ. All letters were used equally often and were paired with all other letters randomly. The size of the letters was 5 x 7 pixels [59 pixels/inch] which equates to an overall visual angle of approximately 14 x 19.5 minutes of arc. Because discrimination between letters, e.g., E vs. F, will be based on a few pixels, the actual effective stimulus is often smaller than these overall dimensions.

The possible spatial positions of the letters is shown in Figure 4-11. The two letters for a trial appeared on a given radius, i.e., positions 1 and 2, 13 and 14, etc. The center of the figure represents the fixation point for the start of a trial. The separation between the center fixation point, the inner circle and the outer circle was approximately 6°. Because the test subject did not know where the letters would occur on a given trial, he was encouraged to fixate the center. Indeed, the initiation of a trial was started by the test subject when he felt he was looking at the center point. To start the trial, he pressed the space bar on a keyboard and the two letters appeared shortly thereafter.

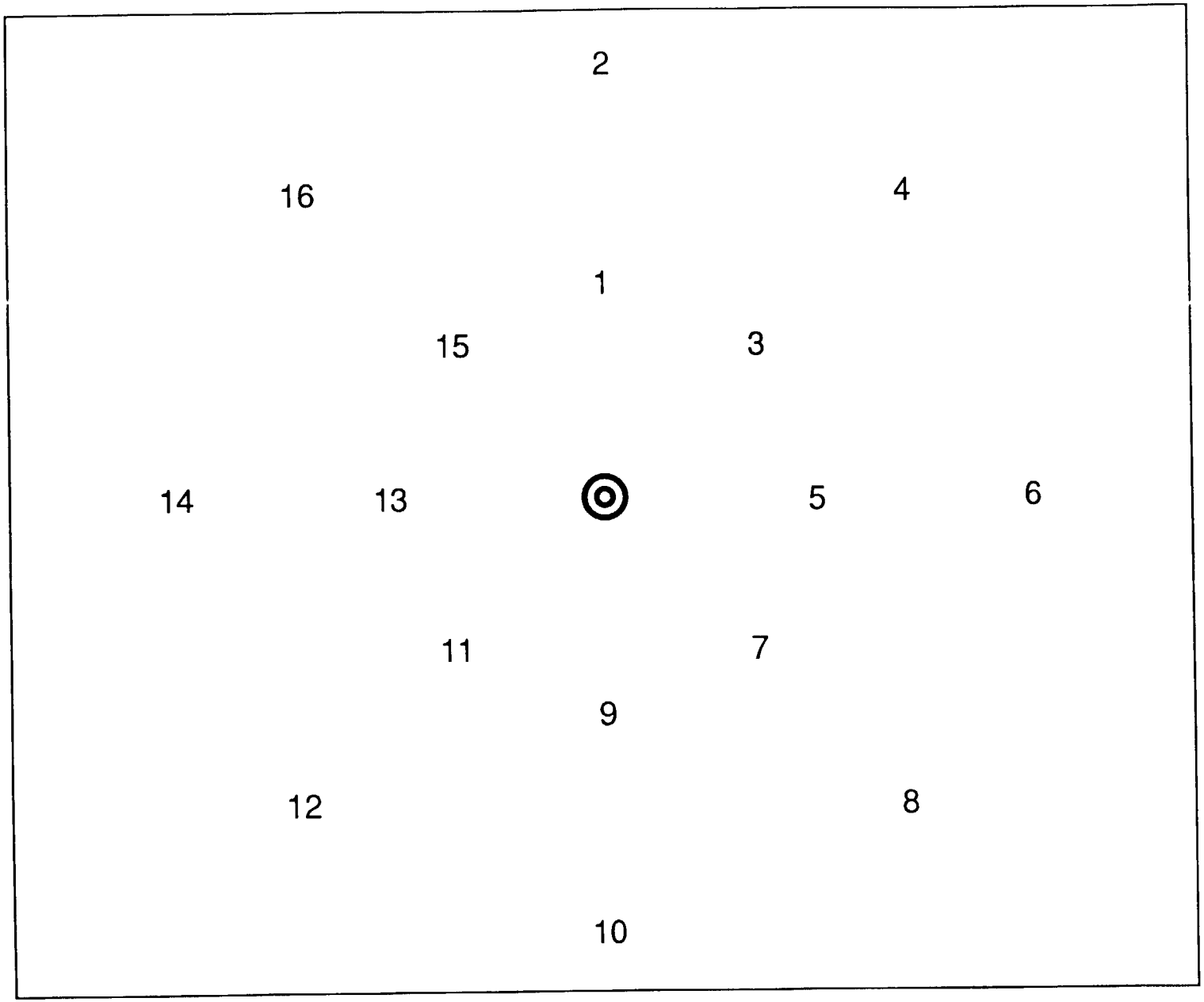

Figure 4-11. Schematic layout of potential stimulus positions.

The duration of display of the two letters was varied. The time periods were 300, 400, 500, or 600 msec. These durations allowed time for the test subject to move his eyes from the fixation point to the position of one or both of the letters. At the end of the exposure duration, each letter was replaced by a mask which inhibited post-exposure processing. To indicate his response for the inner position, the test subject pressed the appropriate letter key on the keyboard followed by a press on the space bar. The space bar response indicated the completion of the response for that stimulus position. The letter and space bar sequence was then repeated for the outer stimulus position. The test subject could change his response simply by pressing an alternative key before pressing the space bar. The computer recorded all responses, including multiple responses for a trial. The last letter pressed before pressing the space bar was taken as the final response for purposes of scoring.

The combination of conditions were presented randomly within a block with different randomizations of conditions for each block. The horizontal and vertical meridians occurred equally often and randomly occupied 40 of the trials. The oblique meridians were presented equally often on the other 20 trials. The exposure durations were used randomly, each for 15 trials. Thus, the meridian by exposure combinations were not necessarily tested equally often within a block. New calibrations were carried out before each block of 60 trials. This technique permitted evaluation of the calibration procedure by block.

One test subject was run for four blocks. This individual also participated in the previous experiment as test subject number 2. The Masscomp system was used together with the helmet mounted oculometer. The helmet was restrained to prevent head movement and resulted in a viewing distance of 21 inches. This was done to reduce the number of possible factors contributing to the data.

Results

The analysis of eye position was accomplished using a special purpose program. This program uses the successive lookpoint data obtained and written to file by CORS. The scoring procedure incorporates the temporal portion of the filter (10/12) and the spatial setting at a radius of 0.316 inches (52 minutes of arc) at the calibration plane. The scoring for the region, however, was more relaxed. Circles were drawn around the letter positions so as to be as large as possible without overlapping. This yielded region fixation circles of slightly less than 6° in diameter. The lookpoint data were then examined manually by stepping through the data and examining the calculated POGs after each frame. A fixation which fell within the criterion region circle while the letter was being displayed was considered to be coincident with the letter for that trial.

As indicated in Figure 4-10, there are four possible outcomes for a given trial: *Both correct* (test subject correct with CORS identifying the position), test *Subject only* correct (CORS missed the position), *CORS only* gets position (test subject incorrect), and *Null* trials (neither

performed correctly). The results for all four of these outcomes for each of the exposure durations are presented in Table 4-4. As would be expected, performance on the inner letter was high. As exposure duration is increased, performance on the outer letter improved dramatically. This is a result of the test subject having time to move his eyes to the outer position while the letter is still being exposed. The two cases of primary interest are those two in which the letter was reported correctly. The upper right cells of Table 4-4 provide the data.

Calibrations were carried out for each of the blocks of trials. Table 4-5 shows the data recast in terms of Blocks. The principal point of this table is to show that Block # 1 has a poor calibration. This one block accounted for 68 % of the CORS failures. The two rightmost columns in the table provide a ratio of the number of CORS 'misses' (test subject correct) to the total number reported correctly by the test subject.

The results show that CORS is capable of identifying eye position with the head fixed. The experiment also indicates that calibration is a crucial factor. Specifically, in Block #1, the CORS inaccuracy ratio is 0.279 which indicates that the system did not perform nearly in parallel with the test subject. For the inner letters, the test subject correctly reported 55 out of 60, indicating a high level of performance whereas CORS identified only 44 out of the 55 correct. The other blocks, with different calibrations, show apparent acceptable performance by CORS within the parameters used.

One purpose of the experiment was to examine the spatiotemporal filter. The extent to which fixations are identified regardless of location provides evidence for the viability of the spatiotemporal filter settings. The level of performance in most of the runs indicate that the spatiotemporal filter performed well, with a high percent of fixations reported. This is represented in the table as the two entries, *Both Correct* and *CORS only*. Further, CORS reported fixations for the outer letter about 30% of the time when the test subject did not report the letter correctly. This result was fairly stable across exposure duration, indicating the eyes moved but that the test subject could not identify the letter. Thus, CORS is identifying fixations.

The identification of the existence of fixations is necessary, but it is not sufficient. It is of utmost importance to have accurate positioning of the fixation within the region. This was not particularly good. Letter fixation was defined by a circle of almost 3° radius, 6° diameter around the letter. Because CORS identifies POGs and fixations, but only generally in the area of the stimulus, this is further evidence for the problems associated with the calibration procedures and the application of the calibration data to the lookpoint values. This result is analogous to the angular displacement results shown Figure 4-5. Further, the present experiment offers the basis of a technique to check on the adequacy of the calibration.

Table 4-4. Test subject accuracy and CORS accuracy for exposure duration. (Numbers in () are for the outer position.) (Cell entries are number of occurrences out of 60.)

Exposure Duration = 300

		CORS: Correct	CORS: Incorrect	Total
Test Subject: Correct		49 (5)	0 (1)	49 (6)
Test Subject: Incorrect		11 (12)	0 (42)	11 (54)
Total		60 (17)	0 (43)	

Exposure Duration = 400

		CORS: Correct	CORS: Incorrect	Total
Test Subject: Correct		51 (8)	6 (3)	57 (11)
Test Subject: Incorrect		3 (20)	0 (29)	3 (49)
Total		54 (28)	6 (32)	60 (60)

Exposure Duration = 500

		CORS: Correct	CORS: Incorrect	Total
Test Subject: Correct		55 (20)	5 (5)	60 (25)
Test Subject: Incorrect		0 (22)	0 (13)	0 (35)
Total		55 (42)	5 (18)	60 (60)

Exposure Duration = 600

		CORS: Correct	CORS: Incorrect	Total
Test Subject: Correct		54 (33)	4 (4)	58 (37)
Test Subject: Incorrect		0 (21)	2 (2)	2 (23)
Total		54 (54)	6 (6)	60 (60)

Table 4-5. Summary of acuity experiment. (Cell entries are number of occurrences out of 60.)

Block #	Position	Both Correct	Subject only	CORS only	Null (neither)	Sub Only/ Both + Sub	CORS Inaccuracy Ratio
1	Inner	44	11	5	0	11/55	
	Outer	5	8	18	29	8/13	0.279
2	Inner	55	3	2	0	3/58	
	Outer	16	2	18	24	2/18	0.066
3	Inner	54	1	5	0	1/55	
	Outer	24	0	20	16	0/24	0.013
4	Inner	56	1	3	0	1/57	
	Outer	22	2	16	20	2/24	0.037

Experiment on the Effect of Head Motion on System Performance

One of the goals of Phase II experimentation was to determine how head motion affects system performance. The majority of head motion that occurs in a cockpit is rotational with a small amount of translation motion. This experiment considered the initial level of system accuracy, conducted an evaluation of the accuracy at different orientations and angles of incidence with the panels and determined whether system performance degraded during the experiment. The emphasis for this experiment was on spatial point designation where the test subject focused on successive points for a few seconds each. This produced definite fixations which could be correlated to the regions to determine how accurately CORS could reproduce where the test subject was looking.

The experiment was conducted in the mock cockpit, described in Task 1. The test subject was required to look at the calibration points and then at a sequence of regions throughout the cockpit and then at the calibration points again. The regions were placed in panels 3, 4, 5, 6, 8, 12, and 15 (in reference to Figure 3-15, p 31.). These panels correspond to the full spectrum of angular orientations that would commonly be found in a cockpit. Each region is a square with the letter **A** in the center, the length of the edge of the square being one inch. A sequence of regions was defined in the planes program around the letter **A** to evaluate how accurately CORS calculated where the test subject was looking. The largest square was six inches on a side, which corresponds to 8° of deviation from the center of the **A** at 21 inches. During the experiment each fixation that CORS calculated was written to a file and then reviewed by the play back program. Additionally, the output of the scene camera was recorded on a VCR to

be played back to show where the oculometer calculated the test subject to be looking. Ten experimental runs were conducted using one test subject.

The results from the head free runs are inconclusive; the majority of the runs showed varying levels of degradation of the calibration at the conclusion of each run. These degradations were not consistent across the runs, but the majority of the degradations seem to be a result of hardware deficiencies of the helmet mounted oculometer as described in Task 1. On some occasions the visor slid as the test subject tilted his head to look at panels 3, 12, and 15. Helmet slippage occurred frequently during the runs as the test subject was released or made rapid head motions. Additionally, the scene camera would occasionally move during the run, removing the only means of independently verifying the results produced by CORS. These problems preclude being able to define the performance of the CORS system numerically with respect to head motion or panel fixation, but some qualitative observations can be drawn from the data.

Generally, the system performed as expected for most of the regions. The best performance was in panel 8. This was to be expected since this is the panel that contains the calibration points and is perpendicular to the test subject's line of sight, i.e., directly in front. In a cockpit, it is also the location of many primary instruments.

CORS system error is an angular displacement from the test subject's line of sight. As a result, when the test subject looks at a panel at an oblique angle to the line of sight the linear error is magnified as a function of the angle between the line of sight and the panel. This was most dramatically shown in panel 15 where the angle of incidence was on the order of 20°. CORS usually calculated the test subject to be looking at the background of the panel instead of at a six inch region that included the letter **A**. CORS usually calculated to within two inches of the correct position in panels 3, 4, and 12 which had angles of incidence of approximately 70 to 80°.

The worst results were obtained for panels 5 and 6, which correspond to the left and right sides of the cockpit. In both of these panels CORS had difficultly calculating the correct location as to where the test subject was looking. Review of the videotape usually showed that the oculometer was providing what should be the correct coordinates for **A**, and the angle of incidence was close to perpendicular. The only difference between these two panels and better panels, beside the obvious rotation, was that panels 5 and 6 were much closer to the test subject. At this point it is unknown whether the problems associated with these two panels are a system deficiency in the algorithms or a hardware related problem in either the helmet or the head tracking system. Unfortunately, the constraints imposed by the hardware and the conclusion of the contract precluded a more thorough examination of the effect of head motion on overall system performance.

Summary of Experimental Issues

A number of issues were to be studied within the experiments. In retrospect, several of these issues were based on questions that were not necessary to study. The most important reason for the change in relative importance of the research issues was the availability of technologically improved computer hardware in which processing could be performed at a much higher rate than anticipated. Other issues included the study of calibration. However, it was not possible to modify the calibration routines without having the oculometer manufacturer perform this function.

Some of the proposed issues were studied in the experiments described above. For completeness and convenience, we address all the issues identified in the original proposal here in summary form. This is done independently of whether the experiments investigated them or not.

A Characterization of System Head Motion Tolerance

As indicated in the Task 1 equipment discussion, the helmet presents considerable problems as currently configured. Whenever there is head movement, there is often helmet movement and movement of the associated devices mounted on the helmet. Specifically, the helmet may move in relation to the head, the visor may move in relation to the helmet, and the scene camera may move in relation to the helmet. The combinations and effects of these variable movements defy any system of compensation within the constraints of the contract.

System Accuracy Relative to Head Motion/Location

The two Masscomp experiments indicate that tolerable accuracy can be achieved without head movement. However, when the helmet is released, CORS performance degrades. The combination of the helmet problems and the calibration problems made it difficult to characterize the errors in any formal manner. These random variables have also made it difficult to test the algorithms involving the integration of head and eye position data. Nevertheless, several observations point to potential problems in the algorithms. One of these involves the angle of incidence which may cause disruptions in the calculations and relates to accommodating the depth of the panel.

While these results are not as good as one would like, they do not negate the CORS concept. They do, however, emphasize the extreme importance of the hardware used and indicate that further work is needed to test and develop the system, including the algorithms.

Clearly, improving the helmet system would be of considerable benefit as a first step in any such future research.

Optimization of Calibration Procedures

The EVM provides modified output based on fitting the individual x,y observations to the calibration points using the calibration plane. That is, the lookpoints are modified as a result of having been passed through the calibration routines.

Experiments were carried out to characterize the accuracy of the oculometer and the CORS system. The findings of these experiments suggest the CORS oculometer accuracy is variable and is dependent on, at least, the following variables:

- Time since calibration,
- Location in the visual field,
- Test subject, including the size of pupil and other physiological variables

It should be noted that the calibration routines are proprietary, and therefore it was not possible to modify these routines under this effort. Thus, the accuracy and errors noted are characterized in relation to the calibration, but were not corrected.

Optimization of Eye Position Sample Rate (samples per second)

The consideration of optimization of the eye position sample rate is based on two separate issues. One of these relates to the real time processing capabilities of the CORS computer and the other has to do with accuracy or fidelity in capturing the movements of the eye.

One of the concerns prior to developing CORS was whether a PC could keep up with the necessary calculations required for CORS if the data rate occurred at 60Hz. For each new frame of data, the computer has to do calculations on up to 12 time frames of data. These calculations include integrating the eye and head position data for each lookpoint, averaging a number of lookpoints, and possibly looking up a dwell region and recording data.

Within reason, it is easy to argue that the greater the sample rate, the better the accuracy. The duration of a saccadic movement has a range between 20 and 100 msec (Hallett, 1986), however, the standard deviation was not reported, and consequently one can only guess about the shape of the temporal distribution. (Simply using the middle of the range would put the typical duration at 60 msec.) The purpose, however, is not to capture the eye while it is motion but to know where it is between movements. Thus, the intent is to use the eye movement as a 'trigger' to determine the end of a fixation and the beginning of the next. Accordingly, the objective is to filter this movement out.

Different sampling rates have been used in oculometer studies. At 60Hz sampling rate the data are sampled about every 17 msec; at 32Hz the data are sampled about every 31 msec. These sample rates are approximately two to four times faster than the midrange of the saccadic movement times (20-100 msec). The primary effect of a sampling rate change is on selection of the appropriate parameters for the spatiotemporal filter. Stated differently, halving the sample rate requires changing the spatiotemporal filter from 10 out of 12 lookpoint frames to 5 out of 6 to maintain the similar accuracy relations.

Neither the oculometer nor the head tracker provides a provision to alter the data sample rate. To change the sample rate, we are left with the sole alternative of ignoring some of the data. However, such steps were not required, since the preset data rate of 60Hz was processed by the CORS computer.

Trade-off between Data Reduction and System Accuracy

There are several points in the CORS system where data reduction and system accuracy trade-offs could occur. One such point resides in the spatiotemporal filter. Changing the size of the spatial area leads to a more rigorous criterion (smaller radius - fewer fixations) or a more lax criterion (larger radius - more fixations). Similarly, changing the temporal parameter also relaxes or tightens the accuracy, i.e., the number of frames (x) required to be within the range relative to the total number of frames (n) contained in the POG window.

A second data reduction routine is based in the recording option , i.e., on and off fixation records vs. dwell records (Figure 3-12). This point clearly influences the accuracy of the data recorded. Because dwells will often contain fixations with null regions interspersed, the fine detail of oculometer data will be lost when only dwells are recorded.

Both the spatiotemporal filter and the mapping can be changed within CORS, depending upon the specific situation. Accordingly, the user has control over the data reduction/ system accuracy factor. Further experiments are required, however, to provide appropriate guidelines and recommendations so the end user can make these decisions.

System Response as a Function of Scan Rate

This, too, was an issue that was not important after the final selection of the CORS computer. Basically, CORS can handle any eye scan rate. The limitations within the prototype were defined by the spatiotemporal filter along with a desire not to drive the recording system too hard. Because of the number of words being written to the DFDR and the speed of the CORS computer, we intentionally eliminated dwells shorter than 200 msec. This is not a permanent

limitation, however, and can be changed in an operational system, provided suitable substitute hardware is available.

CORS Prototype Demonstration

A final goal of the CORS effort was to demonstrate the integration of the prototype equipment as a functioning system. This demonstration utilized the cockpit mockup to exercise the system in a representative environment that provided dynamic eye movements throughout defined regions. The primary factor influencing the demonstration protocol was that of verifying the proof-of-concept by showing the ability to reconstruct pilot eye movement history from the DFDR recorded data to an acceptable degree of fidelity.

As implemented, the CORS computer performed all data analysis prior to recording the output on the DFDR. Accordingly, data actually recorded consisted of eye dwells coded by region and time of initiation (delayed slightly to account for the decision criteria of 10 of 12 acceptable measurements. Thus, the system demonstration involved collecting, reducing, coding, formatting, and writing data to the recorder and then retrieving the data from the DFDR.

Being a research project, the CORS software is implemented to provide flexibility and insight to its operation and performance. While the data collection and processing steps are, in general, basic and common throughout, the writing step has several alternatives. Processed data may be written to disk, to the computer screen, or to a recording device, in this case the DFDR. During the early steps of development and testing the data were written to the screen and the disk so that they could be analyzed quickly, modified if necessary, and then reanalyzed prior to formatting in the FDAU-M and recording on the DFDR. In the final stages of the effort data were formatted in accordance with the ARINC standard and written to the DFDR. The CORS results discussed previously attest to the capability to collect, process, and write eye history data.

The ability to write data to and retrieve data from the DFDR was demonstrated in conjunction with the CORS computer. A test routine was developed which wrote a series of records to the DFDR from the CORS computer through the FDAU-M onto the DFDR. The FDAU-M, in addition to formatting and automatically transmitting the record series to the DFDR, also generates its own validation records which are written to the DFDR. These parallel data are retrieved by reversing the the process, i.e., the CORS computer activates the playback mode to the DFDR through the FDAU-M. Comparison of the dual records retrieved via the software demonstrates the playback capability of CORS. The software used was tested repeatedly in this fashion with the FDAU-M and the DFDR. This effort constituted the prototype demonstration.

FUTURE DIRECTIONS AND POTENTIAL IMPROVEMENTS

A variety of improvements can be made to the prototype system. Many of these are straightforward and, in some cases, the equipment already exists. Generally, to implement the improvements would mean replacing the oculometer and improving the helmet mounted sensor design.

The Helmet

The difficulties with the helmet were documented in the other sections. Clearly, a better fitting helmet would be of considerable value. One way to accomplish this would be to use pads attached with velcro to adjust the helmet size. Another possibility is to use several sizes with the means to transfer the associated sensors from one to the other. Further the attachments currently have too much freedom of movement. The visor, the scene camera, and the eye camera mounts tend to loosen with no means to tighten the fittings.

To correct these mechanical aspects is clearly possible and would result in better overall performance.

The Oculometer

An overall issue central to implementing CORS is obtaining an oculometer that is able to track the pupil and corneal reflections reliably. This overall issue can be broken into two separate subissues: (a) The technique used in the oculometer and (b) the manner in which the calibrations are integrated into the eye position data. Of the two, the calibration issue seems to be the more important. In general, a dark pupil tracking scheme, along with a sophisticated algorithm to track both the corneal and pupil reflections, appears substantially superior to a bright pupil tracker. Unfortunately, our present oculometer uses bright pupil technology with a more rudimentary pupil discrimination algorithm There are advantages and disadvantages with either approach, however, changes in VLSI and digital processing technology now make the dark pupil approach the more viable. In a demonstration provided by a manufacturer, a dark pupil oculometer was always successful in tracking the pupil even under conditions in which our bright pupil system typically fails.

General Technology Considerations

There are two different approaches for identifying the pupil. These approaches to eye tracking are known as bright pupil and dark pupil, respectively. The bright pupil approach shines

an infrared light into the eye and looks for a "white" reflection from the pupil (as seen by a black and white video camera). A "white" reflection will result if the light source and the camera are coaxial, a condition generated by the optics. The dark pupil approach utilizes an infrared light off axis from the camera and looks for a dark pupil.

The hardware utilized for the initial pupil and corneal reflection discrimination is largely analog in nature. Different approaches involve different timing for conversion of the analog signal to digital form. A computer is used to handle some of the more complex calculations associated with determining the centroid of the pupil and corneal reflections.

A bright pupil signal is much greater intensity than a dark pupil signal and it is therefore easier for an analog circuit to process it. This approach was developed at a time when analog-to-digital conversion was not fast enough to process a video image. Hence, analog circuitry was the only viable alternative, and since the bright pupil approach was better suited to analog technology, it was the approach used.

The Bright Pupil Approach

The present bright pupil oculometer system takes the video input from a head mounted camera and outputs eye position data. The eye tracking and calibration portions of the system are designed in such a way that one cannot be separated from the other. The present oculometer has a complex calibration algorithm that maps eye centroid data to real world coordinates. It is difficult, however, to assess the capabilities of these algorithms because problems in discrimination are such that is difficult to assess what proportion of the error is attributable to discrimination and what proportion of the error is attributable to calibration. In order to get only centroid data, we would have to make a modification to the software to permit access to these centroid data. This program is proprietary and not available to Analytics.

The Dark Pupil Approach

The dark pupil oculometer takes a video image of the eye (either from a remote camera or a head mounted system) and produces digital outputs denoting the centroid of the pupil, the centroid of the corneal reflection and the diameter of the pupil. These digital outputs can be sent to a host computer or they can be sent to another unit which then maps the data onto a video image.

A dark pupil eye tracker is completely different from the present system. Pupil and corneal reflection tracking have been reduced to sixteen application specific integrated circuits or "custom chip" components. The video signal is digitized to eight bit resolution prior to signal processing, thereby reducing signal noise and permitting the use of complex signal processing algorithms. The entire system is controlled by software in EPROMs, thereby allowing minor systems modifications without substantial changes to the hardware. All of the hardware is contained in a single board inside the unit.

Dark pupil images involve scanning for objects whose voltages are at or near 0.0 volts (i.e., ground or video black level). A purely analog system trying to analyze a dark pupil signal is susceptible to signal noise. Analog-to-digital conversion has made significant progress in the past few years, and it is now possible to digitize a video signal. When the video image is digitized much of the signal noise can be eliminated. Further, digital technology has progressed to the point where this digitized information can be processed by elaborate algorithms to eliminate other random signals. With these changes in technology it becomes feasible to process a dark pupil image more effectively.

Performance

In evaluating system performance, special emphasis is placed on the ability to track the pupil and corneal reflection under various conditions of eye occlusion and ambient light since these two factors have the greatest impact on a CORS system. Neither of these factors can be controlled in an operational environment.

Our current oculometer is particularly sensitive to ambient light. This seems to affect the system in two ways. First, bright light causes the pupil to shrink and, hence, reduces the amount of light reflected off the retina bounded by the pupil. Second, if the ambient light contains infrared light (as is the case with incandescent light) the image of the surrounding skin is intensified thereby reducing the contrast between the skin and the pupil reflection. When either of these conditions occur, the oculometer invariably has trouble tracking the pupil. Further, the oculometer has difficulties with occlusions such as eye lashes and eyelids. These problems are, to some extent, inherent to the overall bright pupil approach, but most of it is due to the manner in which the oculometer processes the pupil image. The hardware and algorithms, apparently, cannot deal with erroneous information adequately.

A dark pupil oculometer seems to contain solutions to many of the problems associated with ambient light and occlusions which would be important in the operational environment. First, it can perform in a brightly lit room. Second, it is able to handle eye occlusions better. Such results indicate that pupil discrimination algorithms are extremely robust. However, there may be problems when shadows are present in the video image. This system can be adapted to track a bright pupil if there is such a requirement.

The Computer

The CORS computer is capable of performing within the laboratory setting but it has marginal capacity to support an operational system. The CORS computer is based on a 32 bit, 20 MHz CPU. The speed and power of a computer depend not only on the cycle time of the CPU but also on a number of other associated characteristics, such as the operating system, the input/output facilities, and the instruction set. The operating system, for example, was not

designed for on-line data acquisition and processing and does not take full advantage of the 32 bit architecture. Replacement with an operating system designed for such on-line applications would improve overall performance. Similarly, reduced instruction set computers (RISC technology) typically show instruction execution two to four times faster than larger instruction set machines and would increase the data processing capacity. Finally, the communication between the primary CPU on the motherboard and the two other CPUs in the system (on the parallel board and the serial board) was not balanced for optimal performance. This imbalance should be corrected.

New Flight Data Recording Technology

Most of the aircraft parameters currently being recorded on DFDRs are continuous temporal data which do not change rapidly. Interpolation between data points is reasonable. Over the years, flight data recorder applications have gradually become more sophisticated with more variables being recorded.

Eye movement time histories are dramatically different from the aircraft parameters. The eye moves in a discontinuous manner and it moves frequently. Time intervals (dwells) of as little as a 100 msec can be important. CORS is capable of capturing these short time frames and thus, CORS can generate a large (huge) amount of data relative to other variables being recorded. For CORS to be effective in an optimal manner, it will be necessary to incorporate advanced technology into new flight data recording systems.

Write once, read many (WORM) optical disks are one possibility and may well be used in future DFDRs. They have the advantage of greatly increased recording speeds, as well as greatly enhanced storage capabilities. Use of WORMs would permit expanded data recording in modern airliners, including that of pilot eye tracking.

The Ideal System

Having discussed some of the possible improvements to the prototype, it is now appropriate to consider what an ideal operational system might look like sometime in the future. It is entirely within the practical realm to envisage the day when CORS will be an operational device used every day in aviation. The components of CORS would look somewhat different from the prototype discussed in this report; however, most of the components of this ideal system utilize realizable technology.

The weight of the components would be a consideration. The flight data recorder is already on board so that item is not a consideration. However, the CORS computer, the oculometer, and the head tracker would need to be added. These items have some considerable

weight in the prototype. However, the use of very large scale integration (VLSI) digital circuitry along with miniaturization of the other components would permit future development of a light weight system. The software would be put in read only memory (ROM) eliminating the need for an onboard disk drive. For maintenance purposes, the keyboard, the monitor, and a disk drive could be plugged into the system but would not be needed in operation.

The biggest obstacle is the engineering of the sensor devices to meet with acceptable human engineering practices for safety, convenience, and comfort. For both laboratory and prototype purposes, a helmet mounted oculometer is acceptable. However, the CORS sensors need to be integrated with other devices. For example, commercial pilots currently need and use a microphone and an ear phone for communications. Many pilots also wear glasses. For this reason alone, it is impractical to wear a helmet. Combined with other considerations such as safety, helmet weight, and a probable lack of pilot acceptance of a helmet, it is clear that the future operational system would not include a helmet.

Because many pilots already wear spectacles, it would seem that an approach utilizing eye glass frames may be a viable one. A number of items could be integrated with the eye glass frame:

- The boom microphone could be conveniently attached to the eye glass frame.
- Prescription lenses would individualize the eye glass frames for each pilot.
- The eye monitor camera which would be light weight and mounted on the frame. It would measure light reflected off the eye glass lens just as a half silvered mirror would.
- The head tracker transmitter could also be attached to the glass frame. Use of an infrared head tracking system could provide separation of signals for the head movements of the pilot and the co-pilot.

Another advance would include simplified and automated calibration procedures. These automated routines could be integrated into the checklist and preflight checkout procedures. While this approach would not totally eliminate the need for calibration, it would reduce the steps currently required in the prototype.

Finally, the future operational CORS system might also integrate the OASIS concept. OASIS provides eye-voice integration to provide hands free command and control of many or all aircraft system functions.

CONCLUSIONS

The overall goal of developing a prototype system to record eye scan data on a flight data recorder was accomplished. The present CORS system was built as a laboratory prototype and therefore does not meet the performance requirements of an operational system. The transformation of CORS from a laboratory prototype to an operational system was beyond the scope of this effort; however, the potential capability of CORS was clearly demonstrated during the current research.

The primary function of CORS is the collection and recording of eye scan data, stated in terms of positions and instruments scanned in the cockpit. To this end, a number of detailed aspects of the prototype system were demonstrated:

- The integration of the oculometer and head tracker signals so as to be able to obtain observations throughout the entire cockpit,
- The development of data processing routines on a personal computer,
- The demonstration that a moderately priced personal computer is capable (marginally) of performing the necessary processing,
- The writing to and recovery of data from a commercial digital flight data recorder, and that
- The entire system can be assembled from off-the-shelf components.

The equipment components were assembled into a functional prototype system with data processing algorithms providing the integration. One purpose of a prototype is to demonstrate the concept and to identify areas for improvement. Accordingly, there are several suggestions discussed here. First we provide a brief summary of the capabilities of CORS which provides the background for the improvements and then a discussion of possible future improvements.

Although CORS does a reasonable job in identifying each dwell region, CORS is currently less accurate in areas off the test subject's midline (the longitudinal axis of the mockup cockpit) than on the test subject's midline. Performance of CORS is an interaction of concatenating individual variables and although we have identified the important variables, we cannot isolate and improve the first link in the chain, calibration. Several problems in the components were identified:

- The calibration routines within the oculometer,
- The reduced capabilities of the oculometer in the lower portion of the field-of-view, and
- The helmet which contributes to sensor instabilities.

Several other accuracy issues in the prototype were also identified. For the first, this is simply a matter of geometry. In the second case, it is not presently known where the basis of the accuracy deficiency exists. These are:

- For processing a POG within a plane in which the line of sight is not perpendicular to the plane and
- For processing a POG within planes to the left or right of the test subject.

The combination and chaining of problems as well as completion of the period of performance has precluded testing the head movement/eye position integration more fully. This is certainly an area where additional work should be done. However, it is both appropriate and necessary to correct the hardware problems first.

REFERENCES

Dick, A. O. (1980). *Instrument scanning and controlling: Using eye movement data to understand pilot behavior and strategies.* NASA Contractor Report 3306.

Hallett, P. (1986). Eye movements. In K. R. Boff, L. Kaufman, & J. P. Thomas (Eds.), *Handbook of perception and human performance. Volume I: Sensory processes and perception.* New York: John Wiley.

Harris, R. L., Sr., & Christhilf, D. M. (1980). What do pilots see in displays? *Proceedings of the Human Factors Society 24th Annual Meeting.* Santa Monica, CA: Human Factors Society.

Harris, R. L., Sr., Glover, B., J. & Spady, A. A., Jr. (1986). *Analytical techniques of pilot scanning behavior and their application.* NASA Technical Paper 2525.

APPENDIX A

Glossary

Glossary

Harris, Glover, and Spady (1986) developed a number of definitions. The use of terms in this report is intended to be consistent with and parallel to the use by those authors. Additional terms are also defined.

bps. Bits per second, an electronic data transmission rate.

Dwell time. The time spent looking within the boundaries of a region. *

Fixation. A series of continuous lookpoints which stay within a circle [of 52 minutes radius at the calibration plane]. *

Lookpoint. The current coordinates of where the test subject is looking within a single time frame. *

Background region. A region which does not contain an instrument.

Oculometer. A device which measures the lookpoint of a test subject. *

Out of track. A state in which the oculometer cannot determine where the pilot is looking, such as during a blink or when the subject's head movement has exceeded the tracking capabilities of the oculometer. [Not applicable in CORS due to head movment tracking, but see null region.] *

Panel. A surface area in the cockpit. A panel may contain instruments or could be, for example, a window.

Plane. A three dimensional representation of a panel in CORS.

Point of gaze. A term parallel to fixation. The point of gaze is determined with reference to the EVM calibration plane and has to be converted to a region. It is a moving window containing 12 lookpoint frames and spatially represented by a circle of 52 minutes radius

Point of regard. The lookpoint translated into regions on a plane, e.g., an instrument.

Region. An area on a panel, the perimeter of which corresponds to instrument boundaries.

Saccade. The spatial change in fixations. [The duration of a saccade is within the range of 20 to 100 msec.] *

* Indicates definitions found in Harris, et al. (1986). Material in [ ] has been added to the Harris et al. definition.

APPENDIX B

Data for Individual Subjects, Accuracy Experiment

Table B-1. Cluster size data, Subject 1.

RUN	POINT	100%			90%		
		AVG deg	RMS deg	MAX deg	AVG deg	RMS deg	MAX deg
1	1	0.8438	0.9660	2.6253	0.7518	0.8480	1.4157
	2	0.4194	0.5840	2.5211	0.3089	0.3550	0.7893
	3	0.3649	0.4550	1.6200	0.3049	0.3390	0.6237
	4	0.5647	1.0630	7.6846	0.4045	0.4460	0.8384
	5	0.4528	0.5280	1.4301	0.3942	0.4480	0.8510
2	1	0.5665	0.6480	1.4694	0.4975	0.5550	1.0269
	2	0.3513	0.4140	1.1464	0.3004	0.3420	0.6864
	3	0.6431	1.1960	5.0805	0.3847	0.4150	0.7437
	4	0.4348	0.4880	1.3011	0.3824	0.4150	0.7198
	5	0.2345	0.2620	0.7365	0.2088	0.2270	0.3852
3	1	0.8037	0.8630	1.8144	0.7374	17.3200	1.2700
	2	0.4257	0.5930	2.5693	0.3125	7.8300	0.8664
	3	0.6233	0.9660	4.9258	0.4636	11.3100	0.9173
	4	1.0292	1.4040	8.6984	0.7802	20.3220	2.1395
	5	0.4357	0.8260	16.7731	0.3608	5.8400	0.7230
4	1	0.4911	0.5650	1.6452	0.4275	10.6000	0.8979
	2	0.5606	1.0990	7.2548	0.3806	9.7100	0.8447
	3	0.7581	1.1560	4.9673	0.5177	13.6800	1.3580
	4	0.8948	2.1680	13.9147	0.5331	12.9200	1.0206
	5	0.9291	1.4000	3.6071	0.6458	20.2300	3.0370
5	1	0.7775	0.8110	1.6628	0.7302	0.7530	1.0021
	2	0.4122	0.4700	1.2651	0.3653	0.4080	0.7166
	3	0.4253	0.6120	3.0650	0.3297	0.3640	0.6319
	4	0.9309	1.2540	5.3858	0.7000	0.7950	1.7287
	5	0.4131	0.4660	1.0797	0.3644	0.3990	0.7180

Table B-2. Cluster size data, Subject 1 (cont.).

RUN	POINT	100%			90%		
		AVG deg	RMS deg	MAX deg	AVG deg	RMS deg	MAX deg
6	1	0.5444	0.6370	2.8102	0.4736	0.5100	0.8560
	2	0.5525	0.6330	1.6060	0.4862	0.5440	0.9899
	3	0.4352	0.4850	1.2655	0.3883	0.4230	0.7130
	4	1.3097	1.7070	3.6914	1.0499	1.3270	3.6107
	5	0.4884	0.5950	2.4800	0.4131	0.4570	0.8082
7	1	0.8217	0.8650	1.3882	0.7816	0.8210	1.1004
	2	0.2918	0.3360	1.0468	0.2548	0.2820	0.4325
	3	0.3189	0.3690	0.9949	0.2724	0.2990	0.6260
	4	0.5362	0.6370	1.9343	0.4239	0.4770	1.0427
	5	0.3509	0.3940	1.5609	0.3094	0.3350	0.5858
8	1	0.4285	0.4860	1.2763	0.3770	0.4160	0.7541
	2	0.3351	0.3860	0.9187	0.2963	0.3370	0.6102
	3	0.3987	0.4910	1.7575	0.3301	0.3610	0.6255
	4	0.3477	0.4830	2.7137	0.2643	0.2890	0.5150
	5	0.3031	0.4650	2.1883	0.1935	0.2200	0.9110
9	1	0.7703	0.9050	2.0182	0.6490	0.7250	1.6836
	2	0.5877	0.8440	3.0406	0.4163	0.4780	1.1514
	3	0.4487	0.6130	2.5775	0.3437	0.3940	0.7861
	4	1.2118	2.1190	9.4985	0.7581	0.8480	2.2748
	5	0.3549	0.4280	2.4489	0.2981	0.3340	0.6251
10	1	0.5953	0.6770	1.8798	0.5205	0.5670	0.9872
	2	0.3238	0.3770	1.4044	0.2765	0.3050	0.5678
	3	0.4898	0.5570	1.5244	0.4280	0.4700	0.8506
	4	0.7568	0.9760	3.3415	0.5849	0.6710	1.6182
	5	0.4587	0.5070	1.1491	0.4095	0.4410	0.7906

Table B-3. Cluster size data, Subject 2.

RUN	POINT	100%			90%		
		AVG deg	RMS deg	MAX deg	AVG deg	RMS deg	MAX deg
1	1	0.6472	0.7360	2.1111	0.5701	0.6280	1.0806
	2	0.4799	0.5700	2.0448	0.4050	0.4540	0.8952
	3	0.6170	0.8800	6.4741	0.4731	0.5400	1.2790
	4	0.6350	0.7210	1.7246	0.5660	0.6340	1.1158
	5	1.0287	1.1980	3.2725	0.8835	0.9840	1.8198
2	1	0.3843	0.4330	1.1334	0.3396	0.3720	0.6526
	2	0.3563	0.4050	1.4942	0.3116	0.3400	0.6102
	3	0.3473	0.4210	1.3300	0.2900	0.3330	0.6815
	4	0.8560	1.0110	3.3618	0.7302	0.8260	1.6295
	5	0.5371	0.6520	2.1147	0.4411	0.4960	1.0341
3	1	0.3698	0.4270	1.0747	0.3252	0.3680	0.6544
	2	0.4460	0.6060	4.1975	0.3608	0.3920	0.6688
	3	0.4086	0.4810	1.5339	0.3477	0.3860	0.7324
	4	0.7306	0.8830	3.2873	0.6079	0.6900	1.3728
	5	0.5453	0.6670	3.1290	0.4501	0.4940	0.9079
4	1	0.3919	0.4350	1.0436	0.3500	0.3780	0.6512
	2	0.3703	0.4200	1.2899	0.3252	0.3560	0.6188
	3	0.4244	0.5220	1.8144	0.3504	0.3970	0.7708
	4	0.7802	0.8920	3.0573	0.6833	0.7470	1.2786
	5	0.4077	0.4890	2.1982	0.3450	0.3860	0.6792
5	1	0.3464	0.3830	1.1464	0.3080	0.3300	0.5827
	2	0.7225	1.9990	13.2215	0.4014	0.4430	0.8181
	3	0.3635	0.4200	0.9940	0.3184	0.3600	0.6625
	4	0.7211	0.8560	2.5621	0.6165	0.7080	1.3995
	5	0.3193	0.3580	0.8876	0.2805	0.3030	0.5371

Table B-4. Cluster size data, Subject 2 (cont.).

RUN	POINT	100%			90%		
		AVG deg	RMS deg	MAX deg	AVG deg	RMS deg	MAX deg
6	1	0.4591	0.5810	2.3759	0.3644	0.4040	0.8055
	2	0.5335	0.6310	1.8121	0.4492	0.5020	1.0346
	3	1.2578	1.6040	4.[illegible]	1.0319	1.2660	2.5337
	4	0.7306	0.8410	2.1946	0.6382	0.7120	1.2678
	5	1.0883	1.2750	6.8728	0.9309	1.0300	2.0047
7	1	1.2145	1.3990	4.3210	1.0486	1.1490	2.1607
	2	0.7960	1.1490	4.1884	0.5480	0.6300	1.8937
	3	0.7410	1.0350	4.5023	0.5922	0.6060	1.4653
	4	0.7771	0.9100	2.8963	0.6598	0.7300	1.3940
	5	0.3901	0.4600	1.2520	0.3319	0.3750	0.7211
8	1	0.3143	0.3550	1.1613	0.2760	0.2990	0.5196
	2	0.2927	0.3480	1.0617	0.2494	0.2850	0.5385
	3	0.8055	1.1010	4.8685	0.5913	0.7020	2.2013
	4	1.0373	1.2080	3.1841	0.8934	1.0030	1.8924
	5	0.4064	0.4740	2.2365	0.3513	0.3920	0.7081
9	1	0.4073	0.4700	1.3616	0.3540	0.3970	0.7442
	2	0.3843	0.4400	1.3142	0.3346	0.3670	0.6454
	3	0.3883	0.4520	1.3070	0.3346	0.3750	0.7284
	4	0.8772	1.0510	3.8186	0.7469	0.8570	1.5591
	5	0.4253	0.4820	1.4549	0.3766	0.4180	0.7595
10	1	0.3157	0.3630	1.1753	0.2724	0.2980	0.5732
	2	0.3594	0.4040	1.1843	0.3193	0.3490	0.6057
	3	0.4533	0.5890	2.6704	0.3545	0.4050	0.8118
	4	1.1068	1.3610	5.1152	0.9043	1.0250	1.9961
	5	1.4292	2.3500	16.4457	1.0932	1.1930	2.1423

Table B-5. Cluster size data, Subject 3.

RUN	POINT	100%			90%		
		AVG deg	RMS deg	MAX deg	AVG deg	RMS deg	MAX deg
1	1	0.3044	0.3420	0.9052	0.2683	0.2920	0.5141
	2	0.2602	0.2990	0.8574	0.2282	0.2550	0.4492
	3	0.2810	0.3300	1.0242	0.2422	0.2750	0.5191
	4	0.2751	0.3110	0.7496	0.2431	0.2670	0.4776
	5	0.3301	0.3850	1.1203	0.2873	0.3260	0.6079
2	1	0.2733	0.3050	0.8668	0.2435	0.2660	0.4524
	2	0.2769	0.3100	0.7847	0.2481	0.2720	0.4645
	3	0.3554	0.4080	0.9521	0.3116	0.3500	0.6521
	4	0.3243	0.3600	0.9890	0.2873	0.3080	0.5038
	5	0.2729	0.3030	0.9557	0.2444	0.2640	0.4384
3	1	0.3031	0.3440	0.8758	0.2652	0.2910	0.5074
	2	0.3234	0.3590	0.9448	0.2900	0.3140	0.5277
	3	0.2927	0.3460	1.1009	0.2499	0.2840	0.5520
	4	0.3590	0.4040	1.1383	0.3157	0.3410	0.6102
	5	0.2932	0.3650	1.9267	0.2444	0.2730	0.5038
4	1	0.2692	0.3010	0.7509	0.2377	0.2570	0.4316
	2	0.2517	0.2910	0.7175	0.2187	0.2440	0.4447
	3	0.3310	0.3670	0.8921	0.2968	0.3220	0.5471
	4	0.3834	0.4320	1.0175	0.3405	0.3740	0.6693
	5	0.3216	0.3680	1.1307	0.2774	0.3020	0.5660
5	1	0.2909	0.3300	0.7405	0.2566	0.2850	0.5272
	2	0.3157	0.3680	1.2421	0.2720	0.3030	0.5430
	3	0.3125	0.3490	0.8601	0.2778	0.3020	0.5209
	4	0.3040	0.3420	0.8704	0.2688	0.2950	0.5254
	5	0.2647	0.3070	0.8587	0.2278	0.2520	0.4681

Table B-6. Cluster size data, Subject 3 (cont.).

RUN	POINT	100%			90%		
		AVG deg	RMS deg	MAX deg	AVG deg	RMS deg	MAX deg
6	1	0.3044	0.3410	0.8312	0.2724	0.3000	0.5173
	2	0.3107	0.3440	0.8344	0.2787	0.3010	0.5123
	3	0.3202	0.3580	1.0215	0.2828	0.3060	0.5358
	4	0.3049	0.3590	1.1879	0.2598	0.2920	0.5498
	5	0.5015	0.5640	1.2817	0.4433	0.4860	0.8682
7	1	0.3193	0.3530	0.8587	0.2877	0.3120	0.5308
	2	0.3549	0.3970	1.1004	0.3162	0.3450	58.8104
	3	0.3432	0.3800	0.8298	0.3116	0.3410	0.5547
	4	0.2932	0.3230	1.1970	0.2647	0.2840	0.4623
	5	0.2823	0.3190	0.7090	0.2503	0.2780	0.4920
8	1	0.2656	0.3040	0.7284	0.2327	0.2600	0.4785
	2	0.2810	0.3170	0.7653	0.2476	0.2720	0.4907
	3	0.2841	0.3230	1.2975	0.2503	0.2770	0.4799
	4	0.2968	0.3440	0.9827	0.2557	0.2860	0.5525
	5	0.2963	0.3280	0.9566	0.2647	0.2840	0.4772
9	1	0.3035	0.3370	0.8456	0.2679	0.2880	0.4993
	2	0.2692	0.3230	1.1487	0.2273	0.2550	0.4812
	3	0.4032	0.4350	0.9710	0.3671	0.3870	0.6192
	4	0.3148	0.3580	0.9236	0.2774	0.3060	0.5606
	5	0.3067	0.3390	0.9701	0.2760	0.2970	0.4835
10	1	0.4542	0.5010	1.2921	0.4077	0.4400	0.7392
	2	0.2787	0.3190	0.8808	0.2422	0.2670	0.4821
	3	0.2620	0.2990	0.8145	0.2291	0.2530	0.4578
	4	0.2819	0.3420	0.9945	0.2363	0.2740	0.5809
	5	0.3928	0.4370	1.0752	0.3513	0.3830	0.6571

Table B-7. Cluster offset data, Subject 1.

RUN	POINT	RMS	RUN RMS
1	1	0.871	.786
	2	1.256	
	3	0.273	
	4	0.691	
	5	0.446	
2	1	1.679	2.662
	2	2.311	
	3	3.297	
	4	3.314	
	5	2.326	
3	1	1.414	1.06
	2	0.889	
	3	0.356	
	4	0.243	
	5	1.625	
4	1	1.574	1.155
	2	1.552	
	3	0.29	
	4	0.112	
	5	0.941	
5	1	0.965	0.824
	2	1.178	
	3	0.81	
	4	0.338	
	5	0.555	

RUN	POINT	RMS	RUN RMS
6	1	1.3453	2.0796
	2	1.0166	
	3	2.1792	
	4	1.979	
	5	2.2654	
7	1	0.4875	0.9128
	2	1.1604	
	3	0.7667	
	4	1.0675	
	5	0.9255	
8	1	0.5484	0.8217
	2	0.9426	
	3	0.6733	
	4	0.8163	
	5	1.0323	
9	1	1.022	1.2127
	2	1.5059	
	3	1.2867	
	4	1.8757	
	5	1.422	
10	1	1.2642	0.7221
	2	0.7581	
	3	0.1033	
	4	0.5444	
	5	0.3572	

Table B-8. Cluster offset data, Subject 2.

RUN	POINT	RMS	RUN RMS
1	1	2.237	2.448
	2	1.782	
	3	1.706	
	4	1.556	
	5	4.057	
2	1	0.277	1.638
	2	0.667	
	3	0.674	
	4	3.498	
	5	0.451	
3	1	1.395	2.333
	2	0.612	
	3	0.666	
	4	4.918	
	5	0.51	
4	1	1.726	2.549
	2	0.675	
	3	1.297	
	4	5.134	
	5	1.001	
5	1	0.093	1.911
	2	0.267	
	3	0.355	
	4	4.159	
	5	0.869	

RUN	POINT	RMS	RUN RMS
6	1	0.822	2.373
	2	0.52	
	3	1.222	
	4	3.695	
	5	3.472	
7	1	0.635	1.262
	2	1.21	
	3	0.621	
	4	2.062	
	5	1.211	
8	1	1.015	1.371
	2	1.086	
	3	0.634	
	4	2.45	
	5	0.888	
9	1	1.006	1.686
	2	0.851	
	3	0.595	
	4	3.295	
	5	1.122	
10	1	2.235	3.277
	2	1.398	
	3	1.059	
	4	4.62	
	5	4.926	

Table B-9. Cluster offset data, Subject 3.

RUN	POINT	RMS	RUN RMS
1	1	2.098	1.994
	2	1.825	
	3	1.918	
	4	2.021	
	5	2.096	
2	1	0.53	0.674
	2	1.029	
	3	0.686	
	4	0.181	
	5	0.656	
3	1	1.04	1.012
	2	0.854	
	3	0.818	
	4	1.175	
	5	1.125	
4	1	0.554	0.762
	2	0.662	
	3	0.656	
	4	0.263	
	5	1.287	
5	1	0.768	1.289
	2	1.139	
	3	0.98	
	4	1.438	
	5	1.843	
6	1	1.02	1.137
	2	1.231	
	3	1.045	
	4	1.17	
	5	1.585	
7	1	0.49	0.445
	2	0.301	
	3	0.476	
	4	0.51	
	5	0.413	
8	1	0.639	0.939
	2	0.677	
	3	0.746	
	4	1.13	
	5	1.306	
9	1	0.301	0.622
	2	0.873	
	3	0.359	
	4	0.175	
	5	0.96	
10	1	2.047	1.437
	2	1.157	
	3	1.327	
	4	1.524	
	5	0.845	

Table B-10. Angular offset data, Subject 1.

RUN	POINT	OFFSET ANGLE deg	AVG OFFSET deg
1	1	112.53°	112.75°
	2	36.56°	
	3	59.70°	
	4	111.74°	
	5	22.33°	
2	1	3.31°	60.32°
	2	1.99°	
	3	4.27°	
	4	16.07°	
	5	15.04°	
3	1	46.78°	52.35°
	2	6.46°	
	3	11.47°	
	4	34.00°	
	5	57.78°	
4	1	15.19°	78.36°
	2	2.36°	
	3	3.04°	
	4	1.98°	
	5	18.62°	
5	1	32.64°	64.99°
	2	11.00°	
	3	1.15°	
	4	39.51°	
	5	2.97°	
6	1	15.44°	5.81°
	2	14.73°	
	3	14.20°	
	4	5.14°	
	5	21.11°	
7	1	72.53°	7.18°
	2	32.23°	
	3	7.04°	
	4	60.49°	
	5	37.23°	
8	1	55.99°	9.50°
	2	36.57°	
	3	2.80°	
	4	26.13°	
	5	69.24°	
9	1	17.29°	30.78°
	2	1.77°	
	3	7.31°	
	4	15.64°	
	5	10.74°	
10	1	97.55°	19.10°
	2	40.14°	
	3	88.19°	
	4	13.89°	
	5	35.61°	

Table B-11. Angular offset data, Subject 2.

RUN	POINT	OFFSET ANGLE deg	AVG OFFSET deg
1	1	19.02°	173.30°
	2	0.32°	
	3	29.75°	
	4	11.24°	
	5	0.18°	
2	1	62.27°	23.52°
	2	6.01°	
	3	15.83°	
	4	125.38°	
	5	72.92°	
3	1	3.35°	118.54°
	2	27.73°	
	3	30.99°	
	4	3.77°	
	5	65.87°	
4	1	15.71°	94.83°
	2	5.01°	
	3	4.23°	
	4	12.36°	
	5	28.90°	
5	1	103.67°	51.23°
	2	58.85°	
	3	4.05°	
	4	160.62°	
	5	4.57°	

RUN	POINT	OFFSET ANGLE deg	AVG OFFSET deg
6	1	8.33°	150.06°
	2	51.42°	
	3	11.44°	
	4	29.09°	
	5	19.22°	
7	1	36.25°	22.76°
	2	25.85°	
	3	11.80°	
	4	89.17°	
	5	66.96°	
8	1	4.40°	119.72°
	2	55.88°	
	3	11.55°	
	4	107.31°	
	5	35.43°	
9	1	15.45°	133.75°
	2	49.27°	
	3	31.70°	
	4	22.82°	
	5	119.26°	
10	1	2.23°	105.35°
	2	15.28°	
	3	36.14°	
	4	3.33°	
	5	45.85°	

Table B-12. Angular offset data, Subject 3.

RUN	POINT	OFFSET ANGLE deg	AVG OFFSET deg
1	1	2.28°	93.05°
	2	3.74°	
	3	6.26°	
	4	15.99°	
	5	3.69°	
2	1	10.31°	21.46°
	2	28.47°	
	3	28.80°	
	4	80.47°	
	5	33.50°	
3	1	38.16°	187.44°
	2	18.94°	
	3	5.37°	
	4	11.36°	
	5	63.10°	
4	1	40.93°	39.95°
	2	0.92°	
	3	5.99°	
	4	14.26°	
	5	33.59°	
5	1	5.46°	99.96°
	2	9.41°	
	3	11.07°	
	4	13.40°	
	5	1.61°	

RUN	POINT	OFFSET ANGLE deg	AVG OFFSET deg
6	1	17.75°	100.69°
	2	8.34°	
	3	15.06°	
	4	7.81°	
	5	8.31°	
7	1	41.79°	172.81°
	2	23.53°	
	3	5.98°	
	4	19.78°	
	5	39.56°	
8	1	31.47°	103.46°
	2	17.06°	
	3	22.19°	
	4	10.54°	
	5	2.76°	
9	1	2.41°	86.66°
	2	27.08°	
	3	42.76°	
	4	71.32°	
	5	3.90°	
10	1	7.42°	131.15°
	2	6.79°	
	3	7.00°	
	4	0.63°	
	5	6.99°	

C-2

APPENDIX C

Oculometer Survey

Table C-1. Oculometer Manufactures and models by characteristics of each device.

OCULOMETER MAKE	COST($)	HEAD RESTRAINT	ACCURACY	TEMPORAL RESOLUTION	MOUNT TYPE/ INTRUSIVE	METHOD OF DETECTION	SUBJECT DISCOMFORT/ AWARENESS	GLASSES/ CONTACTS COMPATIBILITY	VISUAL INTERFERENCE
ASL 1998 <1>	150,000 to 175,000	NONE	1° W/ IN 20° OTHERWISE 2°-3°	16.67 ms	RACK MOUNTED CAN IMPLEMENT HELMET	LIGHT PUPIL & CORNEA	MODERATE	MODERATE SOME GLASSES PROBLEM	MINIMAL
HONEYWELL	400,000	NONE	.5°	16.67 ms	HELMET MOUNTED	IR BEAM PUPIL & CORNEA	MODERATE	MODERATE SOME GLASSES PROBLEM	MINIMAL
NAC Eyemark V	14,300	HEADSET	1°	16.67 ms	GOGGLE MOUNT	IR BEAM BACK OF CORNEA	MODERATE	MINIMAL SOFT CONTACTS ONLY	MODERATE PERIPHERAL OBSTRUCTION
MICROMEASUREMENTS SYSTEM 1200 <2>	10,000	CHIN RESTRAINED	1° W/ IN 20°	16.67 ms	TABLE MOUNT	DARK PUPIL & CORNEA	MODERATE	MODERATE SOME GLASSES PROBLEM	MODERATE LEFT-SIDE OBSTRUCTION
MICROMEASUREMENTS SYSTEM 1200 <2>	10,000	NONE	3°-4°	16.67 ms	HELMET MOUNT	CORNEA & ARTIFICIAL CORNEA	MODERATE	MODERATE SOME GLASSES PROBLEM	MODERATE LEFT-SIDE OBSTRUCTION
DENVER RESEARCH INSTITUTE EYEGLASSES	2,000	NONE	2°-3°	UNKNOWN	GLASSES MOUNTED	CORNEA	MINIMAL	COMPLETELY COMPATIBLE	NONE
ASL 1996 <1>	100,000 + 30,000 w/ head movement	NONE	1°	16.67 ms	RACK OR HELMET MOUNT	LIGHT PUPIL & CORNEA	MINIMAL	MODERATE HARD LENS PROBLEM	NONE
ISCAN RK426 <3>	20,000	NONE	1°	16.67 ms	FIXED OR HELMET	DARK PUPIL, CORNEA	MINIMAL	MAXIMAL	NONE
SST EYETYPER 300	8,000	NONE	2°-3°	16.67 ms	UNINTRUSIVE	VIDEO CAMERA	MINIMAL	MINIMAL NO GLASSES	NONE
UNIVERSAL INTRAM CO. OFTALMOGRAF	13,000	MOUTH RESTRAINED	<.5°	1 ms	HELMET/ HEADSTRAP MOUNTED	4 IR BEAMS CAMERA	MAXIMAL	MODERATE SOME GLASSES PROBLEM	MODERATE SLIGHTLY BELOW OBSTRUCTED
FORWARD TECHNOLOGY <4>	60,000 +	CHIN RESTRAINED	1'	1 ms	CHIN REST	1ST AND 4TH PURKINJE IMAGE	MAXIMAL	MODERATE SOME GLASSES PROBLEM	MINIMAL
STOELTING CO.	10,000	NONE	1°	16.67 ms	CHIN REST	DARK PUPIL	MAXIMAL	MODERATE SOME GLASSES PROBLEM	MINIMAL

Table C-1. Oculometer Manufactures and models by characteristics of each device. (Cont.)

OCULOMETER MAKE	EYE MOVEMENT W/ RESPECT TO HEAD	HEAD MOVEMENT W/ RESPECT TO CABIN	HEAD/BODY TRANSLATION	AMBIENT LIGHT CONSIDERATIONS	VIBRATION STABILITY CONDITIONS	SIZE/WIEGHT	CALIBRATION TIME/ EXPERTISE	CALIBRATION PATTERN
ASL 1998 <1>	20° ANY DIRECTION	TRACKING MIRROR OR POLHEMUS	1 CUBIC INCH	MODERATE BRIGHT LIGHT PROBLEM	MAXIMAL CAN BE MINIMIZED WITH HELMET	HELMET 10 OZ UNIT FAIRLY LARGE	MAXIMAL LONGER THAN 20 MINUTES	9PTS
HONEYWELL	FULL RANGE	FULL RANGE	1 CUBIC FOOT	MODERATE BRIGHT LIGHT PROBLEM	MINIMAL	HELMET 4 LBS RACK HUGE	MINIMAL SEVERAL MINUTES	UNKNOWN
NAC Eyemark V	30° LEFT-RIGHT 22° UP-DOWN	FULL USES POLHEMUS MAGNETIC SENSOR	FULL RANGE	MINIMAL	MODERATE	HELMET 1.7 LBS RACK 8 LBS MODERATE	MAXIMAL 15 MINUTES	UNKNOWN
MICROMEASUREMENTS SYSTEM 1200 <2>	20° ANY DIRECTION	NONE	NONE YET	MINIMAL	MINIMAL	SYSTEM 35 LBS 17" x 18" x 5"	MINIMAL SEVERAL MINUTES	9 PTS
MICROMEASUREMENTS SYSTEM 1200 <2>	20° ANY DIRECTION	FULL POLHEMUS HEAD TRACKING AVAILABLE	FULL RANGE	MINIMAL	MINIMAL	HELMET 10 OZ SYSTEM 35 LBS 17" x 18" x 5"	MINIMAL SEVERAL MINUTES	9 PTS
DENVER RESEARCH INSTITUTE EYEGLASSES	15° ANY DIRECTION	NONE	NONE	MINIMAL	MINIMAL	SEVERAL OUNCES	MAXIMAL 30 MINUTES	NONE
ASL 1996 <1>	20° LEFT-RIGHT 25° UP 5° DOWN	TRACKING MIRROR OR POLHEMUS	2 CUBIC INCHES	MINIMAL	MAXIMAL	HUGE	MAXIMAL 15-20 MINUTES	9 PTS
ISCAN RK426 <3>	15° ANY DIRECTION	FULL POLHEMUS HEAD TRACKING	FULL BODY	MINIMAL	MODERATE	RACK 12 LBS 19" x 5.5" x 16"	MODERATE 5-10 MINUTES	5 PTS
SST EYETYPER 300	45° ANY DIRECTION	NONE	NONE	MINIMAL	MAXIMAL	20 LBS	MODERATE 5-10 MINUTES	2 PTS
UNIVERSAL INTRAM CO. OFTALMOGRAF	50° LEFT-RIGHT 40° UP-DOWN	NONE SUGGEST USING CAMERA	NONE YET	MODERATE DARKNESS PROBLEM	MINIMAL	HELMET 3 LBS BAR MOUNT 7 OZ	MINIMAL SEVERAL MINUTES	UNKNOWN
FORWARD TECHNOLOGY <4>	25° ANY DIRECTION	NONE	1 CUBIC CM	MODERATE BRIGHT LIGHT PROBLEM	MODERATE	HUGE	MINIMAL SEVERAL MINUTES	UNKNOWN
STOELTING CO.	45° ANY DIRECTION	NONE	NONE	MODERATE BRIGHT LIGHT PROBLEM	MAXIMAL	FAIRLY SMALL	MINIMAL SEVERAL MINUTES	5 PTS

Table C-1. Oculometer Manufactures and models by characteristics of each device. (Cont.)

OCULOMETER MAKE	SERIAL CAPABILITY (BAUD RATE)	PARALLEL CAPABILITY	ANALOG CAPABILITY MAXIMAL VOLTAGE LEVEL	POWER REQUIREMENTS	# OPERATORS REQUIRED	PRESENTLY USING SYSTEM	ANTICIPATED UPGRADES
ASL 1998 <1>	NONE	20 BITS 10 BITS HORIZ. 10 BITS VERT.	+/- 5VDC	120 VAC 60 CYCLE	1	NAVAL TRAINING CENTER ORLANDO, FL.	IMPROVE HELMUT SYSTEM DESIGN & REDUCE SIZE
HONEYWELL	CAN EASILY BE ADDED AT ANY BAUD	16 BITS 9 WORDS	EASY TO ACCOMMODATE CAN BE MODULATED TO 400 HZ ALSO	120VAC 60 CYCLE CAN USE 400 CYCLE	AT LEAST 2	INFORMATION UNAVAILABLE	ANY CUSTOMIZATIONS
NAC Eyemark V	9600	NONE	+/- 5VDC	12VDC	2 FOR CALIB. 1 TO OPERATE	S. COLLEGE OF OPHTHALMOLOGY	NONE
MICROMEASUREMENTS SYSTEM 1200 <2>	NONE	9 BITS HORIZ. 9 BITS VERT. 9 BITS PUPIL AREA	+/- 5VDC TO +/- 10VDC	120 VAC 60 CYCLE	1	UNIV. OF ALABAMA & OHIO STATE	REDUCE SIZE IMPLEMENT HELMET
MICROMEASUREMENTS SYSTEM 1200 <2>	NONE	9 BITS HORIZ. 9 BITS VERT. RAW DATA	+/- 5VDC TO +/- 10VDC	120 VAC 60 CYCLE	1	UNIV. OF ALABAMA & OHIO STATE	NONE
DENVER RESEARCH INSTITUTE EYEGLASSES	300	10 BITS 5 BITS HORIZ. & VERT. RAW DATA	NONE	120 VAC 60 CYCLE 24V NO PROBLEM	2 FOR CALIB. 1 TO OPERATE	NATIONAL INSTITUTE OF HEALTH	INFORMATION UNAVAILABLE
ASL 1996 <1>	NONE	20 BITS 10 BITS HORIZ. 10 BITS VERT.	+/- 5VDC	120 VAC 60 CYCLE	AT LEAST 2	ANALYTICS, INC.	REDUCE SIZE & IMPROVE SYSTEM
ISCAN RK426 <3>	NONE	45 BITS <5>	6 LINES ANALOG +/- 5VDC	120 VAC 60 CYCLE CAN BE 24VDC	1 W/ CONSIDERABLE TRAINING	VARIOUS MEDICAL UNITS	OVERALL IMPROVEMENT
SST EYETYPER 300	9600	8 BITS X 8 BITS Y 8 BITS PUPIL DIAM.	NONE	120 VAC 60 CYCLE	1 W/ CONSIDERABLE TRAINING	CUSTOMIZED FOR SPECIFIC HANDICAPS	POINT OF GAZE SYSTEM FOR NAVY
UNIVERSAL INTRAM CO. OFTALMOGRAF	NONE	NONE	+/- 12 VDC OR 24 VDC	120 VAC 60 CYCLE 24 VDC OR 12 VDC	1	STEVE RUDOLF BETH ISREAL MED CENTER	IMPROVE CHIN RESTRAINT DESIGN
FORWARD TECHNOLOGY <4>	NONE	NONE	4 +/- 5VDC LINES H, V, Hvel, Vvel	120 VAC 60 CYCLE	1 W/ TRAINING	BROOKS AIR FORCE BASE SAN ANTONIO, TX.	EXPAND MARKETABILITY
STOELTING CO.	NONE	22 BITS 7 BITS X &Y 8 BITS PUPIL DIAM.	+/- 5VDC TO +/- 10VDC	120 VAC 60 CYCLE	2	UNIV. OF ILLINIOS	IMPLEMENT FIBER OPTICS HEAD MOUNT

Table C-1. Oculometer Manufactures and models by characteristics of each device. (Cont.)

OCULOMETER MAKE	POINT OF CONTACT	PHONE NUMBER	DELIVERY TIME
ASL 1998 <1>	JOSE VALEZ 335 BAIR HILL RD WALTHAM, MA. 02154	617-890-5100	9 MONTHS
HONEYWELL	JOHN BAHR MINNEAPOLIS, MN	612-542-5837	1 YEAR
NAC Eyemark V	CAREY CLAYTON 820 S. MARAPOSSA BURBANK, CA 91506	203-668-4803	30 DAYS
MICROMEASUREMENTS SYSTEM 1200 <2>	KEITH SHERMAN 1921 HOPKINS ST. BERKELEY, CA 94707	415-542-0125	120 DAYS
MICROMEASUREMENTS SYSTEM 1200 <2>	SAME AS ABOVE	SAME AS ABOVE	120 DAYS
DENVER RESEARCH INSTITUTE EYEGLASSES	GEORGE RINARD 303-871-4370	303-871-4370	3 MONTHS
ASL 1996 <1>	JOSE VALEZ (SAME AS ABOVE)	SAME AS ABOVE	9 MONTHS
ISCAN RK426 <3>	RIKKI RAZDEN 755A CONCORD AVE CAMBRIDGE, MA 02238	617-868-5353	4-6 WEEKS
SST EYETYPER 300	GARY KILANY 5011 BAUM BLVD PITTSBURGH, PA 15123	412-682-0144	30 DAYS
UNIVERSAL INTRAM CO. OFTALMOGRAF	HENRY MICHEAL P.O. BOX 1915 DEMMING, NM 88031-1915	505-546-8205	6 WEEKS
FORWARD TECHNOLOGY <4>	WARREN WOOD 8652 MAGNOLIA SU. 52 SANTEE, CA 92071	619-258-8789	18 MONTHS
STOELTING CO.	CHARLES SCOUTEN 1350 S. KOSTNER AVE CHICAGO, IL 60628	312-860-9700	4 MONTHS

FOOTNOTES:

<1> ASL oculometers can be adapted for head mounted optics with helmet.

<2> Micromeasurements System 1200 yields raw eye position data. This data can be input to Micromeasurements System 7000 for proprietory processing. System 7000 is an IBM AT compatible with propietory software. Software alone can be purchased for $4,000.

<3> ISCAN System RK416 yields raw eye position data. This data can be input to ISCAN System RK520 for proprietory processing.

<4> Forward Technologies manufactures and develops eyetrackers utilizing and perfecting technology initiated at Stanford Research Institute (SRI). This work was headed by:
Dr. Hewitt Crane EK-150
Menlo Park, CA 94025
415-326-6200

<5> Raw eye position data as follows:

Pupil Diam.-	9 bits
Pupil horiz.-	9 bits
Pupil vert.-	8 bits
Corneal reflec. horiz.-	9bits
Corneal reflec. vert.-	8 bits
Pupil diam. pos. sel.-	1 bit
Data storage -	1 bit